1 Introduction

1.1 History and commercial importance of vinyl acetate

In 1914 Dr. Fritz Klatte[1] patented a process for the production of esters of vinyl alcohol (including vinyl acetate, VAc) and within a few years he had made poly(vinyl acetate), pVAc. In 1924 Herrmann and Haehnel described a process[2] for the production of poly(vinyl alcohol), pVOH, by alkaline saponification of pVAc because vinyl alcohol itself cannot be polymerized directly. In fact vinyl alcohol exists only in minute quantities as the enol form of acetaldehyde. 1926 saw the first major industrial use of pVAc - as the intermediate in the production of pVOH, which in turn was used for sizing textiles.

About 3×10^9 kg of vinyl acetate are manufactured annually worldwide, mainly by the oxidative addition of acetic acid to ethylene in the presence of a palladium catalyst[3].

$$CH_3COOH + CH_2{=}CH_2 + \tfrac{1}{2}O_2 \xrightarrow{Pd} CH_3COOCH{=}CH_2 + H_2O \qquad 1.1$$

The polymerization of VAc for pVOH production was, and still is, done by free-radical solution polymerization in methanol. This has several attractive features from an industrial point of view but suffers several drawbacks as well, not the least of which is the difficulty of achieving high molecular weights. When high molecular weight pVAc is required it is generally produced by emulsion polymerization.

Poly(vinyl acetate) latexes were the first synthetic polymer latexes made on an industrial scale, beginning in Germany in the 1930s. With the addition (and/or generation in situ) of pVOH as an emulsifier, pVAc latexes became one of the major products of the adhesive and surface coating industries. Low cost and good performance, further enhanced by copolymerization with acrylates and other vinyl esters, have ensured its continued pre-eminence.

From a manufacturer's perspective emulsion polymerization has many attractive features:

(i) no solvents are required, a not inconsiderable virtue in an era of ever more stringent pollution controls

(ii) polymer latexes of high solids content have low viscosities and as such are easily pumped and are amenable to continuous flow processing - features highly regarded by chemical engineers

(iii) high monomer conversion is readily achieved. This has both an economic benefit and the desirable environmental outcome of low residual volatile organics

(iv) the high heat capacity of water helps deal with the large amount of heat of reaction evolved in polymerizations, and finally

(v) as already mentioned, high molecular weights can be achieved which enhance the polymer's properties.

The kinetics of emulsion polymerizations are responsible for the evolution of high molecular weight material and it is hoped that this work can cast further light on the kinetics of the emulsion polymerization of vinyl acetate.

1.2 Overview of free-radical emulsion polymerization

An emulsion polymerization is one that takes place in a heterogeneous dispersion. There are many different types of emulsion polymerizations depending on:

(i) the type of dispersion ("oil-in-water" or "water-in-oil")

(ii) regimes of particle sizes (micro and mini emulsions)

(iii) surfactant (anionic, non-ionic, cationic, amphoteric or surfactant free)

(iv) reactor type and

(v) feed regimes (batch, starved feed, continuous stirred tank).

Of the above, the most commonly used process in industry is the free-radical polymerization of a surfactant-stabilised oil-in-water emulsion. Consequently, when the term emulsion polymerization is used without qualification, it is generally understood to mean polymerization of a surfactant-stabilised oil-in-water emulsion. The "oil" (i.e. monomer) is usually an olefin with molecular weight in the range 60-200 daltons. The most widely used monomers in emulsion polymerizations are styrene, butadiene, vinyl chloride, various acrylates and vinyl esters. Copolymerization of two or more monomers is practised extensively to produce polymers with enhanced properties.

Poly(vinyl acetate) is manufactured by a free-radical surfactant-stabilised oil-in-water emulsion polymerization and in the following sections the kinetics of this type of emulsion polymerization are outlined. The process takes place in three stages, usually called intervals I, II and III[4] (figure 1.1).

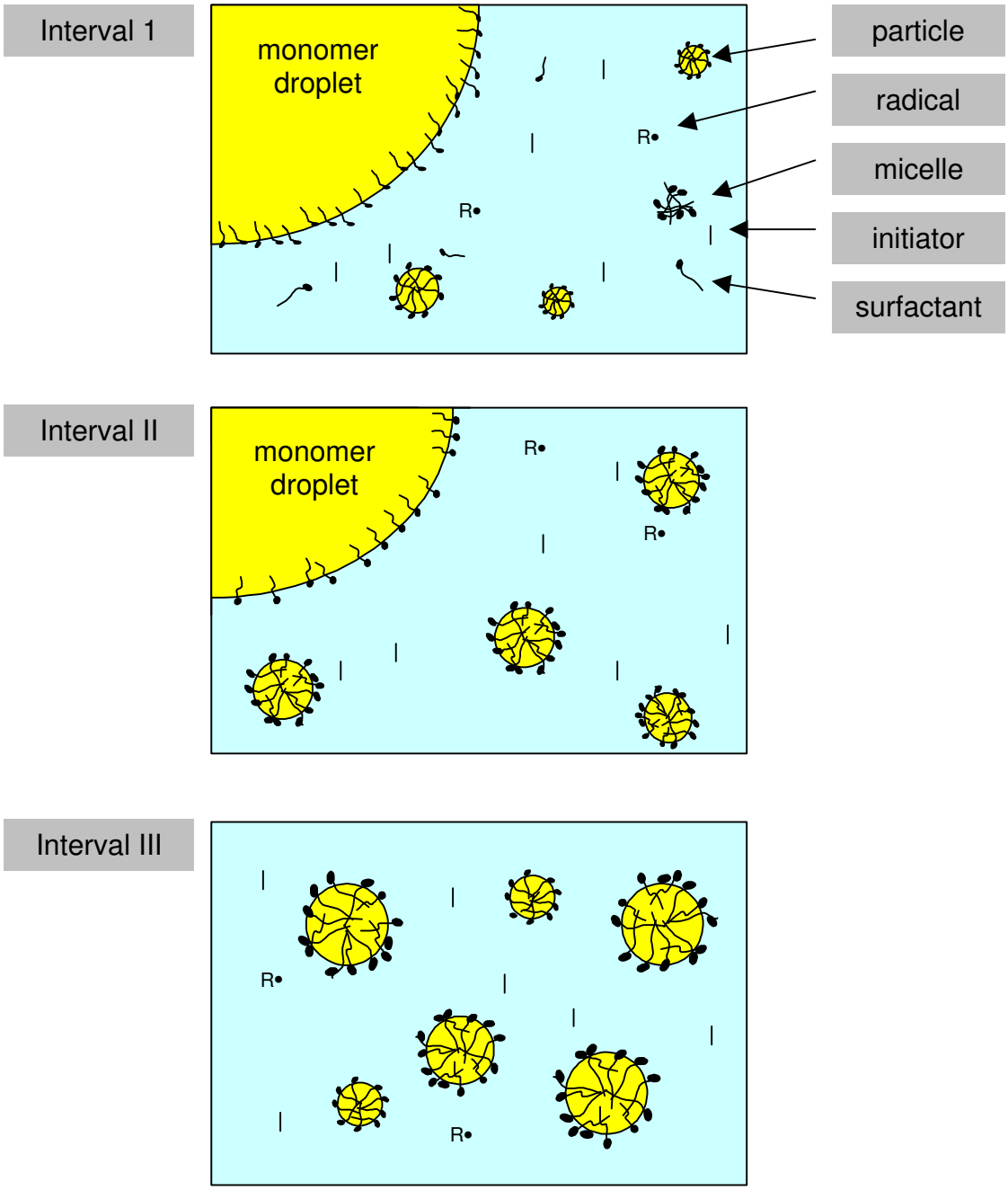

Figure 1.1: The three stages of an emulsion polymerization.

1.2.1 Interval I – particle formation

Interval I is defined as the period of particle formation. It commences with an emulsion of surfactant-stabilised monomer droplets (typically a few microns in diameter) in water. To this is usually added a water-soluble initiator which decomposes to produce the free radicals that initiate polymerization. Most monomers have limited water solubility and as the oligomeric radicals grow they become even less water soluble and tend to precipitate. The degree of polymerization at which precipitation occurs is denoted j_{crit} and such an oligomeric radical is called a j_{crit}-mer. In the presence of surface-active species, oligomeric radicals may also enter micelles or become solubilised. In either case a precursor particle is formed (typically a few nanometres in diameter). Such particles are rapidly swollen with monomer and are the main locus of polymerization thereafter[5-7].

When persulfate is used (figure 1.2) the free-radical fragment that initiates polymerization is the sulfato free radical ($SO_4^{-}\bullet_{(aq)}$). This negatively charged end group imparts surface activity to the growing aqueous-phase oligomeric radical. This has two immediate consequences. The first is that these surface-active oligomers may stabilise particles. (This is seen in surfactant-free emulsion polymerizations and is also likely to be a contributing factor in the observed dependence of particle number on initiator concentration[8,9].) Second, and most importantly, this is the mechanism whereby the free radicals generated in the aqueous phase enter particles.

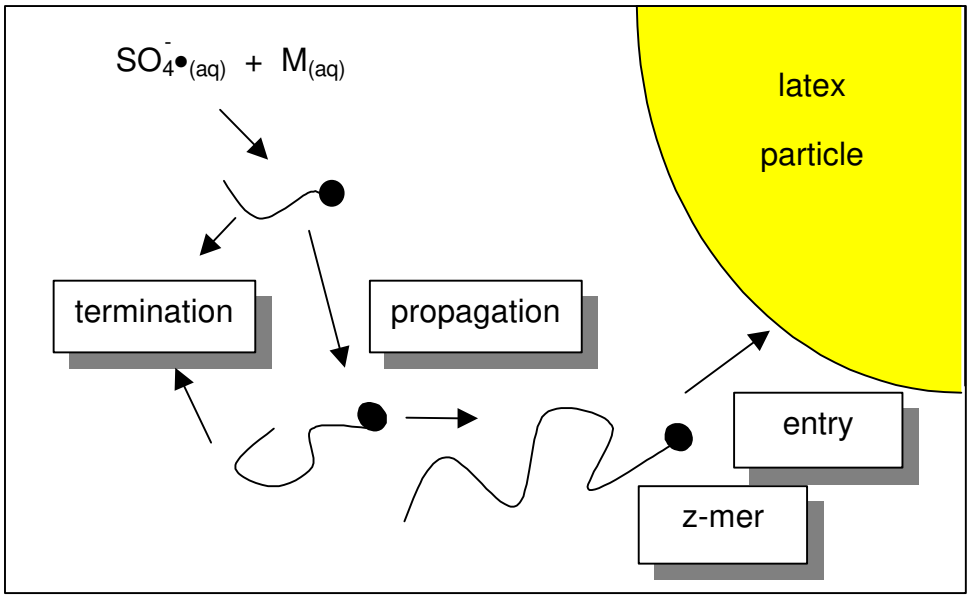

Figure 1.2: Mechanism of free radical entry into particles.

If an aqueous-phase oligomeric radical grows to a degree of polymerization, z, where it becomes sufficiently surface active that it is unlikely to desorb from a particle it encounters, it is called a z-mer.

As the number of particles increases, the probability for a z-mer to encounter and enter a particle before it can grow to a j_{crit}-mer increases, thereby decreasing the rate of new particle formation. When a sufficient number of particles have formed (typically 10^{17} - 10^{18} dm^{-3}) the probability of an aqueous-phase oligomeric radical growing beyond a z-mer is negligible.

At some point early in the polymerization nearly all the surfactant is adsorbed onto droplets and particles. Hence, very little surfactant is available in the aqueous phase to stabilise precursors and (in a well behaved system) particle formation ceases.

1.2.2 Interval II – particle growth

This is the period of particle growth. The droplets act as monomer reservoirs and as polymerization proceeds in the particles monomer is replenished from the droplets. Hence, the particles grow until all the droplet phase monomer is consumed. This process is thermodynamically driven as the system strives to minimise the sum of the (favourable) free energy of mixing of monomer and polymer and the (unfavourable) surface free energy of the particle/water interface. This process is referred to as "swelling" and determines the equilibrium saturation concentration of monomer in the particles.

The main feature of interval II is that the concentration of monomer in the particles remains constant at the equilibrium saturation concentration. Macroscopically, interval II is usually characterised by a constant rate of polymerization.

1.2.3 Interval III – final stage

Interval III commences when the monomer droplets are exhausted. During this period monomer concentration in the particles decreases and is usually accompanied by a decrease in polymerization rate.

The simple picture outlined above is far from a complete one and many systems deviate in some of the details. Often the distinction between intervals I and II is not sharp, or even non-existent, and particle nucleation continues during the period of particle growth. The other major deviation occurs during interval III where, as monomer concentration decreases, many polymers pass through a "glass transition".

This significantly reduces diffusion rates which in turn reduce termination rates to such an extent that polymerization rates increase despite the decrease in monomer concentration. This is called the "Trommsdorf-Norrish" gel effect[10,11] and is particularly evident in the emulsion polymerizations of so-called glassy polymers such as styrene and methyl methacrylate.

1.2.4 Compartmentalization

Compartmentalization is the term used to describe the fact that the propagating radicals in an emulsion polymerization are physically separated from one another by virtue of the compartmentalized nature of an emulsion polymerization. This property may drastically reduce the incidence of bimolecular termination otherwise available in a bulk or solution polymerization and defines the kinetics of emulsion polymerization and the properties of the resultant polymers.

1.3 Types of emulsion polymerization systems

1.3.1 Zero-one emulsion polymerizations

The term zero-one is used to describe the "usual" situation found in emulsion polymerizations whereby two or more radicals cannot co-exist within a particle. This is because they are constrained to such a small volume that bimolecular termination is almost instantaneous. By this, the kineticist means bimolecular termination occurs at a much greater rate than any of the other kinetic events that influence the fate of the radicals (such as entry of a third radical or exit of a radical subsequent to transfer to monomer).

This constraint weakens as particles grow and as intra-particle viscosity increases with conversion during interval III. Often it is lifted completely for systems at or near the glass transition. As will be shown in section 2.4, monomers possessed of a high propagation rate coefficient may also escape this classification.

The main consequence of zero-one kinetics is that when a z-mer enters a "live" particle (i.e. a particle containing a growing polymer chain) "instantaneous" bimolecular termination ensues and the system loses two radicals.

1.3.2 Pseudo-bulk emulsion polymerizations

Pseudo-bulk emulsion polymerization describes the case where radicals may cohabit a particle without terminating instantaneously. This situation arises when there exists a chain-length dependence of the termination rate coefficient and intra-particle termination becomes rate-determining: for example, in glassy systems where diffusion rates are so low as to reduce the termination rate below that of the entry rate. This may cause $\bar{n}$ to be larger than 0.5 and is believed to be the case, for instance, for methyl methacrylate at high conversions[12]. This is also often the case for large particles (for instance in styrene emulsion polymerizations) where the radicals do not "see" each other[13].

1.3.3 Compartmentalized pseudo-bulk emulsion polymerizations

This is a special case of pseudo-bulk kinetics, sometimes called zero-one-two kinetics, which arises when termination is not instantaneous and $\bar{n}$ is low. Zero-one-two kinetics are favoured by high propagation rate coefficients, whereby radicals grow to a cumbersome size rapidly and centre-of-mass diffusion becomes so hindered that bimolecular termination of radicals is no longer "instantaneous" in the zero-one sense. However, termination is faster than entry (due to relatively rapid transfer to monomer and small particle size) and thus, $\bar{n}$ remains low. This behaviour is sometimes called zero-one-two kinetics because, as the name implies, particles may contain zero, one or two radicals.

1.4 Aim of this work

In most emulsion polymerizations the exhaustion of the separate monomer phase (onset of interval III) is followed by a decrease in conversion rate due to the decrease in monomer concentration in the latex particles. An unusual feature of vinyl acetate emulsion polymerization is that the conversion rate remains approximately constant throughout most of interval III[8,9].

The primary aim of this work was to determine rate coefficients for the emulsion polymerization of vinyl acetate using the γ radiolysis relaxation techniques and molecular weight distribution analysis techniques developed by Gilbert's group at the University of Sydney[13]. These rate coefficients were then to be used to test kinetic models that were proposed to explain the independence of conversion rate from monomer concentration.

-oOo-

2 Kinetics of vinyl acetate emulsion polymerizations

The first thing one notices when researching the emulsion polymerization literature for references to vinyl acetate is that vinyl acetate is often mentioned as the extreme case or even the exception to the "normal" behaviour of the other common monomers. It is more polar and hence more water soluble than any of the other common monomers whose polymers are insoluble in water. The propagation rate coefficient is in the very high range along with the acrylates (see table 2.1). The rate coefficient for transfer to monomer is very high compared with the other common monomers (see table 2.2), and vinyl acetate induces accelerated decomposition of persulfate to a much greater extent than any of the other common monomers for which such data exist (see section 4.2). Finally, reactivity ratios are extremely unfavourable for inclusion of vinyl acetate in copolymer chains (see table 2.3).

The essentials of emulsion polymerization can be understood in terms of the behaviour of a small group of representative common monomers such as the vinyl and acrylic monomers listed in table 2.1. The following sections on the general mechanisms of free radical polymerization in emulsions will therefore focus on these monomers and include discussion of the peculiarities of vinyl acetate polymerization.

Finally, three kinetic models are identified that could account for the observed independence of the rate of polymerization from the monomer concentration in the emulsion polymerization of vinyl acetate. It will be seen that each of the models has certain requirements, that may be tested experimentally.

2.1 Initiation and entry

Primary free radicals are usually generated by thermal homolysis or photolysis of a chemical initiator, denoted I_2. Radiolysis is a special case and is described in detail in chapter 3. Most industrial processes rely on thermal homolysis of a chemical initiator, often accelerated by redox couples. In any case, two (not necessarily identical) primary radicals, denoted I•, are formed according to:

$$I_2 \xrightarrow{k_d} 2I\bullet \qquad 2.1$$

where k_d is the dissociation rate constant.

Initiation of free-radical polymerization is a two step process. Reaction 2.1 describes the production of primary free radicals and reaction 2.2 requires that at least some of

the free radicals from reaction 2.1 react with monomer rapidly enough to avoid recombination reactions. In practice, of course, initiators are used which produce primary radicals that do react rapidly with monomers.

The primary free radicals from reaction 2.1 may then react with monomer, M, according to:

$$\mathrm{I}\bullet + \mathrm{M} \overset{k_{\mathrm{p,I}}}{\rightarrow} \mathrm{IM}\bullet \qquad 2.2$$

hence $k_{\mathrm{p,I}}$ is the rate coefficient for addition of the primary radical to monomer. The (monomeric) radicals so formed may then propagate to z-mers and enter particles as described in section 1.2.1.

$$\mathrm{IM}\bullet + \mathrm{M} \overset{k_{\mathrm{p,aq}}^{i}}{\rightarrow\rightarrow\rightarrow} \mathrm{IM}_z\bullet \qquad 2.3$$

where $k_{\mathrm{p,aq}}^{i}$ is the propagation rate coefficient for an aqueous-phase oligomer of degree of polymerization i.

Aqueous-phase radicals may be lost in bimolecular termination reactions. Initiator-derived primary radicals may terminate via reaction 2.4 and aqueous-phase oligomeric radicals may terminate before they can grow to z-mers via reaction 2.5, in which case two radicals are lost, or via reaction 2.6 in which case no radical loss occurs but initiator is consumed:

$$\mathrm{I}\bullet + \mathrm{T}\bullet \overset{k_{\mathrm{t,aq}}}{\rightarrow} \text{inert products} \qquad 2.4$$

$$\mathrm{IM}_i\bullet + \mathrm{T}\bullet \overset{k_{\mathrm{t,aq}}}{\rightarrow} \text{inert products} \qquad 2.5$$

$$\mathrm{IM}_i\bullet + \mathrm{I}_2 \overset{k_{\mathrm{tr,I}}}{\rightarrow} \mathrm{IM}_i\mathrm{I} + \mathrm{I}\bullet \qquad 2.6$$

where $i < z$, T• represents any aqueous-phase radical, $k_{\mathrm{t,aq}}$ is the aqueous-phase bimolecular termination rate coefficient and $k_{\mathrm{tr,I}}$ is the rate coefficient for chain transfer to initiator by oligomeric radicals.

The most widely used initiator in emulsion polymerizations, and the one used in this work, is the peroxodisulfate anion, $S_2O_{8\,(aq)}^{2-}$ (commonly referred to simply as persulfate). It undergoes thermal homolysis to produce sulfato radical anions at a convenient rate for both industrial and laboratory applications:

$$S_2O_{8\,(aq)}^{2-} \xrightarrow{k_d} 2\ SO_4^{\bullet-}{}_{(aq)} \qquad 2.7$$

2.1.1 Efficacy of initiator systems in emulsion polymerization

There are three major factors relevant to the overall efficacy of initiator in emulsion polymerizations. The first is wastage of initiator through non-radical producing side reactions such as reaction 2.6, above. The second is the efficiency of the reaction of monomer with the initiator fragments formed by decomposition of the initiator. The third is the entry efficiency, in other words the probability that an aqueous-phase oligomeric radical will grow to a *z*-mer and enter a particle.

2.1.1.1 Initiator efficiency of persulfate-initiated emulsion polymerization.

Accelerated decomposition of persulfate is significant in the presence of some monomers and surfactants[14-17]. This may have the undesirable effects of introducing a large uncertainty in the value of k_d, if the induced decomposition proceeds via a radical producing pathway, thus significantly reducing initiator concentration during polymerizations. These aspects of persulfate decomposition are considered in detail in chapter 4.

The probability, f_{init}, that a sulfato radical initiates polymerization rather than terminating with another radical in the aqueous phase can be seen from the competing reactions (2.2 and 2.4) to be:

$$f_{init} = \frac{k_{p,I}[M_{aq}]}{k_{t,aq}[T\bullet] + k_{p,I}[M_{aq}]} \qquad 2.8$$

f_{init} is called the scavenger efficiency as it relates to the efficiency with which radicals are "scavenged" by, in this case, monomer. An estimate of the upper limit for [T•] is given by Casey[18] as:

$$[T\bullet] = \left\{ \frac{k_d[I]}{k_{t,aq}} \right\}^{1/2} \qquad 2.9$$

The activation energy for reaction 2.4 is negligible and the aqueous-phase radicals one would expect in emulsion polymerizations are small species so it is reasonable to assume that $k_{t,aq}$ will be close to the diffusion limit for small species[19]

i.e. ~ 4×10^{9} M^{-1} s^{-1}. Hence, under typical emulsion polymerization conditions [T•] < 2×10^{-9} M (at 50°C and [$S_2O_8^{2-}$] < 10^{-2} M).

For the vinyl and acrylic monomers $k_{p,I}$ is in the range[20] 2×10^{8} - 2×10^{9} M^{-1} s^{-1}. The least water-soluble of the common monomers listed in table 2.1, vinyl neo-decanoate, (which would be expected to have the lowest scavenger efficiency) has a saturation aqueous-phase concentration of 4×10^{-5} M at 20°. Substituting the above in equation 2.8 gives $f_{init} > 0.999$. Hence, in typical emulsion polymerizations reaction with monomer accounts for virtually 100% of the sulfato radicals produced by thermal homolysis of persulfate.

2.1.1.2 Entry efficiency in persulfate-initiated emulsion polymerization.

The size of the entering oligomeric radical is an important parameter in the determination of entry efficiency, f_{entry}. This is because the time spent in the aqueous phase growing to a z-mer determines the likelihood of bimolecular termination occurring before entry can take place. From thermodynamic considerations Maxwell et al.[21] postulated that, for persulfate-initiated oligomers, z may be estimated from equation 2.10:

$$z \approx 1 - \frac{23\ (\text{kJ mol}^{-1})}{RT \ln C_w^{sat}} \qquad 2.10$$

where T is the reaction temperature and C_w^{sat} is the saturation concentration of aqueous-phase monomer. Predicted values of z for the common monomers are shown in table 2.1.

They also showed that the entry efficiency, f_{entry}, can be estimated, if the value of z is known, from a simple analytical approximation to the complete set of rate equations that describe all the aqueous-phase events[21]:

$$f_{entry} = \left\{ \frac{(k_d[I]k_{t,aq})^{0.5}}{k_{p,aq}C_w} + 1 \right\}^{1-z} \qquad 2.11$$

where k_d is the rate coefficient for decomposition of initiator, [I] is the initiator concentration, $k_{t,aq}$ is the average rate coefficient for bimolecular termination of aqueous-phase radicals, C_w is the aqueous-phase concentration of monomer and $k_{p,aq}$ is the rate coefficient for propagation in the aqueous phase. It has been shown[22,23] that $k_{p,aq}$ is generally about the same as k_p measured in bulk for ordinary monomers; however there may be a significant effect for polar monomers such as vinyl acetate.

The entry rate coefficient for initiator-derived radicals, (i.e. the number of initiator-derived propagating radicals entering per particle per second) ρ_{init}, may then be predicted from the "Maxwell-Morrison" equation[21]:

$$\rho_{init} = \frac{2k_d[I]N_A}{N_c}\left\{\frac{(k_d[I]k_{t,aq})^{0.5}}{k_{p,aq}C_w} + 1\right\}^{1-z} \qquad 2.12$$

where N_c is the particle number concentration.

Table 2.1: Predicted values of z (degree of polymerization of entering oligomeric radicals) for some common monomers in persulfate initiated emulsion polymerizations. Calculated from equation 2.10 , all values at 50°C, $[S_2O_8^{2-}] = 10^{-2}$ M . Entry efficiency calculated from lower value of z, $k_{p,aq}$ assumed equal to k_p.

	C_w^{sat} (M)	ref	k_p (M^{-1} s^{-1})	ref	z	f_{entry}
styrene	0.0043	24	2.6×10^2	25	2 – 3	3%
butyl acrylate	0.0062	26	1.1×10^4	27	2 – 3	99%
methyl methacrylate	0.15	28	6.5×10^2	25	4 – 5	94%
n-butyl methacrylate	0.0025	29	5.4×10^2	30	3	15%
vinyl neo-decanoate	0.00004	31	5.3×10^3	31	2	2%
vinyl acetate	0.3	32	6.7×10^3	33	8	95%

2.1.1.3 Surface anchoring

Termination, subsequent to entry of a sulfato derived oligomeric radical into a "live" particle, is complicated by the possibility of "surface anchoring" whereby the charged sulfato endgroup may resist "true" entry. In this case, diffusion of the radical will be limited to reaction diffusion, i.e. the radical moves within the particle by propagation. This is very much slower than centre-of-mass diffusion for small *i*-mers. Consequently, the termination rate for an otherwise zero-one system will be reduced while the propagation rate remains largely unaffected.

2.1.1.4 Initiation by gamma radiation

As discussed in detail in chapter 3, the majority of the primary radicals produced in the γ radiolysis of emulsion polymerizations react by addition to the double bond of the monomer[34] in the aqueous phase. The monomeric free radicals so formed may propagate to *z*-mers and enter particles. It should be noted that *z* for an aqueous-phase oligomeric radical initiated by γ radiolysis will be less than that for an aqueous-phase oligomeric radical initiated by persulfate. This is because the initiator fragments in the

former case do not include a charged end group. Hence, entry efficiency should be greater for initiation by radiolysis than persulfate.

2.1.2 Efficacy of initiation by persulfate in vinyl acetate emulsion polymerization.

2.1.2.1 Induced decomposition of persulfate by vinyl acetate

It has been known for many years that vinyl acetate accelerates the decomposition of persulfate to a much greater extent than any of the other common monomers[14]. Various mechanisms have been proposed and these are discussed in detail in section 4.2. The important thing as far as entry is concerned is whether the accelerated decomposition produces a significant number of "extra" radicals. If it does then k_d and hence ρ_{init} (equation 2.12) may be increased substantially.

2.1.2.2 Entry efficiency of persulfate-initiated vinyl acetate emulsion polymerization

Applying equation 2.10 to VAc at 50°C gives $z \approx 8$. This result is supported by the recent work of Poehlein[35] wherein z was found to be in the range 6 - 14. Also, as will be shown in section 4.4.3, indirect evidence and theoretical considerations support the contention that oligomers of degree of polymerization less than eight with one sulfate end group are soluble in water whereas longer oligomers are expected to be surface active. Hence, from equation 2.11 the entry efficiency may be estimated to be greater than 99% for VAc emulsion polymerization initiated by 10^{-3} M persulfate at 50°C. This estimate is not very sensitive to the calculated value of z or to the assumed value for $k_{p,aq}$. Even if z is taken as the upper limit found in Poehlein's work, $k_d[I]$ increased by a factor of ten and $k_{p,aq}$ halved, the calculated entry efficiency is still found to be greater than 90%.

2.1.2.3 Entry efficiency of gamma radiolysis-initiated vinyl acetate

In the case of initiation by gamma radiolysis of VAc, about 98% of the aqueous-phase radicals produced by γ radiolysis of the emulsion (97% of the OH• and 100% of the e^-) react by addition to the monomer double bond[34]. From the foregoing discussion it can be concluded that most of the monomeric free radicals so formed propagate to z-mers rapidly and enter particles with an even higher efficiency than that calculated for persulfate-derived oligomeric radicals.

2.2 Propagation

Propagation is the process whereby a macroradical adds to the double bond of a monomer molecule. Addition to monomer increases the degree of polymerization by one:

$$R_i + \mathrm{M} \xrightarrow{k_p^i} R_{i+1} \qquad 2.13$$

where the propagation rate coefficient for a macroradical of degree of polymerization i is denoted by k_p^i and the macroradical itself by R_i. (Species propagating within a particle are not necessarily initiator-derived and so the nomenclature $IM_i\bullet$ has been replaced with the more general R_i). For i greater than about three or four, (which includes the vast majority of macroradicals) $k_p^i = k_p$, the long chain propagation rate coefficient. It follows that the rate equation for monomer concentration with respect to time is given by:

$$\frac{\mathrm{d}[\mathrm{M}]}{\mathrm{d}t} = -k_p[\mathrm{M}]\sum_{i=1}^{\infty}[R_i] \qquad 2.14$$

In emulsion polymerizations the latex particles are the locus of polymerization so the effective monomer concentration, [M], is that in the particles, and is denoted C_p. The radical concentration:

$$\sum_{i=1}^{\infty}[R_i] = \bar{n}\frac{N_c}{N_A} \qquad 2.15$$

The rate of depletion of monomer, -d[M]/dt, is usually called the polymerization rate and may be replaced by the widely used symbol R_p. Equation 2.14 may then be written as:

$$R_p = k_p C_p \bar{n}\frac{N_c}{N_A} \qquad 2.16$$

2.2.1.1 Chain length dependence of propagation rate coefficients

The propagation rate coefficient is essentially constant for a given temperature except for very short chains and "glassy" regimes. Quantum calculations[36,37] have shown that the partition function that describes hindered rotations in the propagation transition state is affected by the size of the macroradical and causes k_p to increase with decreasing chain length. It has been argued that this effect is only significant for very short chains[38,39] and as such has little effect on the average polymerization rate coefficient.

Chain length dependent k_p is denoted k_p^i. Evidence exists that suggests that k_p^1 may be much greater than the average k_p. Lorand[40] has compiled rate coefficients for small model radicals which shows that this applies to such systems. Moad et al.[41,42] have shown that for methyl acrylate and methacrylonitrile k_p^1 is about ten times average k_p. Gridnev and Ittel[43] have shown that k_p^1 and k_p^2 for MMA are about seventeen times and four times the long chain k_p at 60°C respectively, while k_p^1 for methacrylonitrile is about six times the long chain k_p at 60°C.

A high value of k_p^i for small i may have a significant effect on the overall kinetics of an emulsion polymerization as several kinetic steps are dependent on competing processes which involve very short chains. For instance, persulfate-derived z-mers for most of the common monomers are very short chains ($z = 2 – 5$, see table 2.1) so it can be seen from equation 2.11 that $k_{p,aq}^i$ may have a significant effect on entry efficiency especially for systems with low entry efficiency[13]. Also, termination, especially in glassy systems, exhibits a dependence on the concentration of short chains, which in turn depends on how quickly the short chains can grow.

2.2.1.2 Propagation rate coefficients

The overall propagation rate coefficient, k_p, is related to is the diffusion-controlled propagation rate coefficient, $k_{p,diff}$, and the chemically-controlled propagation rate coefficient, $k_{p,chem}$ by[13]:

$$\frac{1}{k_p} = \frac{1}{k_{p,diff}} + \frac{1}{k_{p,chem}} \qquad 2.17$$

At very high viscosities such as are found in glassy regimes, $k_{p,diff} < k_{p,chem}$, the rate determining step for propagation is diffusion and k_p is said to be diffusion controlled. $k_{p,diff}$ is given by the Smoluchowski equation for diffusion controlled reactions[44]:

$$k_{p,diff} = 4\pi N_A \sigma D \qquad 2.18$$

where σ is the reaction radius and D is the mutual diffusion coefficient for the monomer and the macroradical. It has been argued that a reasonable value to ascribe to σ is the Lennard-Jones diameter of the monomer molecule[45,46] which is around 6 Å. Given the reasonable assumption that $D_{mon} >> D_{pol}$ (where D_{mon} and D_{pol} are the diffusion coefficients for centre-of-mass diffusion of monomer and polymer respectively) D_{mon} may be used to approximate the combined centre-of-mass diffusion coefficient for propagation.

Combining equations 2.17 and 2.18 with the known[13] dependence of D_{mon} on W_p allows one to estimate whether or not propagation in a given system is diffusion controlled. D_{mon} ($cm^2\ s^{-1}$) has been determined empirically for styrene at 50°C as a function of $W_p < 0.82$ (i.e. below the glass transition)[13] {p121}:

$$D_{mon}/cm^2\ s^{-1} = 3.188\times10^{-5} - 5.607\times10^{-5}W_p + 4.078\times10^{-6}W_p^2 + 2.096\times10^{-5}W_p^3 \quad 2.19$$

and for MMA at 50°C and $W_p < 0.8$[13]:

$$\log(D_{mon}/cm^2\ s^{-1}) = -4.386 - 3.200W_p + 9.049W_p^2 - 12.079W_p^3 \quad 2.20$$

Above the glass transition, D_{mon} has been determined for methyl methacrylate[47,48]. The data and the empirical fits are plotted in figure 2.1.

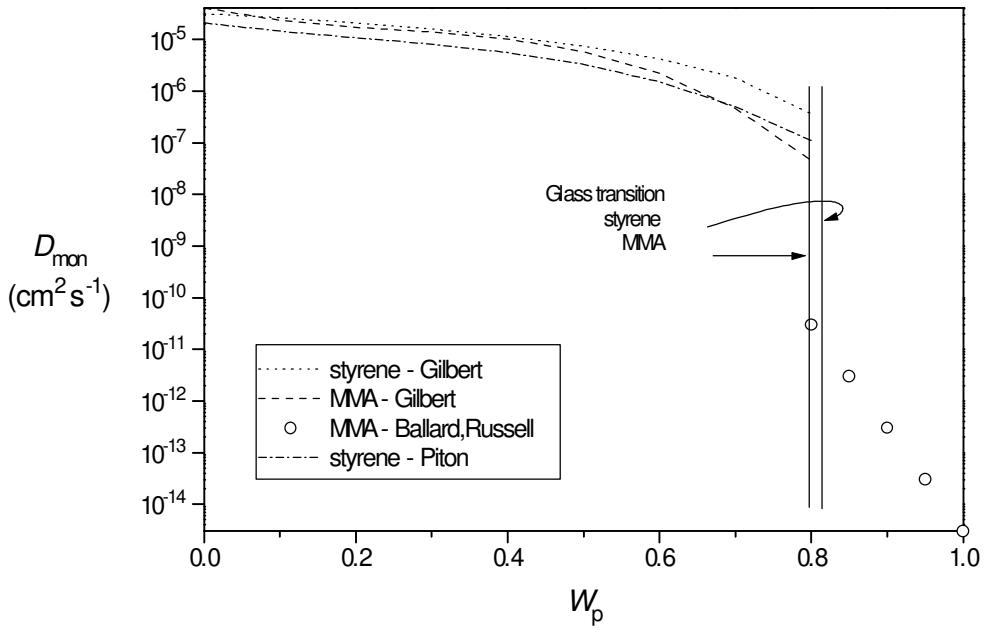

Figure 2.1: Dependence of D_{mon} on W_p for styrene and methyl methacrylate at 50°C, based on equations 2.19 and 2.20.

From figure 2.1 it can be seen that above the conversion at which the glass transition occurs, D_{mon} decreases dramatically. For $D_{mon} < 10^{-11}\ cm^2\ s^{-1}$ equation 2.18 gives $k_{p,diff} < 4\times10^3\ M^{-1}\ s^{-1}$ which is comparable to typical k_p values. As W_p increases k_p eventually becomes diffusion controlled.

Conversely, it is clear that for rubbery systems (systems below the conversion, and/or above the temperature, T_g, at which the glass transition occurs) $D_{mon} >> 10^{-8}\ cm^2\ s^{-1}$ up

to very high conversions and hence $k_{p,diff} > 4\times10^6$ M^{-1} s^{-1}. Thus, $k_{p,diff}$ is 2 - 4 orders of magnitude greater than k_p for any of the common monomers, above their respective T_g, and in such systems k_p is chemically controlled and does not vary significantly with conversion.

2.2.1.3 High propagation rate coefficient of vinyl acetate.

Vinyl acetate has a high propagation rate coefficient, k_p. Recent improvements in pulsed laser polymerization techniques, particularly in relation to faster laser repetition rates, have allowed for the reliable determination of k_p for a number of monomers including VAc. The Arrhenius relationship for VAc has been most recently reported as[33]:

$$\ln(k_p / M^{-1} s^{-1}) = (16.50 \pm 0.14) - (2485 \pm 41)/T(K) \qquad 2.21$$

giving a frequency factor of $10^{7.17 \pm 0.05}$ M^{-1} s^{-1} and activation energy of 20.66 ± 0.34 kJ mol^{-1}. Hence, $k_p = 6.7\times10^3$ M^{-1} s^{-1} at 50°C.

2.3 Transfer, branching and exit

Transfer, in the broadest sense, refers to the transfer of radical activity from one radical species to another. In the case of a macroradical growing in an emulsion polymerization, the usual mechanism is hydrogen abstraction by the macroradical (though other functional groups may also be abstracted when they are present) thereby terminating the growing chain. This can be represented as:

$$R_i + XH \xrightarrow{k_{tr,x}} P_i + X\bullet \qquad 2.22$$

where R_i is a macroradical of degree of polymerization i, P_i is a dead polymer chain of degree of polymerization i and $k_{tr,x}$ is the transfer rate coefficient for transfer to species X.

In the absence of especially reactive chain transfer agents (adventitious or deliberately included to control molecular weight) most transfer is to polymer, monomer, or, as has been suggested for styrene, perhaps to a Diels-Alder dimer[49-53].

Table 2.2: Chain-transfer constants of some common monomers, all values for 50°C. C_M ($=k_{tr}/k_p$) from Polymer Handbook (1989)[54] except [a]this work and [b]obtained recently in Gilbert's group by R. Balic. k_{tr} calculated using k_p data in table 2.1.

monomer	$C_M \times 10^4$	$k_{tr} \times 10^3$
styrene	0.35-0.78	9.1-20.2
methyl acrylate	0.80	N/A
methyl methacrylate	0.1-0.85	6.5
n-butyl methacrylate	0.54	29.2
vinyl neo-decanoate	4[b]	2120
vinyl acetate	1.28[a]	859

2.3.1.1 Transfer to monomer and exit of monomeric free radicals

Transfer to monomer has significant implications for molecular weight distribution (MWD), branching and kinetics. MWD's are affected by, and in some instances dominated by, transfer to monomer because it results in the formation of dead polymer chains. Secondly, transfer to monomer may influence the extent of branching and consequently investigation of branching may give insight into mechanisms of transfer to monomer (see section 2.3.1.2). Finally, in emulsion polymerizations, if $M_{tr}^{\bullet}$ does not reinitiate rapidly, it may exit the particle and terminate with another radical thereby causing the loss of two radicals and influencing the polymerization kinetics. This is one of the most important kinetic processes and is discussed below.

It is usually assumed that only monomeric radicals may desorb from a particle as the solubility of oligomers in the aqueous phase is very low. The probability that $M_{tr}^{\bullet}$ will exit before it can propagate, P_{ex}, is given by[13]:

$$P_{ex} = \frac{k_{dM}}{k_{dM} + k_{p,M}^{1} C_p} \qquad 2.23$$

where k_{dM} is the desorption rate coefficient for monomeric free radicals and $k_{p,M}^{1}$ is the propagation rate coefficient for the following reaction:

$$M_{tr}^{\bullet} + M \xrightarrow{k_{p,M}^{1}} R_2 \qquad 2.24$$

It should be noted that the radical centre on $M_{tr}^{\bullet}$ is usually completely different to that in the "normal" propagating macroradical; hence $k_{p,M}^{1}$ may be quite different to k_p. Unfortunately, $k_{p,M}^{1}$ is not known for any monomers, which is not surprising as even the structure of $M_{tr}^{\bullet}$ is not known with any certainty for many monomers.

However, it is possible to estimate k_{dM}[13] from which one can then estimate the sensitivity of P_{ex} to $k^1_{p,M}$:

$$k_{dM} = \frac{3D_W}{r_s^2}\frac{D_M}{(qD_M + D_W)} \qquad 2.25$$

where D_W is the diffusion coefficient of monomeric free radicals in the aqueous phase, D_M is the diffusion coefficient of monomeric free radicals inside the swollen latex particle, r_s is the radius of a swollen latex particle and q ($=C_p/C_w$) is the partition coefficient of monomeric free radicals between the particle and aqueous phases.

For the sake of simplicity, the remainder of this section will consider only interval II, though the argument is readily extended to interval III for specific cases. Diffusion rates for radicals are approximately equal to those of their stable parents (±25%[55]), and so $D_M \approx D_{mon} \approx 1\times10^{-5}$ cm^2 s^{-1} for a typical interval II W_p (figure 2.1). D_W for typical monomer size molecules is ~1.5×10^{-5} cm^2 s^{-1} and so $D_M \approx D_W$. For the "representative" monomers listed in table 2.1 q is in the range 55,000 – 26 so $qD_M >> D_W$ and equation 2.25 simplifies to:

$$k_{dM} \approx \frac{3D_W}{r_s^2}\frac{C_w}{C_p} \qquad 2.26$$

The sensitivity of P_{ex} to $k^1_{p,M}$ is plotted in figure 2.2 below. It should be noted that figure 2.2 is only intended to demonstrate the range over which P_{ex} is sensitive to $k^1_{p,M}$ for each of the "representative" group of monomers. A more precise treatment incorporating the small, but not insignificant, dependence of D_{mon} on the exact interval II weight fraction of polymer for each system has not been attempted here. However, inspection of equation 2.25 shows that only systems with relatively small q (i.e. hydrophilic monomers) and small D_M (due to a "gel" effect or inordinately high interval II W_p) can be significantly affected. Methyl methacrylate may be affected in this way and so no conclusions may be reliably drawn in regard to its exit behaviour.

From figure 2.2 it is clear that only an extremely small $k^1_{p,M}$ could result in significant exit for vinyl neo-decanoate, VnD, while a large $k^1_{p,M}$ would be required (and this is entirely possible) to prevent exit for VAc. The specific case of VAc will be taken up again in section 2.3.1.7. The remaining monomers show marked sensitivity of P_{ex} to $k^1_{p,M}$ in the range one might expect $k^1_{p,M}$ to lie, i.e. $10^2 – 10^4$ M^{-1} s^{-1} and no firm conclusions about their exit behaviour can be drawn without more information.

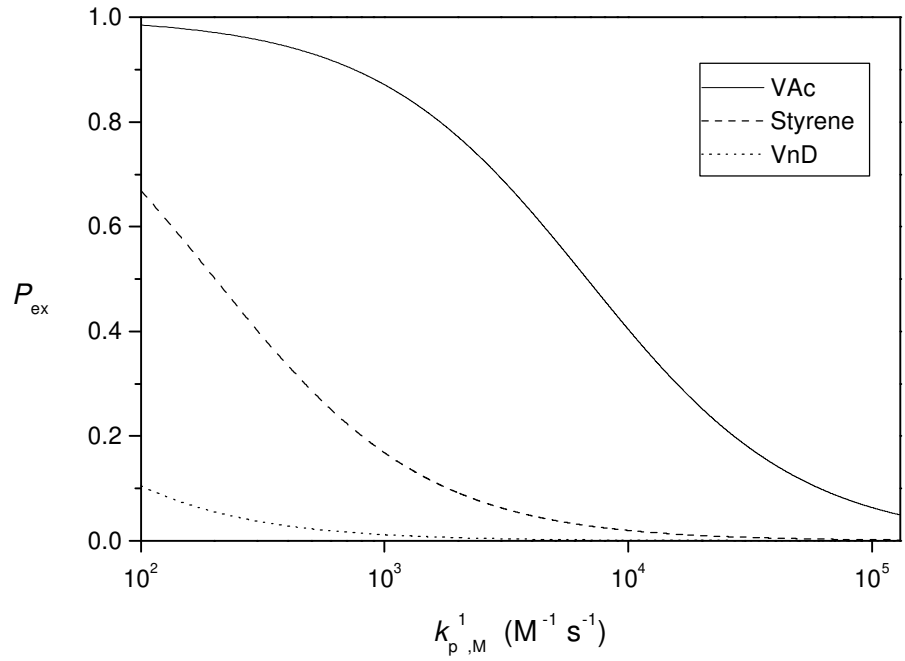

Figure 2.2: P_{ex}, the probability of desorption of $M_{tr}^{\bullet}$, as a function of $k_{p,M}^1$. Calculated from equations 2.23 and 2.26, 120 nm diameter swollen particles, interval II, 50°C.

Theoretical prediction of $k_{p,M}^1$ is fraught with uncertainty and needs to account for steric effects, polarity, resonance stabilisation, nucleophilicity and electrophilicity of the attacking radical and olefinic substrate. As mentioned previously, in many systems the chemical structure of $M_{tr}^{\bullet}$ has not even been identified.

It is possible, when all goes well, to infer values of $k_{p,M}^1$ from kinetic experiments[43]. Also, direct measurements have been made of rate coefficients for the addition of many carbon centred radicals to monomers[56] from which inferences about the magnitude of $k_{p,M}^1$ can be made for some monomers. This is discussed further for the case of VAc in section 2.3.1.7.

2.3.1.2 Branching resulting from transfer to polymer

Transfer to polymer, or even dimer, has little effect on kinetics except in rare instances where the "new" radical is so unreactive (possibly through a combination of resonance stabilisation and steric hindrance) that it is effectively a radical trap awaiting the arrival of another radical with which it may terminate. The main consequence of transfer to polymer is chain branching which commonly occurs in three ways:

(i) Hydrogen may be abstracted from sites on the backbone thereby transferring radical activity and initiating a "long" chain branch:

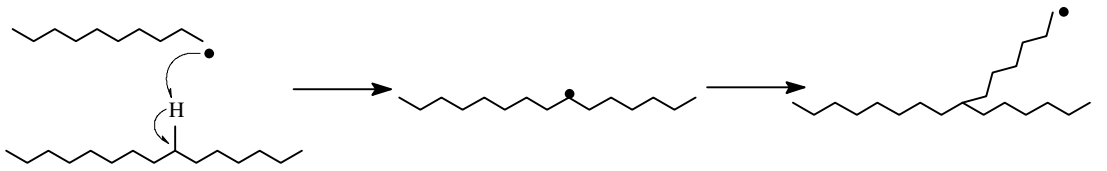

(ii) A hydrogen atom may also be abstracted from a substituent carbon:

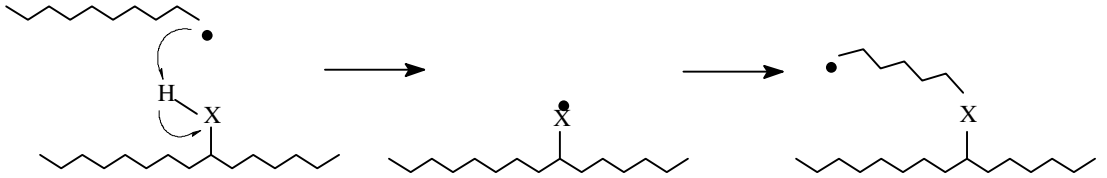

(iii) "Short" chain branches may be formed by intra-molecular atom transfer (backbiting). In this case the propagating radical abstracts a backbone hydrogen from a nearby carbon (typically C5) which then initiates what is technically a "long" branch as in 2.3.1.2(i) above. However, the net result of this mechanism is a "short" chain branch usually two monomer units in length. This reaction is favoured by the high frequency factor associated with the five-membered-ring transition state[57].

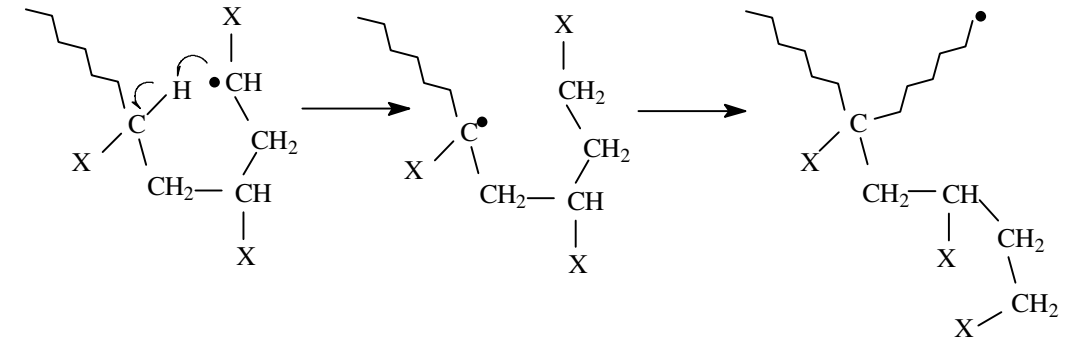

2.3.1.3 Branching resulting from transfer to monomer

(i) The free radical formed by transfer to monomer, $M_{tr}^{\bullet}$, may reinitiate polymerization, thereby forming a chain with an unsaturated end group. This may, in

time, be incorporated into another growing macroradical thereby forming a “long” chain branch.

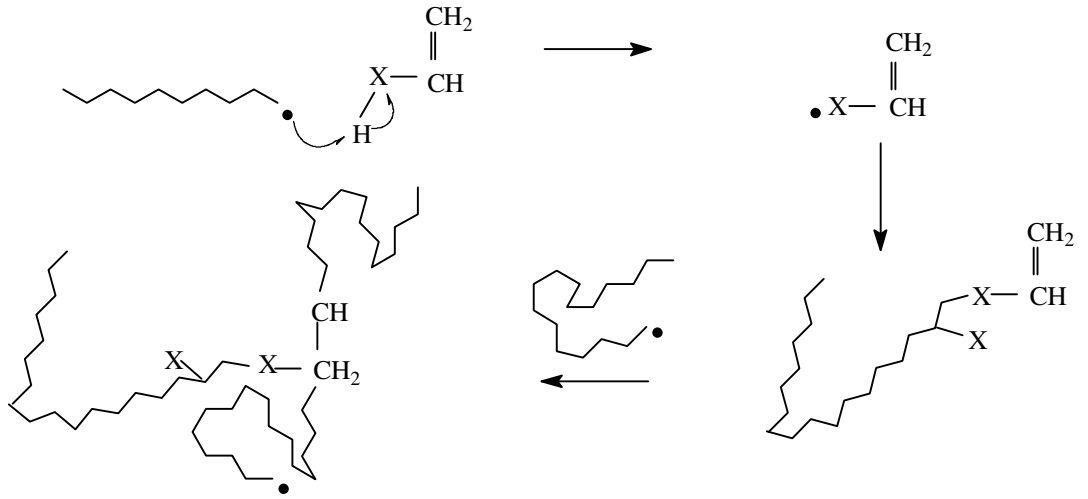

(ii) If $M_{tr}^{\bullet}$ does not reinitiate polymerization rapidly it may undergo bimolecular termination with a macroradical, thereby forming a chain with an unsaturated end group. As in 2.3.1.3(i) above, the terminal double bond may be incorporated into another growing macroradical. However, it may be noted that the connection to the “long” chain branch is likely to be from the substituent to a “head” group rather than the tail addition one would expect in 2.3.1.3(i).

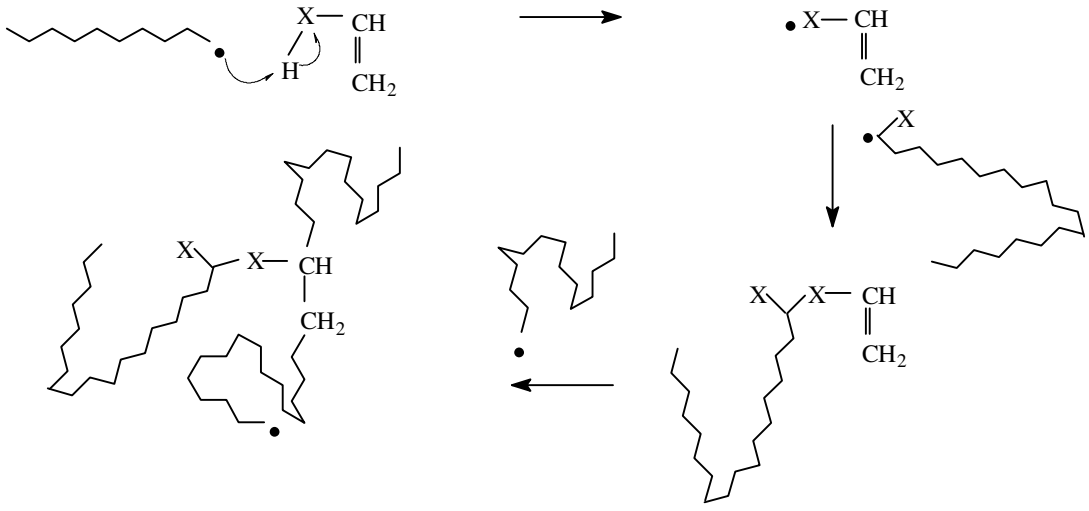

2.3.1.4 High transfer rates in vinyl acetate polymerizations

The high reactivity of the pVAc macroradical is responsible for the high transfer rate coefficients to both monomer and polymer[54] {table II/235}. Based on reactivity rates

towards a range of transfer agents, it has been claimed that the pVAc macroradical is 1500 to 2000 times as reactive as the polystyrene free radical[58,59]. It has been suggested that the high rate of transfer may be at least partly due to the radical formed by "head-to-head" addition[60]. The radical so formed is on a primary carbon atom so it seems likely that the radical should be very reactive. It has also been demonstrated that a high proportion (~20%) of the vicinal diols formed by hydrolysis of pVAc are 2,3-diols[61] as one would expect if the radical formed by "head" addition were active in transfer reactions.

Flory[62,63] showed that, depending on reaction conditions, about 1- 2% of additions in VAc polymerization are head additions. This was determined by the reduction in molecular weight subsequent to hydrolysis and periodate cleavage of the vicinal diols formed therefrom. This finding has been independently confirmed by ^{13}C NMR spectroscopy[64].

Literature values for $k_{tr,M}$ are usually reported as C_M, the ratio of $k_{tr,M}$ to k_p. This is because the method used for their determination (the Mayo method[65]) determines C_M and until quite recently, values for k_p were very uncertain.

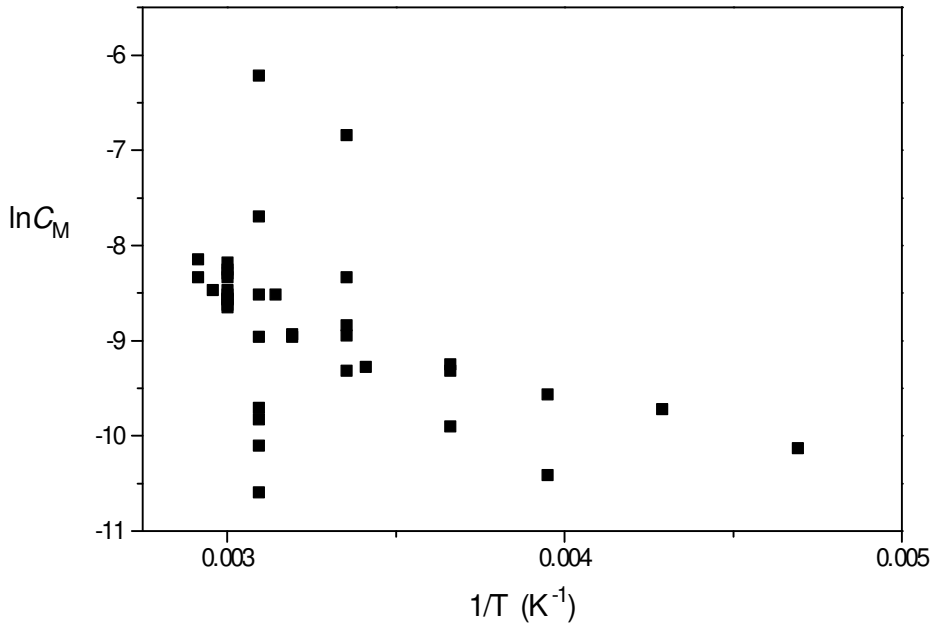

Figure 2.3: Arrhenius plot of literature values of the chain transfer constant to monomer for VAc (C_M)[54].

Although there is a lot of scatter in the literature data the activation energy for transfer to VAc monomer may be estimated as approximately 30 kJ mol^{-1}. This is quite low

compared to that of most other monomers for which it is usually greater than 40 kJ mol^{-1}.

An improved method has been developed to determine rate coefficients for transfer to monomer for a number of monomers[13]. It is called the ln$P(M)$ method and has been applied to VAc as part of this work; the results are presented in chapter 5.

2.3.1.5 Mechanism of transfer to poly(vinyl acetate)

A small point on nomenclature. Throughout the literature, the methyl group of VAc is referred to variously as the *methyl, acetyl, acetoxy* and *acetoxymethyl* group. In this work, the term *acetyl* will be used.

In the case of pVAc, transfer to the acetyl carbon (figure 2.4) has been shown to be a major pathway for transfer[64,66-68]. As the branch is connected to the original chain through an ester linkage, hydrolysis causes branch scission. Upon reacetylation a decrease in molecular weight compared to that before hydrolysis has been interpreted as confirmation of transfer to the acetyl group[69-71]. However, it should be noted that branches formed through the acetyl group may arise through transfer to polymer as above, and/or through transfer to monomer as in 2.3.1.3. Acetyl branches formed by either process are chemically indistinguishable.

Nozakura et al. grafted ^{14}C labelled VAc onto a specially crosslinked pVAc which could be separated from newly formed homopolymer on the basis of vastly different solubilities[72-74]. After separation, de-crosslinking, hydrolysis and reacetylation they claim to have shown that 70% of transfer to polymer is to the backbone α-carbons and 30% to the acetyl carbons. Subsequently, they calculated chain transfer constants to the backbone and the polymer acetyl group from the increase in viscosity average molecular weight of the crosslinked fraction (after de-crosslinking and again after hydrolysis). They found chain transfer constants to the backbone, $C_{p,2} = 3.03\times10^{-4}$, and to the acetyl group, $C_{p,1} = 1.27\times10^{-4}$ at 60°C and $C_{p,2} = 2.48\times10^{-4}$, $C_{p,1} = 0.52\times10^{-4}$ at 0°C. They also claimed that a large number of acetyl branches result from the reaction of the terminal double bond of polymer formed by the mechanism of 2.3.1.3(i) but did not consider 2.3.1.3(ii).

The presence of long chain branches in pVOH, made by hydrolysis of pVAc, shows that branching occurs from the backbone in pVAc[69] since any acetyl branches in the parent pVAc would be hydrolysed during the preparation of the pVOH. Long chain branching is not easily quantified by NMR spectroscopy alone as the branch points are liable to be confused with those of the short branches produced by backbiting.

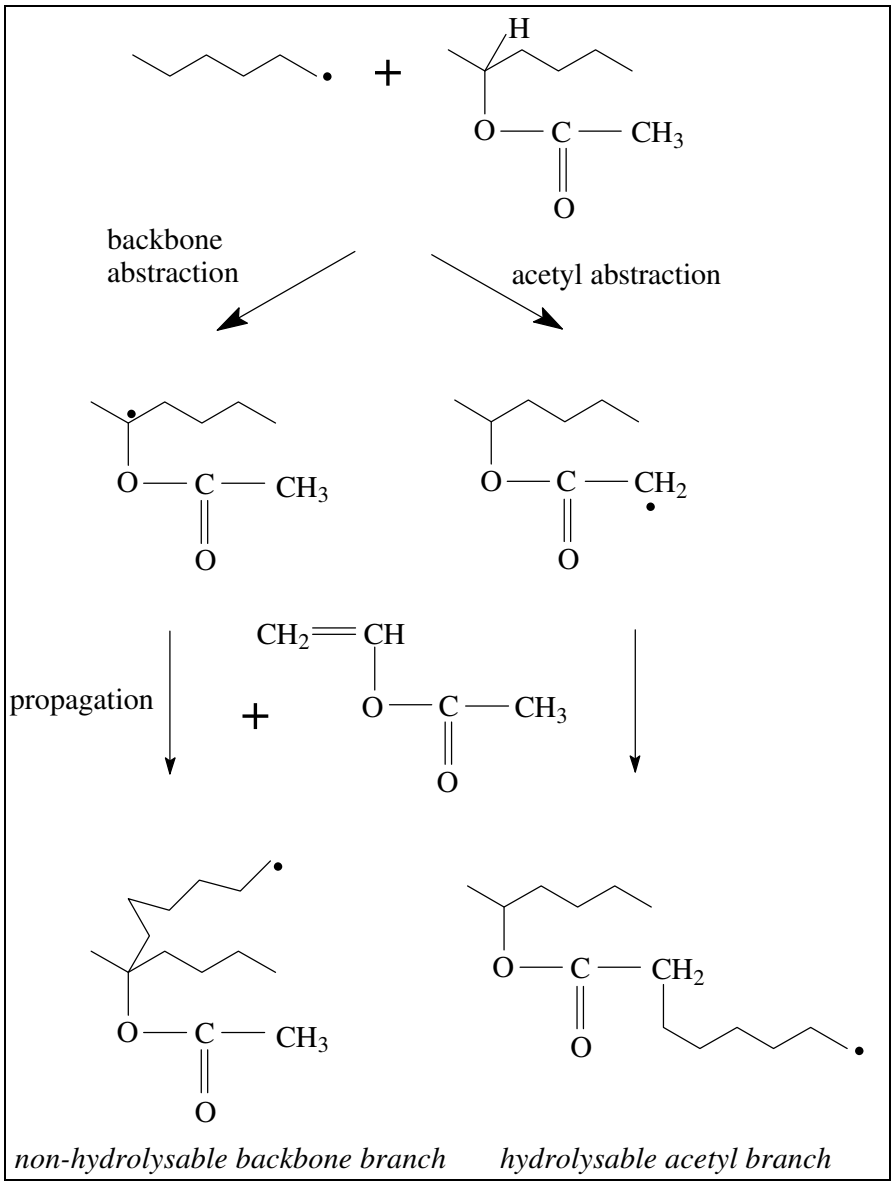

Figure 2.4: Hydrolysable and non-hydrolysable branching in vinyl acetate.

It has also been shown that significant backbiting occurs in the polymerization of VAc[75-77]. Bugada et al.[69] employed ^{13}C and ^{1}H NMR to determine total, i.e. long and short, non-hydrolysable branches and GPC-LALLS to determine long branches. From the difference they claim that ~95% of non-hydrolysable branches in the commercial poly(vinyl alcohols) they studied were short chains resulting from backbiting.

Most recently, Britton et al.[64] have quantified total branching in pVAc as a function of conversion at 60 and 70°C by ^{13}C NMR. Having shown that most, if not all, hydrogen abstraction is due to the pVAc macroradical (as against abstraction by initiator) and that the hydrogen donors are primarily monomer and polymer (with an insignificant

contribution from surfactant) they argue that the quantity of the end group formed by hydrogen abstraction is equivalent to the total number of branch points. They conclude that (*i*) most chain transfer is to the acetyl group, though whether this is primarily to the polymer or monomer is not certain, and (*ii*) that the extent of branching is 0.61 mol% at 60°C and 0.75 mol% at 70°C in emulsion polymerization.

From the above it seems that VAc participates significantly in all modes of transfer available to it. The reported activity of each mode depends on reaction conditions, such as temperature, and the method used to determine the frequency and type of branch involved. Finally, the fate of the transferred radical may also depend on reaction type and conditions. For example, much of the research into transfer rates is done in bulk and solution polymerizations where the kinetics are quite different to those in emulsion polymerizations, due particularly to compartmentalisation, aqueous-phase termination and surface anchoring of entering oligomers. Even within the realm of emulsion polymerizations such variables as particle size and number can have a significant effect on the fate of transferred radicals. The fate of the monomeric free radical formed by transfer, $M_{tr}^{\bullet}$, is particularly important and is considered in the next section.

2.3.1.6 The monomeric vinyl acetate free radical

There is still some debate about the exact nature of $M_{tr}^{\bullet}$. Most researchers[74,78] argue for the abstraction of an acetyl hydrogen given that the vinylic C-H bond is ~50 kJ mol^{-1} stronger than the acetyl C-H bond.

The vinyl radical

Litt and Chang[79] proposed abstraction of a vinylic hydrogen to produce a vinylic free radical which they argue is likely to be relatively unreactive. Their experiments were based on the "isotope effect" whereby it is argued that the rate of transfer to a deuterated carbon is less than that for a hydrogenated carbon. This was ascribed to the greater strength of the carbon-deuterium bond. Bartlett and Tate[80] demonstrated that this was indeed the case for deuterated allyl acetate (CD_2=$CHCH_2OOCCH_3$) wherein both the polymerization rate and molecular weight were increased by a factor of ~2.5 on deuteration of the monomer.

Litt and Chang polymerized VAc, trideuterovinyl acetate and vinyl trideuteroacetate in bulk and in emulsion on a non-deuterated seed. They found that the ratio of the viscosity average molecular weights for poly(trideuterovinyl acetate) to both the pVAc and the poly(vinyl trideuteroacetate) was ~2.5 (reported for the bulk polymerizations only, as presumably the seed would interfere with molecular weight determinations for

the emulsion polymerizations). They also reported the ratio of the polymerization rates for the trideuterovinyl acetate to that of the vinyl acetate and the vinyl trideuteroacetate polymerizations as ~1.75 in both bulk and emulsion. This ratio is quite close to the square root of the ratio found for the molecular weights, as one would expect for the bulk polymerizations if both the polymerization rate and molecular weight are determined by transfer.

One might be prepared to accept that occasional abstraction of a vinylic hydrogen occurs and that this may be a kinetically significant event, perhaps even rate determining. However, in consideration of the large amount of evidence that supports abstraction of acetyl hydrogens, it seems extremely unlikely that abstraction of vinylic hydrogens could be the exclusive mode of transfer to monomer and thus determine the molecular weight as Litt and Chang's deuterated monomer experiments apparently suggest. This appears to be an insurmountable contradiction in Litt and Chang's results.

Clarke et al.[58] have shown that the chain transfer constant for transfer from pVAc to ethyl acetate (the saturated analogue of VAc) is slightly greater than that for VAc. Though this is not proof, it further undermines the proposition that the vinylic α-hydrogen is somehow easily abstracted.

The acetyl radical

Numerous studies of branching discussed in the preceding section have demonstrated the facility of abstraction from the acetyl group in pVAc. Nozakura et al.[74] determined the transfer constant to the monomer acetyl group to be $C_M = 2.26\times10^{-4}$ at 60°C and also, that within experimental error, no transfer to the vinyl carbons of the monomer occurred.

In an exhaustive ^{13}C NMR study, Starnes and Chung[81] prepared samples of pVAc under conditions designed to maximise the number of end groups formed by transfer to monomer (72°C, [AIBN] = 10^{-3} M and low conversion, 4.2%). They then further enhanced the proportion of end groups by sequential partial precipitation, thereby isolating the low molecular weight fraction (M_n ~129,000). A model compound was prepared to determine the exact chemical shifts for the olefinic end group expected to be formed by transfer to the acetyl group and subsequent reinitiation. They succeeded in correlating end group resonances (141.28 & 97.58 ppm) with those of the model compound's terminal double bond (141.24 & 97.58 ppm) and found no resonances which corresponded to those arising from either vinylic abstraction or butyrolactonyl groups (see below).

Finally Starnes and Chung[81] repeated Litt and Chang's[79] crucial "isotope effect" experiment comparing the viscosity average molecular weights obtained from low conversion (8% - 14%) bulk polymerization of VAc and vinyl trideuteroacetate. Their experimental conditions were the same as Litt and Chang's except that polymerization was initiated by AIBN instead of gamma radiolysis. They found that the ratio of the molecular weight of poly(vinyl trideuteroacetate) to pVAc was 2.0. This result proves conclusively that most transfer to monomer is to the acetyl group, as this is the only explanation for the increase in molecular weight resulting from deuteration of the acetyl group. Furthermore, their NMR results (above) strongly support re-initiation by the acetyl radical[81].

The contradictory results of Litt and Chang remain unresolved. Interestingly, the molecular weights found by Starnes and by Litt and Chang for pVAc were nearly the same (± 5%) while Starnes' poly(vinyl trideuteroacetate) and Litt's poly(trideuterovinyl acetate) were also nearly the same (± 10%). The possibility that Litt's student simply mislabelled a bottle cannot be discounted.

The butyrolactonyl radical

Litt et al.[9] have argued that the radical formed by acetyl hydrogen abstraction should cyclize rapidly to form the butyrolactonyl radical:

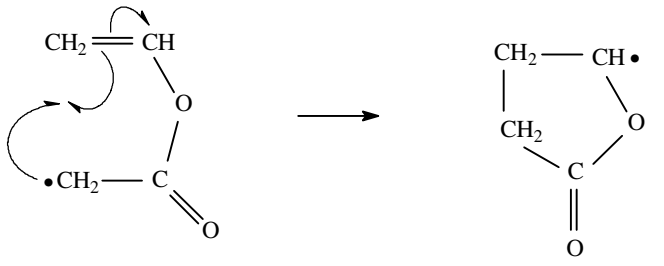

The butyrolactonyl radical was then proposed to partition almost exclusively into the aqueous phase and subsequently terminate with other aqueous-phase radicals. However, several arguments mitigate against (a) its formation and (b) its potential as an aqueous-phase spin trap. The formation of cyclic "endo" radicals such as the butyrolactonyl radical pictured above is not favoured[82] while formation of the otherwise favoured "exo" iso-butyrolactonyl radical is discounted on the grounds of excessive ring strain. Secondly, the butyrolactonyl radical site looks electronically very similar to the normal propagating pVAc macroradical. Hence, it seems likely that $k_{p,M}^{1}$ would be large (~ k_p) and hence, one would expect the butyrolactonyl radical to propagate in the particle or aqueous phase before it could terminate. Finally, as

discussed above, the end groups that would be produced by propagation of, or termination with, the butyrolactonyl radical have been looked for and not seen[81].

2.3.1.7 Exit versus re-initiation for vinyl acetate

As can be seen from equation 2.23 the probability that a monomeric radical will escape from a latex particle is determined by the competition between re-initiation, $k_{p,M}^{1}$, and desorption. There are reasonable arguments for both a low and a high $k_{p,M}^{1}$ for the monomeric VAc free radical, $M_{tr}^{\bullet}$. It is even possible that there are two distinct $M_{tr}^{\bullet}$ resulting from vinylic or acetyl hydrogen abstraction.

On the one hand, vinyl acetate is a relatively unreactive monomer. Rate coefficients towards a range of alkyl radicals are tabulated[60] and show vinyl acetate to be up to 100 times less reactive towards a range of alkyl radicals than are styrene or methyl methacrylate. This is also seen from its reactivity ratios with other common monomers (table 2.3).

Table 2.3: Reactivity ratios for vinyl acetate with common monomers at 50°C. r_1 is the ratio of the rate coefficient for homoaddition to that of heteroaddition for a macroradical terminating with a vinyl acetate unit. r_2 is the ratio of the rate coefficient for homoaddition to that of heteroaddition for a macroradical terminating with the comonomer.[54,83]

comonomer	r_1	r_2
styrene	0.05	50
acrylamide	0.004	8.25
butyl acrylate	0.018	3.48
acrylic acid	0.021	8.66
acrylonitrile	0.06	5.51
2-chlorobutadiene	0.0	33.52
butyl methacrylate	0.0	30.18
methyl methacrylate	0.0	30
itaconic acid	0.053	31
vinyl neo-decanoate	0.99	0.92

Despite the low reactivity of the monomer, VAc is possessed of a very high polymerization rate. This suggests that for some reason (polar, steric, electrophilicity

or whatever) the pVAc macroradical is exceptionally reactive towards VAc monomer and therefore it is possible that $k_{p,M}^{1}$ could be significantly smaller than k_p.

On the other hand, reactivity ratios of VAc with alkyl monomers such as ethene and butadiene are close to unity and this suggests that the pVAc macroradical is not alone in its high reactivity towards VAc monomer. Furthermore, it has been shown[84] that the substituent on the acetyl radical presumed to be formed by transfer to VAc, (RO_2C-), causes a minimal decrease in spin density on neighbouring carbon centred radicals which implies minimal delocalization of the acetyl radical. Therefore, from the foregoing argument it seems possible that the acetyl radical could be very reactive towards VAc momomer.

The competing arguments above seem to have been resolved by the recent work of Wu, Beranek and Fischer[56] in an ESR study wherein they determined the absolute rate coefficient for the addition of (*tert*-butoxy)carbonylmethyl radicals to a range of alkenes, including VAc and many of the common monomers. They give the following Arrhenius constants for addition of (*tert*-butoxy)carbonylmethyl radicals to VAc: frequency factor = $10^{8.1 \pm 0.3}$ M^{-1} s^{-1} and activation energy = 18.5 ± 3.6 kJ mol^{-1}. The (*tert*-butoxy)carbonylmethyl radical, shown below, is very similar to the acetyl radical and it seems reasonable to apply Wu's rate coefficient to $k_{p,M}^{1}$ (the rate coefficient for the reinitiation reaction one expects in the free-radical polymerization of VAc).

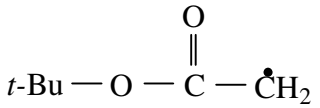

(tert-butoxy)carbonylmethyl radical

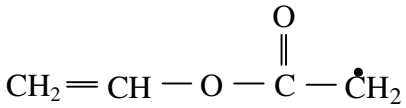

vinyl acetate-derived acetyl radical

If this were the case then $k_{p,M}^{1}$ = 128,000 M^{-1} s^{-1} at 50°C and from figure 2.2 it can be seen that $M_{tr}^{\bullet}$ has a low probability of escape.

2.4 Termination

The ultimate rate-determining process in free-radical polymerizations is the termination mechanism. In zero-one emulsion polymerizations termination is controlled by compartmentalisation and depends on entry and exit (which in turn depend on transfer, initiator efficiency and aqueous-phase solubility as described above). In pseudo-bulk emulsion polymerizations termination rates are governed by diffusion rates. For this reason, various modes of diffusion are described below.

A growing chain may be terminated by transferring radical activity, or as a consequence of combination (equation 2.27) or disproportionation (equation 2.28) with another radical:

$$R_i + R_j \xrightarrow{k^{c}_{t,ij}} P_{i+j} \qquad 2.27$$

$$R_i + R_j \xrightarrow{k^{d}_{t,ij}} P_i + P_j \qquad 2.28$$

where $k^{c}_{t,ij}$ and $k^{d}_{t,ij}$ are the rate coefficients for termination by combination and disproportionation respectively. Whether combination or disproportionation dominates has an obvious effect on molecular weight distributions but little or no effect on the kinetics so, for the purposes of this discussion, the generic bimolecular termination rate coefficient, $k_{t,ij}$, will be used.

2.4.1.1 The Smoluchowski equation

The Smoluchowski equation for diffusion controlled reactions, equation 2.18, may be modified to give:

$$k_{t,ij} = 2\pi p_{ij} D_{ij} (r_i + r_j) N_A \qquad 2.29$$

where p_{ij} is the probability that two radicals, an i-mer and a j-mer, will react if they approach to within the reaction radius, which is taken as the sum of the reactive radii of the radicals ($r_i + r_j$) and D_{ij} is the mutual diffusion coefficient of the radicals. The factors that contribute to these parameters are discussed in the following subsections.

2.4.1.2 Spin multiplicity factor

p_{ij} is dependent on spin multiplicity, viscosity and steric hindrance. The spin multiplicity factor is due to the fact that when two radicals are brought together there is only a ¼ chance that the lone electrons will have opposite spin and be able to combine instantly[13]. In some instances, such as at high W_p, diffusion may become so slow that the radicals remain within the reactive radius long enough for their electron spins to "flip" in which case p_{ij} may be close to 1. On the other hand, steric hindrance at the reaction site may reduce p_{ij} below ¼.

2.4.1.3 Reaction radius

In rubbery systems where termination is dominated by "short-long" termination the reaction radius, ($r_i + r_j$) can be approximated by the Lennard-Jones diameter of the monomer, σ, which is typically ~ 6 Å[48]. In pseudo-bulk systems where "short-long"

termination is not necessarily the dominant mode of termination, the reaction radius may be much larger, due to segmental diffusion[13,48].

Russell et al.[48] describe a bulk (or pseudo-bulk) termination process wherein the "dangling" end of an entangled macroradical, from the ultimate node of entanglement to the chain end, is free to move by configurational rearrangements. As such rearrangements are much faster than propagation steps, the radical samples a volume between propagation events that depends on the length of the flexible portion of the macroradical, denoted by J (monomer units) and the interval between propagation steps. This is the segmental diffusion process alluded to above.

It is impossible to quantify J with any certainty, but it seems reasonable to argue that the length of the dangling chain end should be approximately proportional to the entanglement spacing.

Typical values of J for common polymers are given by Bueche[85] (100 – 380) and by Ferry[86] (59 – 350) with pVAc in the middle of the range at 260. Assuming that the average length of the dangling chain is about half the entanglement spacing, then in pure polymer the length of the dangling chain is of the order of 100 monomer units and, as shown below, substantially more at lower W_p. Russell[48] gives the individual reactive radii as:

$$r_i = aJ^{½} \qquad 2.30$$

where a is the characteristic unit length of a coiled polymer chain, i.e. the root mean square end-to-end distance per square root of the number of monomer units in a polymer chain and hence, r_i is the root mean square end-to-end length of the dangling chain segment. For vinyl and acrylic polymers a is given by:

$$a = 2\omega_{steric}\alpha l \qquad 2.31$$

where ω_{steric} is the steric expansion factor, typically about 2 for small repeat units, α is the solvent expansion factor which, for polymer that is soluble in its own monomer, is usually slightly greater than 1, and l is the carbon – carbon bond length in the polymer backbone. Hence a is about 7Å and this gives r_r a value of about 140 Å in the limit of pure polymer.

However, the dependence of r_r on J must take into account more than just the unperturbed chain dimensions of the dangling chain segments. r_r would also be expected to depend on the mobility of the dangling chain segment (which will decrease

with viscosity and consequently with increasing conversion) and the time available for segmental diffusion (i.e. the time between propagation events which will increase with conversion). Furthermore, J itself will depend on conversion.

The dependence of J on the weight fraction of polymer, W_p (w/v), is given as:

$$J = J_0/W_p \qquad 2.32$$

where J_0 is the entanglement spacing for pure polymer[85]. During interval II, W_p is typically about 0.3, hence the (vinyl acetate) dangling chain is likely to be about 400 monomer units in length. Blind application of equation 2.30 then gives r_i = 140 Å and hence r_r = 280 Å. However, this is clearly not possible in a rubbery system. If the time interval between propagation events was sufficient for the dangling chain-end radical to sample such a large portion of the particle (~1/8th) then the much more rapidly diffusing $M_{tr}^{\bullet}$, from which the macroradical must have grown, would have terminated rapidly and the macroradical would not exist.

It can be seen then, that r_r may be many times greater than the Lennard-Jones diameter of the monomer. However, given the above uncertainties, all that can be said about its dependence on W_p is that r_r would be expected to decrease with increasing W_p.

2.4.1.4 Diffusion coefficient for short-long termination

D_{ij} is the mutual diffusion coefficient of the radical ends. Scheren et al.[87] have shown that nearly all termination in pseudo-bulk emulsion polymerization of styrene is between a "long" chain and an "i-meric" radical where $i \leq 10$. Similar considerations to those discussed in section 2.2.1.2 allow the simplifying assumption for rubbery systems that $D_{ij} \approx D_i$ where i,j are the degrees of polymerization of the "short" and "long" chains respectively. The diffusion rate of i-mers, D_i, is chain length dependent and this must be taken into account when attempting to estimate the "zero-oneness" of emulsion polymerizations.

Griffiths et al.[88] have shown that an approximate "universal" scaling law can be applied to the dependence of diffusion rates of i-mers over the range $0.1 \leq W_p \leq 0.4$ which includes the interval II value of W_p for several monomer/polymer systems:

$$\frac{D_i(W_p)}{D_{mon}(W_p)} = i^{-(0.664 + 2.02W_p)} \qquad 2.33$$

Thus it is possible to estimate the zero-oneness of a given system for three cases of interest kinetically; (i) entry of an initiator-derived oligomeric radical (a z-mer) into a

"live" particle, (ii) entry of an exited $M_{tr}^{\bullet}$ into a "live" particle and (iii) formation of $M_{tr}^{\bullet}$ in a particle containing two radicals.

2.4.1.5 Diffusion rates and zero-oneness

There are two aspects of "zero-oneness" to consider. The first is the probability that a radical that enters a "live" particle, or is formed by chain transfer to monomer in a particle containing two radicals, is prevented from exiting that particle. The processes that prevent exit are "instantaneous" termination and propagation to a *2*-mer, as desorption is negligible for *i*-mers where $i \geq 2$. The second aspect is the probability that short-long termination occurs before the *i*-mer becomes a macroradical itself, whereupon centre-of-mass diffusion becomes very slow and bimolecular termination with another macroradical becomes dependent on reaction diffusion (section 2.1.1.3).

If the entering radical is a *z*-mer the probability of desorption is negligible (by definition). If the entering radical is $M_{tr}^{\bullet}$ then, from the foregoing discussion, it can be seen that the probability of escape from a "live" particle, P_e, is given by:

$$P_e = \frac{k_{dM}}{k_{dM} + k_{t,ij}[R_j] + k_{p,M}^{1} C_p} \qquad 2.34$$

In this case $k_{t,ij}$ is the termination rate coefficient for a monomeric radical and a macroradical which, from equation 2.29, is about 6×10^8 M^{-1} s^{-1} for radicals which are not sterically hindered ($p_{ij} = ¼$, $r_s = 60$ nm, 50°C, $r_i + r_j = 6$ Å). The macroradical concentration, $[R_j]$ is given by:

$$[R_j] = 1/N_A V_s \qquad 2.35$$

where V_s is the volume of a swollen particle and k_{dM} may be calculated from equation 2.25. The dependence of P_e on $k_{p,M}^{1}$ can then be calculated and is presented in figure 2.5.

From figure 2.5 it is clear that, for any reasonable value ascribed to $k_{p,M}^{1}$, a VnD $M_{tr}^{\bullet}$ will remain in the particle in which it was created. On the other hand, for VAc if $k_{p,M}^{1}$ is low ($<<k_p$) the probability of escape approaches one. This could be the case, as argued by Litt and Chang for the radical produced by vinylic abstraction[79]. However, if Wu's rate coefficient for the (*tert*-butoxy)carbonylmethyl radical is applied to $k_{p,M}^{1}$ for VAc, then the probability of escape is very small.

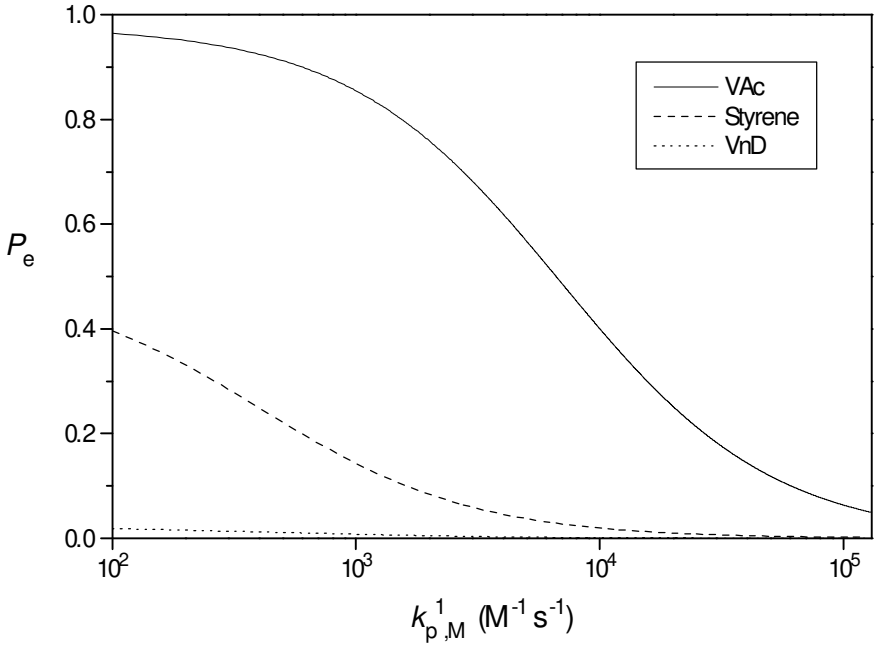

Figure 2.5: Probability that $M_{tr}^{\bullet}$ escapes from a "live" particle as a function of $k_{p,M}^1$, calculated from equation 2.34, 120 nm diameter swollen particle, interval II, 50°C.

2.4.1.6 Short-long versus long-long termination

Consideration of the rates of the competing termination mechanisms, below, shows that long-long termination may dominate in low $\bar{n}$ systems with high k_p and $k_{p,M}^1$. Furthermore, if the dependence of the rate coefficient for reaction/segmental diffusion is taken into account, then R_p is seen to have only a weak dependence on C_p.

The probability, P_m, that a *2*-meric radical, in a particle containing a macroradical, attains a degree of polymerization, m, (where $m < i_{ent}$) without terminating with the "resident" macroradical, is given by the following equation:

$$P_m = \prod_{i=2}^{m} \frac{k_p^i C_p}{k_{t,ij}[R_j] + k_p^i C_p} \qquad 2.36$$

For many monomers, limiting behaviour is easily seen before a degree of polymerization of 50 is reached (figure 2.6).

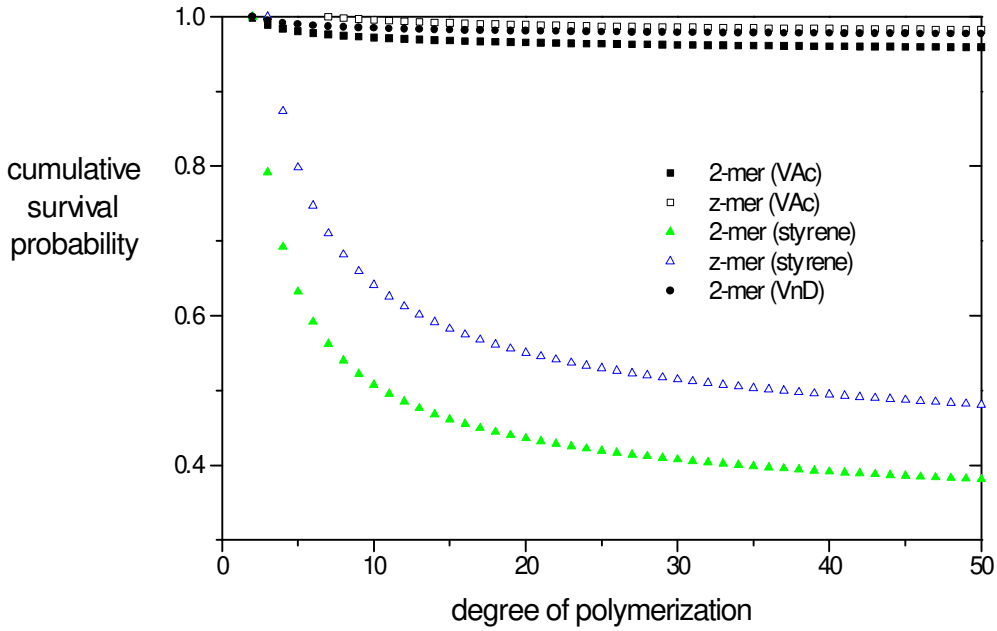

Figure 2.6: Probability that a radical, which enters and propagates in a particle containing a macroradical, grows to a degree of polymerization *i*, without terminating. Calculated from equation 2.36 for 120 nm diameter swollen particles, interval II, 50°C.

As can be seen in figure 2.6, a styrene monomeric radical is quite likely to terminate with a resident macroradical before it grows to a sufficient length to cause entanglement, in accord with the assertion of Scheren et al.[87], that radical loss in such systems is dominated by short-long termination. However, VAc and VnD can be seen to have a high probability of growing to a sufficient length to cause entanglement, primarily because k_p for these monomers is much greater than for styrene.

In intervals II and III, W_p is such that the polymer concentration is always greater than c**, the concentration of polymer above which polymer chains are entangled. Hence, in emulsion polymerizations, once a radical has grown to a sufficient degree of polymerization, i_{ent}, it will become entangled. Russell et al.[48] have shown that the diffusion coefficient for reaction diffusion, D^{rd}, (section 2.1.1.3) is much greater than the diffusion coefficient for centre of mass diffusion for entangled polymers. Hence, diffusion of the radical end of an entangled macroradical will be primarily by reaction/segmental diffusion and D_{ij} is replaced, for $i,j > i_{ent}$, by D^{rd}.

Hence, equation 2.29 may be re-written, for $i,j > i_{ent}$:

$$k_{t,ij}^{rd} = 2\pi p_{ij} 2D^{rd}(r_i + r_j)N_A \qquad 2.37$$

The spin multiplicity factor, p_{ij}, is likely to be close to one as the radicals probably remain within a reactive radius long enough to spin-flip. D^{rd} is multiplied by 2 to account for the contribution to mutual diffusion from both long chains.

Russell et al.[48] give D^{rd} as:

$$D^{rd} = \frac{1}{6} k_p C_p a^2 \qquad 2.38$$

where a is the characteristic length described above. D^{rd} (in interval II at, for example, 50°C) ranges from 1.3×10^{-12} cm^2 s^{-1} for styrene to 5×10^{-11} cm^2 s^{-1} for VAc. These are actually upper limits for D^{rd} as it obviously decreases with decreasing C_p and with decreasing k_p at conversions beyond the glass transition, where applicable.

Combining equations 2.37 and 2.38, and noting that, for reaction diffusion, $r_r = 2r_i$ the long-long termination rate coefficient is given by:

$$k_{t,ij}^{rd} = \frac{8\pi a^2 N_A k_p}{6} C_p r_i \qquad 2.39$$

This gives the interesting result that $k_{t,ij}^{rd} \propto C_p r_i$ to which the discussion will return below.

The cumulative probability of termination for entangled chains is given by:

$$P_m^{rd} = \prod_{i=i_{ent}}^{m} \frac{k_p^i C_p}{k_{t,ij}^{rd}[R_j] + k_p^i C_p} \qquad 2.40$$

where i_{ent} is the degree of polymerization at which entanglement is deemed to occur.

For VAc, D^{rd} was calculated as 5×10^{-11} cm^2 s^{-1} using equation 2.38, $k_p = 6.7\times10^3$ M^{-1} s^{-1}, $a = 7$Å and $C_p = 7.7$ M (interval II, 50°C, section 2.2.1.2). Evaluating equation 2.40 for VAc shows that the cumulative probability of termination is insensitive to i_{ent}. Varying i_{ent} from 100 to 400 makes less than 1% difference in the cumulative probability of termination occurring (before a molecular weight of 10^6 is reached). This can be explained qualitatively as follows. The mobility of the short radical is so reduced before it has attained a degree of polymerization of 100, that it is unlikely to terminate in the period of the subsequent few hundred propagation events, by which time the macroradical will be entangled. Although k_t is much reduced by

entanglement, long-long termination has a much longer timescale in which to effect termination.

However, P_m^{rd} is sensitive to the value assigned to $r_r = r_i + r_j = 2r_i$. As discussed in section 2.4.1.3, the reactive radius is likely to be much greater than the Lennard-Jones diameter (~6 Å). The dependence of P_m^{rd} on r_i for VAc is demonstrated in figure 2.7 where it can be seen that for $r_i = 30$ Å termination by reactive/segmental diffusion is approximately equivalent in importance to short-long termination and for $r_r > 30$ Å long-long termination dominates.

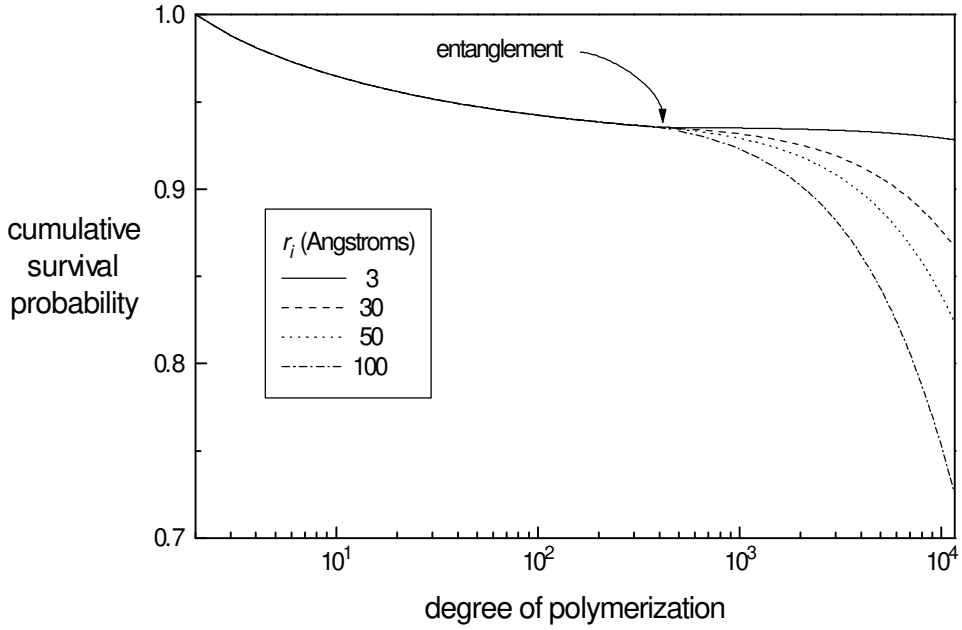

Figure 2.7: Probability that a VAc $M_{tr}^{\bullet}$, which enters and propagates in a particle containing a macroradical, grows to a degree of polymerization *i*, without terminating, as a function of the reactive radius. Calculated from equation 2.40 for 120 nm diameter swollen particles, interval II, 50°C.

Recalling that $k_{t,ij}^{rd} \propto C_p r_i$ and that as r_i decreases with C_p it is possible that $k_{t,ij}^{rd}$ may have an approximately 2nd order dependence on C_p. There is no exact solution to zero-one-two kinetics yet; however, as similar kinetic mechanisms, such as the pseudo-bulk give $R_p \propto C_p k_t^{-0.5}$ then if $k_t \propto C_p^2$ for VAc emulsion polymerizations, R_p may be independent of C_p. This proposition was tested by modelling the complete Smith-Ewart equations, the results are presented in section 2.5.3.

2.5 Modelling Vinyl Acetate Emulsion Polymerization

2.5.1 Introduction

From the foregoing discussion of emulsion polymerization kinetics it can be seen that, for VAc, transfer to monomer is the crucial kinetic event. Furthermore, the value of the rate coefficient for re-initiation, $k_{p,M}^{1}$, is critical to the kinetics. As discussed in section 2.3.1.7, $k_{p,M}^{1}$ is not known and there are reasonable arguments for both high (~10^5 M^{-1} s^{-1} at 50°C) and low (<10^3 M^{-1} s^{-1} at 50°C) values of this critical parameter. The large value, supported as it is by (*i*) direct measurement of the rate coefficient for addition of a model compound to VAc[56] and (*ii*) Starnes' NMR evidence for re-initiation by the acetyl radical[81] seems the more reliable one; however, the possibility of a kinetically significant small $k_{p,M}^{1}$, due perhaps to the occasional abstraction of a vinylic hydrogen, can not be ignored.

Therefore, models for VAc emulsion polymerization fall into two categories: low $k_{p,M}^{1}$ models whose behaviour is dominated by zero-one kinetics and high $k_{p,M}^{1}$ models which, it will be seen, are best described by zero-one-two kinetics. These regimes are discussed in the following subsections.

A good starting point for modelling is a brief summary of the behaviour of VAc in emulsion polymerizations:

(i) most radical transfer to monomer is to the acetyl group, though the possibility remains that the kinetically important transfer is to the vinyl group.

(ii) if $k_{p,M}^{1}$ is small (substantially less than k_p ~ 6.7×10^3 M^{-1} s^{-1} at 50°C[33]) then most $M_{tr}^{\bullet}$ will escape the particle in which they were formed (figure 2.2).

(iii) if $k_{p,M}^{1}$ is very small, less than about 10^3 M^{-1} s^{-1} at 50°C, then exited $M_{tr}^{\bullet}$ may enter and exit many particles, including "live" particles, before terminating or propagating (figure 2.5). This results in a special case of zero-one kinetics where, on entering a "live" particle, $M_{tr}^{\bullet}$'s will terminate with another radical, or exit, before they can propagate.

(iv) as k_p is large, *z*-mers will follow zero-one-two kinetics (figure 2.6).

(v) if $k_{p,M}^{1}$ is large (> k_p), then $M_{tr}^{\bullet}$ will usually reinitiate in the particle in which it was created (figure 2.5).

2.5.2 Zero-one kinetics

The time evolution equations for zero-one kinetics are a trivial subset of the complete Smith-Ewart equations[89], namely:

$$\frac{dN_i}{dt} = \rho[N_{i-1} - N_i] + k[(i+1)N_{i+1} - iN_i] + c[(i+2)(i+1)N_{i+2} - i(i+1)N_i] \qquad 2.41$$

where N_i is the number of particles containing i radicals, ρ is entry rate of propagating radicals per particle, k is the rate of exit per free radical and c is the termination rate coefficient. In this case ρ is the sum of ρ_{init} - the entry rate of initiator-derived radicals described in section 2.1.1.2, ρ_{th} - a usually small but non-negligible contribution from radicals derived by thermal homolysis of species other than the initiator and $\rho_{re\text{-}entry}$ - the contribution from exited radicals that re-enter and propagate. These equations are non-linear (because ρ, k and c are interdependent) and only have analytical solutions for special cases where certain simplifying assumptions are made, particularly concerning the fate of $M_{tr}^{\bullet}$ and the dominant mode of termination. Where the dominant mode of termination is chain-length dependent the Smith–Ewart equations do not hold.

One case that does avail itself of an analytical solution is that of complete termination of the transferred radical. For emulsion polymerizations that follow zero-one kinetics a particle may contain either one or zero radicals. When a second radical enters a particle it must terminate with the resident radical on a faster timescale than the other events that affect $\bar{n}$, namely entry and exit. If the population concentrations of such particles are denoted N_{c1} and N_{c0} respectively, then the total particle number concentration, $N_c = N_{c1} + N_{c0}$ and $N_1 = N_{c1}/N_c$ and $N_0 = N_{c0}/N_c$ are the normalised populations. The average number of radicals per particle, $\bar{n}$ is then given by N_1.

The time evolution of the population of particles containing one radical is:

$$\frac{dN_1}{dt} = \rho N_0 - \rho N_1 - kN_1 \qquad 2.42$$

Assuming constant N_c then the time evolution of $\bar{n}$ is given by:

$$\frac{d\bar{n}}{dt} = \rho(1-2\bar{n}) - k\bar{n} \qquad 2.43$$

If one makes the further assumption that exit is primarily due to desorption of the monomeric free radicals created by transfer, $M_{tr}^{\bullet}$, (and not some adventitious chain transfer agent) then it is possible to estimate k by examining physically reasonable limiting cases for the fate of the exiting radicals.

In the particular case of VAc, entry of a *z*-mer into a "live" particle results in that particle containing two macroradicals which are unlikely to co-terminate (see figure 2.6). However, in VAc emulsion polymerizations $\bar{n}$ is small and transfer to monomer is rapid. Consequently, if $k^{1}_{p,M}$ is small, transfer will be followed by rapid termination or exit and subsequent termination so the system will follow zero-one kinetics. Therefore, the number of particles with two radicals will be negligible.

There are two postulated mechanisms consistent with the observed kinetics[13] - Gilbert's limits 1 and 2b (see figure 2.8). These limits require that the system be zero-one and, in effect, require $k^{1}_{p,M}$ to be small. The attraction of these limiting cases is, as shown below, that the most perplexing aspect of VAc emulsion polymerization, i.e. the zero-order dependence of R_p on conversion, is explained simply and without recourse to any adjustable parameters.

In limit 1, the radical formed by chain transfer to monomer, $M^{\bullet}_{tr}$, always exits the particle and terminates in the aqueous phase with another non-initiating radical species. Hence, $k = k_{tr,M}C_p$ and the time evolution of $\bar{n}$ is given by:

$$\frac{d\bar{n}}{dt} = \rho(1-2\bar{n}) - k_{tr,M}C_p\bar{n} \qquad 2.44$$

where $\rho = \rho_{init} + \rho_{th}$, $k_{tr,M}$ is the rate coefficient for transfer to monomer and C_p is the monomer concentration in the latex particles.

In limit 2b, $M^{\bullet}_{tr}$ re-enter and exit dead particles until they enter a live particle and terminate, thereby eliminating two radicals. Hence, in limit 2b, the time evolution of $\bar{n}$ is given by:

$$\frac{d\bar{n}}{dt} = \rho(1-2\bar{n}) - 2k_{tr,M}C_p\bar{n} \qquad 2.45$$

Both limits require that most $M^{\bullet}_{tr}$ exit the particle and terminate before they can propagate.

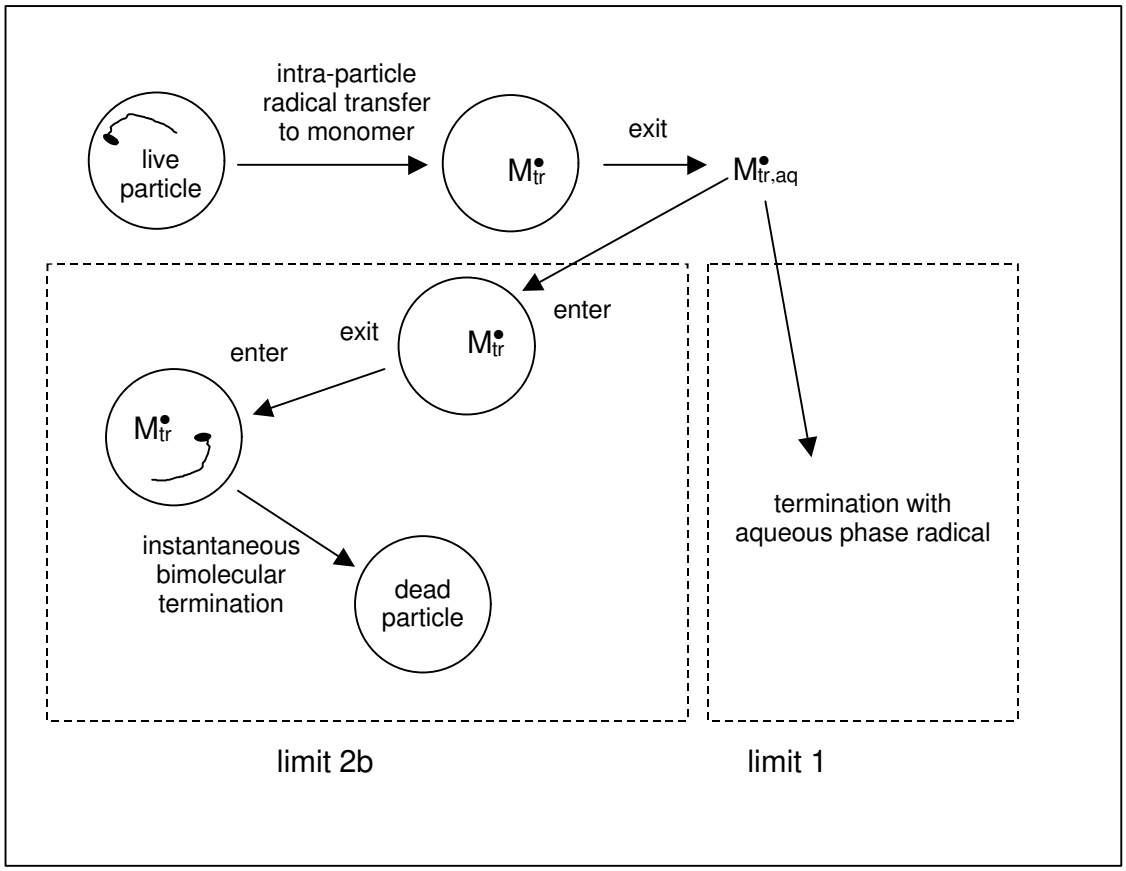

Figure 2.8: Limits 1 and 2b

At steady state:

$$\frac{d\bar{n}}{dt} = 0 \qquad 2.46$$

Hence, for limit 1:

$$\bar{n} = \frac{\rho}{2\rho + k_{tr,M}Cp} \qquad 2.47$$

and for limit 2b:

$$\bar{n} = \frac{\rho}{2\rho + 2k_{tr,M}Cp} \qquad 2.48$$

In VAc emulsion polymerizations $\bar{n}$ is usually very low (<0.1) so $\rho << k_{tr,M}C_p$. Hence, for limit 1:

$$\bar{n} \approx \frac{\rho}{k_{tr,M}C_p} \qquad 2.49$$

Similarly for limit 2b:

$$\bar{n} \approx \frac{\rho}{2k_{tr,M}C_p} \qquad 2.50$$

The general rate equation for emulsion polymerizations is

$$R_p = C_p\bar{n}k_pN_c/N_A \qquad 2.51$$

where R_p is the rate of polymerization, $\bar{n}$ is the average number of radicals per particle, k_p is the propagation rate coefficient and N_c is the particle number concentration.

Combining equations 2.49 & 2.51 we have for limit 1:

$$R_p = \rho\frac{k_pN_c}{k_{tr,M}N_A} \qquad 2.52$$

Similarly for limit 2b:

$$R_p = \rho\frac{k_pN_c}{2k_{tr,M}N_A} \qquad 2.53$$

Thus the independence of conversion rate from monomer concentration can be explained if either of these limiting cases apply to the emulsion polymerization of VAc. The key point is that most transfer to monomer must lead to exit and subsequent termination to satisfy equations 2.44 & 2.45.

However, when these models are applied (assuming a low $k_{p,M}^{1}$, 100% initiator efficiency, and using the literature values for k_p and $k_{tr,M}$) the calculated R_p is lower than the experimental R_p (section 4.3) by about a factor of ten. Consideration of equations 2.52 and 2.53 shows that $R_p \propto \rho$ and $R_p \propto 1/k_{tr,M}$ whereupon two possible explanations are apparent.

(*i*) The kinetically significant transfer (possibly abstraction of a vinylic hydrogen) occurs about $1/10^{th}$ as often as the normal abstraction of an acetyl hydrogen.

(*ii*) The induced decomposition of persulfate, described in section 2.1.2.1, produces about ten times as many radicals as normal thermal decomposition of persulfate.

The initial aims of this project were to test these models by measuring radical-loss rates directly with the γ relaxation experiments described in chapter 3 and to

investigate the mechanism of induced decomposition of persulfate as described in chapter 4.

2.5.3 Zero-one-two kinetics

Vinyl acetate, is expected to follow pseudo-bulk kinetics if $k_{p,M}^{1}$ is large (> k_p) as the probability of escape from a "live" particle is small (see figure 2.5) and the probability of propagating to a macroradical in a particle containing two radicals is large (figure 2.6). As VAc emulsion polymerizations are always low $\bar{n}$ systems, this implies the special pseudo-bulk case called zero-one-two kinetics. As noted by Gilbert[13] the exact solution of the zero-one-two case requires that both compartmentalisation and chain length dependence of termination must be taken into account.

Extensions to zero-one-two-three kinetics are not required as, for a low $\bar{n}$ system, which VAc invariably is, N_2 will be small and N_3 will be negligible. Therefore, $\bar{n}$ is given by:

$$\bar{n} = N_1 + 2N_2 \qquad 2.54$$

Hence, for constant N_c:

$$\frac{d\bar{n}}{dt} = \frac{dN_1}{dt} + 2\frac{dN_2}{dt} \qquad 2.55$$

The time evolution of the radical population (ignoring N_3 and higher and making the simplifying assumption that c is independent of chain length) is given by:

$$\frac{dN_1}{dt} = \rho[N_0 - N_1] + k[2N_2 - N_1] \qquad 2.56$$

$$\frac{dN_2}{dt} = \rho N_1 - 2kN_2 - cN_2 \qquad 2.57$$

where $\rho = \rho_{init} + \rho_{th} + \rho_{re\text{-}entry}$, c is the pseudo-first order termination rate coefficient and $k = k_{tr}C_pP_{ex}$ is the rate of exit per free radical (P_{ex} given by equation 2.23). c will be nearly independent of chain length if most termination is long-long as discussed in section 2.4.1.6 and $W_p > c^{**}$, which is always the case in interval II and III.

Hence, the generalised Smith-Ewart equation for pseudo-bulk kinetics simplifies for zero-one-two kinetics to:

$$\frac{d\bar{n}}{dt} = \rho[N_0 - N_1] + k[2N_2 - N_1] + 2[\rho N_1 - 2kN_2 - cN_2] \qquad 2.58$$

From figure 2.6 it can be seen that VAc has a small probability (~5%) of short-long termination. However, it is well known that VAc emulsion polymerizations are invariably low $\bar{n}$ systems ($\bar{n} < 0.1$). Therefore, there must be a rapid radical-loss mechanism that increases the termination rate in the particles and/or the aqueous phase.

As shown in section 2.1.2.2 entry efficiency is expected to be nearly 100% unless $k_{p,aq}^{i}$ is very much lower than k_p. This may be the case as the effect of a polar solvent on k_p of a polar monomer is not known. Another factor that may affect the aqueous-phase kinetics of VAc is induced decomposition of persulfate. This is discussed in detail and modelled in chapter 4 where it is shown that, at the persulfate concentrations used in emulsion polymerizations, the increase in the aqueous-phase radical concentration due to the induced decomposition of persulfate is insufficient to significantly affect entry efficiency.

It has been shown, above, that increasing the reactive radius has a significant effect on the termination rate (figure 2.7) and further, that r_r decreases with C_p. Therefore, the emulsion polymerization of VAc was modelled by evaluating the complete Smith-Ewart equations, valid for chain-length independent termination as expected here, (equation 2.41) and the equations developed above (2.12, 2.23, 2.26 & 2.39) for exit and entry (with complete re-entry). Unfortunately, in using the reaction/segmental diffusion termination rate coefficient, the contribution from short-long termination is ignored. However, as will be seen, in order to reduce $\bar{n}$ to a comparable value to that seen experimentally, such a large value of r_i is required that the contribution from short-long termination would be relatively small (figure 2.7). Because of the uncertainty regarding aqueous-phase events some modelling was also undertaken for low initiator efficiency by simply reducing the input parameter, ρ. The results are presented in figures 2.9 and 2.10.

It can be seen from figure 2.9 that, given 100% entry efficiency, increasing the segmental diffusion reactive radius beyond about 100 Å has little effect on the predicted $\bar{n}$. Furthermore, the steady-state interval II $\bar{n}$ under these conditions is expected to be about 0.04 (extrapolated from experimental data in section 4.3.3).

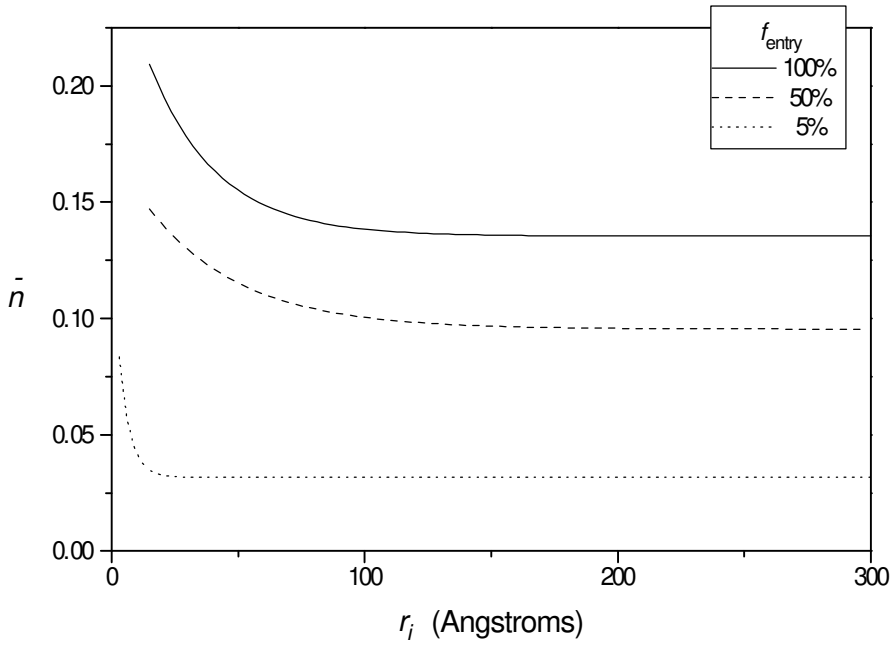

Figure 2.9: Predicted $\bar{n}$ as function of reactive radius, r_i, and entry efficiency, f_{entry}, using reaction/segmental diffusion model for VAc in interval II, C_p = 7.7 M, 50°C, [persulfate] = 2.6 mM, $N_c = 2.33\times10^{17}$ dm^{-3}.

Reducing the entry efficiency predicts an acceptable $\bar{n}$, however, even if a reasonable mechanism were proposed for drastically reducing f_{entry}, which seems unlikely, the dependence of $\bar{n}$ on r_i is weak, particularly for the large r_i required for long-long termination to dominate (i.e. r_i > 30 Å). Recall that the main point of applying reaction/segmental diffusion to VAc emulsion polymerizations was that if a first order dependence of r_i on C_p could be justified (together with the first order dependence of D^{rd} on C_p) then a zero-one-two kinetic model might explain the independence of R_p from C_p. Clearly a weak dependence of $\bar{n}$ on r_i destroys this argument and reduces the dependence of $k_{t,ij}^{rd}$ on C_p to ½ order.

It can be seen in figure 2.10 that even if r_i is forced to decrease in proportion to C_p, zero-one-two kinetics do not predict that R_p should be independent of C_p. This is because as C_p decreases, so too does C_w, the aqueous-phase monomer concentration. This in turn increases the exit rate (equation 2.26) and consequently, at least in a low $\bar{n}$ system, R_p decreases.

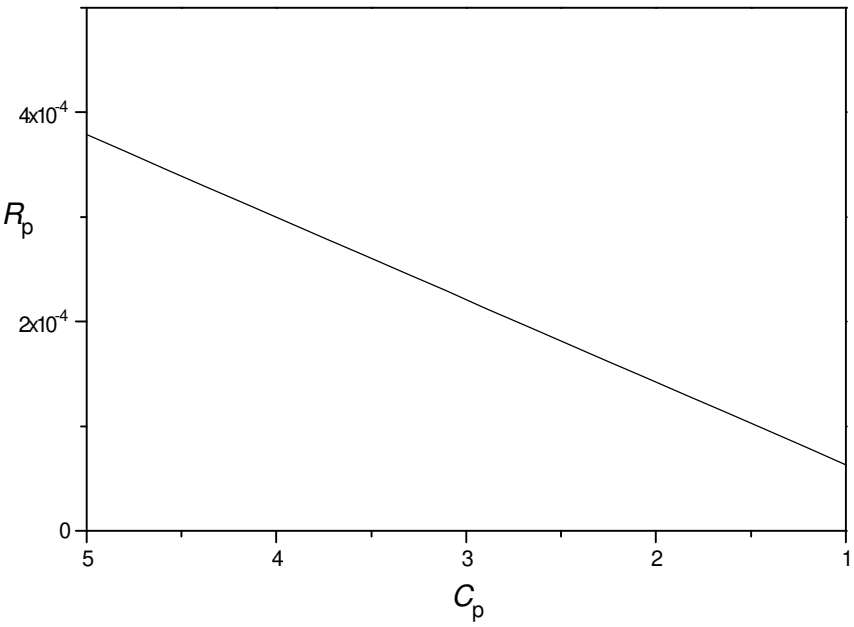

Figure 2.10: Predicted R_p as function of C_p using reaction/segmental diffusion model for VAc in interval III, and setting $r_i \propto C_p$, 50°C, [persulfate] = 0.18 mM.

Thus, the zero-one-two model does not produce the zero-order dependence of R_p on C_p that is generally seen for VAc emulsion polymerizations.

2.6 Conclusions

A large body of evidence reviewed in the literature supports the notion that chain transfer in VAc is primarily to the acetyl group on both the monomer and the polymer. Chain transfer also takes place at the tertiary carbon of the polymer backbone. The possibility that a small, but kinetically significant, amount of chain transfer to the vinyl group occurs can not be discounted.

If the rate coefficient for reinitiation by a monomeric radical, $k_{p,M}^{1}$, is sufficiently small then VAc would be expected to fall into one of the kinetic regimes Gilbert[13] calls limits 1 and 2b. Furthermore, these limits can account for the widely reported independence of R_p from C_p. However, reconciliation of the rate of polymerization predicted by either of these limits with that measured experimentally requires that either (*i*) the induced decomposition of initiator by VAc produces about ten times as many radicals as the normal thermal decomposition or (*ii*) that only about one in ten chain transfers create a radical that is slow to reinitiate. These two hypotheses are tested in chapters 3 and 4.

Finally, a zero-one-two kinetic scheme was modelled using the complete Smith-Ewart equations and a variation of Russell's[48] residual termination mechanism. It was thought that the second order dependence of k_t on C_p may cancel the usual first order dependence of R_p on C_p thereby explaining the unusual independence of R_p from C_p observed in VAc emulsion polymerizations. However, the modelling showed that this was not the case.

-oOo-

3 Gamma Radiolysis of Emulsions

3.1 Introduction

The primary aim of the gamma radiolysis experiments described below was to determine the radical-loss rate in VAc emulsion polymerization. This technique has been used successfully to measure radical-loss rates for styrene[90] and methyl methacrylate[28]. The radical-loss rate was then to be used to test models of kinetic mechanisms, in particular the mechanisms called limits 1 and 2b, described in the previous chapter.

3.2 Why use gamma radiolysis?

The principle behind γ relaxation experiments is that the source of initiating radicals can be switched off "instantaneously". In the absence of initiating radicals the only kinetic events remaining are propagation, transfer and termination. As propagation coefficients have been determined fairly accurately for the monomers used in this work[31,33], relaxation behaviour can be interpreted to determine termination rate coefficients and test models of termination mechanisms.

In principle, the same can be said of UV photolysis but only γ radiation has the penetrating power to provide a homogeneous radical production rate throughout the turbid emulsion. γ radiation also has the advantage of providing a source of radicals in emulsions without the need to introduce another chemical species, namely the photosensitive initiator required for UV photolysis.

However, there are at least two potentially significant drawbacks that must be considered when performing γ relaxations. The first is that the γ source cannot be switched off like a light. Rather the experiment is removed from the source or a thick lead shield is placed between the γ source and the experiment. This takes a few seconds and may result in large experimental uncertainties, especially in systems which relax rapidly. Secondly, the primary radicals formed by γ radiolysis of water are extremely reactive and produce secondary radicals that may complicate the system[91].

Figure 3.1 shows a typical conversion-time plot obtained from a γ relaxation experiment and serves to illustrate the main features of the experiment. The reaction

vessel is placed in the source and after an inhibition and/or retardation period (possibly due to residual oxygen and/or adventitious retardants) polymerization commences.

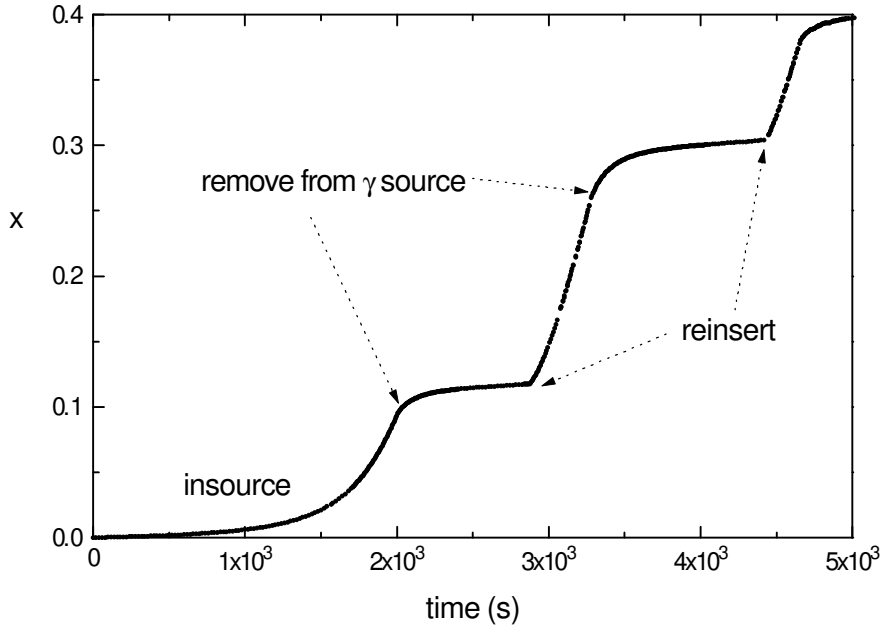

Figure 3.1: A typical γ relaxation experiment plotted as fractional conversion of monomer, x, as a function of time (expt. C1).

When the reaction vessel, in this case a dilatometer, is moved out of the γ source the conversion rate decreases to a much lower steady-state rate. This is called the thermal steady-state rate because the major source of radicals is thought to be from thermal decomposition processes. Upon reinsertion the conversion rate increases to the previous insource steady-state rate very quickly. This procedure can be repeated several times during a single experiment.

The thermally derived radicals may be generated within the particles and as such do not actually enter; however, for the purpose of determining termination rates from relaxations this distinction is irrelevant.

3.2.1.1 Literature review

Only a few reports of gamma relaxation experiments on VAc could be found in the literature and of these only one actually reports relaxation data[92]. The other references to post-irradiation behaviour only mention whether or not there was significant post irradiation polymerization[93,94].

The most recent was the work of Sunardi[92] whose experiments were conducted on ab-initio homopolymerizations at 28-29°C with dose rates ranging from 0.175-0.584 Gy s^{-1}. The results of two intermittent radiation experiments were reported. In the first the emulsion was irradiated for five minutes then allowed to relax for five minutes, this cycle being repeated eight times to achieve 90% conversion. In the second experiment the emulsion was irradiated for five minutes then allowed to relax for fifteen minutes, this cycle also being repeated eight times to achieve 90% conversion. Conversion was measured every five minutes by dilatometry and it appeared that the system did not relax much in the first five minutes out-of-source but relaxed to nearly zero polymerization rate in fifteen minutes. It seems likely that this unusual behaviour is due to an experimental artefact identified in this work and discussed in detail in section 3.3.6.

Sunardi reported a negative order of dependence of polymerization rate and viscosity average molecular weight on emulsifier concentration using Tween 20 – (polyoxyethylene sorbitan monolaurate) as the emulsifier. The order of dependence of polymerization rate on dose rate was reported as 0.6-1.0 increasing with emulsifier concentration. Finally, the conversion-time plots seem to show an increasing rate through to high conversion.

Stannett et al.[94] determined polymerization rates and viscosity average molecular weights between 0°C and 50°C for ab-initio and seeded homopolymerizations. The polymerizations were monitored by dilatometry; however, no account was taken of the small, but non-negligible, non-linearity of the contraction due to polymerization in systems such as this where the monomer has significant water solubility. They reported no significant post-irradiation polymerization at conversions up to 50%.

3.2.1.2 Production of primary free radicals in the irradiation of emulsions

The most commonly used source of γ radiation in research and industry is Cobalt 60. ^{60}Co emits two γ photons from each disintegration. The main interaction between these γ photons and matter is Compton scattering, whereby the incident γ photon ejects an electron losing only a small proportion of its energy in the process. The same γ photon then continues ejecting electrons from subsequent atoms until its energy is exhausted. Some of these ejected electrons also have sufficient energy to eject more electrons and do so until their energy is exhausted.

When an electron is ejected from a stable molecule in this way two radicals are formed and these may initiate (or terminate) free-radical polymerization. ^{60}Co γ photons have

energies of 1.879×10^{-13} & 2.134×10^{-13} J. This is much greater than typical ionization energies ($<10^{-18}$ J/molecule) and so one γ photon may generate many radicals.

Absorption of γ radiation, and subsequent radical production, depends mainly on the electron density of a substance and this in turn is approximately proportional to its mass density (at least for the lighter elements in which we are interested). In emulsion polymerizations the main components have similar densities and so absorption of γ photons is approximately proportional to the relative quantities of each component. The yield of reactive species (in this case free radicals) is called the radiation chemical yield, or G value. Typical G values lie in the range 0.1 to 10 molecules per 1.6×10^{-17} J absorbed. This seemingly odd choice of ratio is a hangover from the pre-S.I. unit era (1.6×10^{-17} J = 100eV).

As γ photons are so energetic that they can break any chemical bond indiscriminately, numerous primary products are possible. These may react or recombine to produce even more secondary products. However, the major species produced by the γ radiolysis of pure water are solvated electrons, protons and hydroxyl radicals.[91] The main reaction pathways are:

$$H_2O + \gamma \rightarrow e^- + H_2O^{\bullet+} \qquad 3.1$$

$$H_2O + \gamma \rightarrow H_2O^* \qquad 3.2$$

$H_2O^{\bullet+}$ decomposes rapidly (~10^{-13} s) to produce protons and hydroxyl radicals.

$$H_2O^{\bullet+} \rightarrow H^+ + OH\bullet \qquad 3.3$$

The exact nature of the H_2O^* species remains undetermined but it seems likely that on decomposition radicals will be produced either directly (equation 3.4) or after ejecting an electron (equations 3.5 & 3.3).

$$H_2O^* \rightarrow OH\bullet + H\bullet \qquad 3.4$$

$$H_2O^* \rightarrow e^- + H_2O^{\bullet+} \qquad 3.5$$

In the absence of reactive species electrons are rapidly (~10^{-11} s) solvated:

$$e^- + nH_2O \rightarrow e^-_{(aq)} \qquad 3.6$$

At any reasonable pH solvated electrons are rapidly protonated:

$$e^-_{(aq)} + H^+ \rightarrow H\bullet \qquad 3.7$$

3.2.1.3 Initiation by the primary radicals formed by the γ radiolysis of water

In the presence of olefins, free electrons add to the double bond and are immediately protonated. This produces a monomeric radical centred on the same carbon atom as that in the propagating macroradical:

$$e^- + CH_2{=}CRX + H^+ \rightarrow CH_3\text{-}\dot{C}RX \qquad 3.8$$

Similarly, for the hydroxyl radical:

$$OH\bullet + CH_2{=}CRX \rightarrow CH_2OH\text{-}\dot{C}RX \qquad 3.9$$

Olefins are effective radical scavengers and at concentrations above 10^{-4} M are thought to account for all diffusing radical species produced in the radiolysis of aqueous solutions[91]. The aqueous-phase concentration of VAc, $[M_{aq}]$, during interval II is 0.3 M (and $[M_{aq}] >> 10^{-4}$ M at the highest conversions in this work) so it is safe to assume close to 100% scavenger efficiency throughout.

Grant, Rizzardo and Solomon showed that, in bulk polymerizations of VAc, the specificity of hydroxyl radicals was as follows[34]:

"tail addition" $OH\bullet + CH_3CO_2CH{=}CH_2 \rightarrow CH_3CO_2\dot{C}HCH_2OH$ 80%

"head addition" $OH\bullet + CH_3CO_2CH{=}CH_2 \rightarrow CH_3CO_2CH(OH)\dot{C}H_2$ 17%

"H abstraction" $OH\bullet + CH_3CO_2CH{=}CH_2 \rightarrow \dot{C}H_2CO_2CH{=}CH_2$ 3%

This indicates how facile hydrogen abstraction by hydroxyl radicals can be. It is clear that H abstraction by the hydroxyl radical may compete, modestly, with addition to the double bond.

3.2.1.4 Production of free radicals in particles

Radiolysis of particle phase monomer and polymer will produce a free electron and a positively charged radical but their chance of avoiding geminate recombination decreases with the dielectric constant of the medium. The relative dielectric constant of pVAc is 3.5 at 50°C[54] and so the efficiency of radical production in the particle phase is very low compared with water ($\varepsilon = 80$). Also in a zero-one system, such as styrene, even if the radicals formed within a particle did initiate polymerization one would expect these to undergo rapid bimolecular termination and hence contribute little to the overall polymerization. Even in a zero-one-two system, such as might be

the case for VAc, intra-particle termination is faster than exit and such radicals will also contribute little to the overall polymerization. If one of the radiolysis products (most likely the free electron) did escape from the particle then the remaining radical may initiate polymerization. However, the locus of origin of the propagating radical is of no consequence in γ relaxations and so this possibility need not concern us in this work.

3.2.1.5 Production of free radicals in droplets

The γ relaxations in this work were all conducted in interval III so there should be no monomer droplets present; however for the sake of completeness we shall consider them briefly.

Monomer droplets are not expected to follow zero-one kinetics and so γ radiolysis of monomer within droplets could result in significant polymerization. However, because of the low dielectric constant the radical production rate generated within droplets is relatively low. More importantly (and similar to aqueous-phase chemical initiation) because of the proportionally small total surface area of droplets compared to that of the large population of small particles, the entry rate (into droplets) of initiating radicals is low. Even in an unseeded batch emulsion polymerization of VAc, interval III commences at about 25% conversion, and hence droplets can account for at most a few percent of the total polymerization.

Aqueous-phase monomer, even for a relatively water soluble monomer like VAc, comprises no more than a few percent of the aqueous phase. Therefore, in a typical γ - radiolysis emulsion polymerization experiment, radiolysis of water will provide more than 95% of the initiating free radicals.

3.2.1.6 Rate of primary radical production in the radiolysis of emulsions

Overall G values for the radiolysis of water in the presence of a dilute (~10^{-3} M) scavenger are slightly pH dependent but in the range pH = 4 - 11 are: OH• = 2.8, H• = 0.55 and $e^-_{(aq)}$ = 2.7 for a total G value of 6.05[91]. In dilute monomer solutions this results in a production rate of aqueous-phase monomeric radicals given by:

$$\left.\frac{d[M^{\bullet}_{aq}]}{dt}\right|_{production} = I \times G / 1.6\times10^{-17} \text{ radicals dm}^{-3}\ (H_2O)\ s^{-1} \qquad 3.10$$

where I is the intensity of the γ radiation (Gy s^{-1}). In the presence of a higher concentration of effective scavenger it is thought that the G value may increase by about 0.3-0.5 for each 10 fold increase in scavenger concentration[95]. It seems likely then, that for VAc and other fairly water-soluble monomers the G value should be

about 7. For a typical experiment in the AINSE source with 2 cm of lead shielding, the calculated aqueous-phase radical production rate was about 1.5×10^{16} radicals dm^{-3} (H_2O) s^{-1}. This is equivalent to chemical initiation by about 8×10^{-3} M potassium persulfate at 50°C in pure water.

As was shown in section 2.1.2.3 entry efficiency for VAc is close to 100% and so the entry rate coefficient can be estimated:

$$\rho = \frac{\left.\frac{d[M_{aq}^{\bullet}]}{dt}\right|_{production}}{N_c} \qquad 3.11$$

where ρ is the number of radicals entering per particle per second and N_c is the number concentration of particles in the reaction flask. It should be noted here that this value of ρ is largely model independent in that it only assumes that most of the radicals formed in the aqueous phase enter particles and propagate.

3.3 Experimental I - vinyl acetate homopolymerization

3.3.1 Introduction

One of the initial objectives of this work was to determine kinetic parameters for the emulsion polymerization of VAc at the temperatures used industrially i.e. around 70°C. Further, it was hoped to determine the radical-loss rate over a range of temperatures and conversions to test the dependence of the radical-loss rate on temperature and monomer concentration. The method used was gamma relaxation monitored by dilatometry.

Unfortunately, experimental limitations precluded accurate determination of the radical-loss rate observed at elevated temperatures in interval II. However, it was expected that the relaxation rate would depend on the exit rate of monomeric radicals subsequent to transfer and so should be reduced by decreasing the reaction temperature (thereby reducing $k_{tr,M}$) and operating at higher conversions (thereby reducing C_p). This was found to be the case and relaxation times were increased from a few seconds to as much as 20 seconds at high conversions at 2°C, thereby permitting acquisition of up to seven data points on the relaxation curve.

At lower temperatures, problems due to an exotherm, (the "heat effect" described below) were much less significant thereby reducing the greatest source of uncertainty

in the early relaxation time data. Consequently, most of the relaxation data reported below were acquired in the 2 – 10°C range.

As mentioned previously, (section 1.4) it has been reported, that in VAc emulsion polymerizations, the polymerization rate is independent of monomer concentration well into interval III. On close inspection of the data presented in many papers however, it appears that the rate actually increased slightly over the course of most VAc emulsion polymerizations up to high conversions (section 3.2.1.1). This was evident in persulfate[96] and radiolysis-initiated emulsion polymerizations[92]. A dependence on initial monomer concentration has also been reported [97]. It would seem most likely that this was related to the formation of a population of secondary particles. However, as the relaxations in this work were conducted well into interval III, these potential complications were largely avoided.

3.3.2 Materials and methods

3.3.2.1 Dilatometry

The crucial part of this work was the measurement of polymerization rates during relaxations by dilatometry. As most monomers are about 20% less dense than their corresponding polymers, polymerization causes a substantial contraction of the reaction mixture. Many different configurations are possible but the main feature common to all dilatometry vessels is that the reaction flask is fitted with a capillary and that any volume change in the reaction mixture causes an equal volume change in the capillary. In a capillary with a suitably narrow bore even a small volume change causes a large change in meniscus height and it is this conveniently accessible parameter which is measured to monitor the progress of the polymerization.

3.3.2.2 Interpretation of relaxation data and calculation of exit rates.

The data acquired from γ relaxations are polymerization rates as a function of time. These are readily converted to $\bar{n}$ as a function of time. This is useful as it provides an intuitive picture of the microscopic behaviour of individual latex particles. From the insource steady-state $\bar{n}$ immediately prior to relaxation, $\bar{n}_0$, and the subsequent decay in $\bar{n}$ on removal of the initiating radical source, the radical-loss rate, k_{rl}, may be determined from equation 3.17, developed below.

For VAc emulsion polymerizations at the temperatures used in this work, ρ_{th} is negligible and the only significant kinetic events taking place during relaxations are

exit and re-entry of monomeric radicals. As this work is intended to test the proposed models, (limits 1 and 2b described in section 2.5.2) the analysis is simplified by noting that k_{rl} is just the exit rate coefficient, k, in limit 1 and twice that in limit 2b.

Recalling equations 2.44 and 2.45 for limits 1 and 2b respectively, one notes that they are readily modified and applied to γ relaxation of emulsion polymerizations. As $\rho_{init} = 0$ during relaxations and $\rho_{re\text{-}entry} = 0$ for limits 1 and 2b, ρ may be replaced by ρ_{th} and the decay in $\bar{n}$ during γ relaxations given by:

$$\frac{d\bar{n}}{dt} = \rho_{th}(1-2\bar{n}) - k_{rl}\bar{n} \qquad 3.12$$

Figure 3.2 shows that the thermally initiated rate, $R_{p,th}$, is small in comparison to the insource rate and from $R_{p,th}$ one can estimate ρ_{th} as follows.

From equation 2.51 one can see that $\bar{n}$ is proportional to R_p. Similarly, $\bar{n}_{th}$, the average number of radicals per particle during the thermally initiated steady-state period, is proportional to $R_{p,th}$ and is therefore, very small. Hence, the low $\bar{n}$ approximation applies and equation 2.49 is readily modified to give:

$$\rho_{th} \approx k_{rl}\bar{n}_{th} \qquad 3.13$$

whereupon, substitution into equation 3.12 gives:

$$\frac{d\bar{n}}{dt} = -k_{rl}(\bar{n} - \bar{n}_{th}(1-2\bar{n})) \qquad 3.14$$

At early relaxation times, $\bar{n} >> \bar{n}_{th}$ and $\bar{n} << 1$, so equation 3.14 reduces to:

$$\frac{d\bar{n}}{dt} = -k_{rl}\bar{n} \qquad 3.15$$

Integrating gives:

$$\bar{n} = \bar{n}_0 e^{-k_{rl}t} \qquad 3.16$$

whence, the radical-loss rate coefficient is given by:

$$k_{rl} = \frac{-\ln[\bar{n} / \bar{n}_0]}{t} \qquad 3.17$$

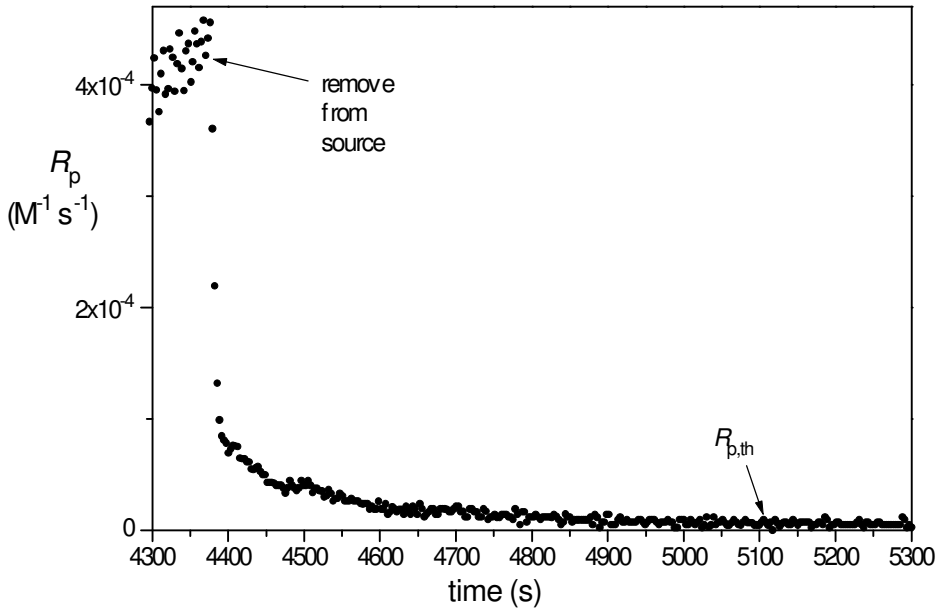

Figure 3.2: VAc γ relaxation at 2°C showing that $R_{p,th}$ is insignificant during the early part of a rapid relaxation. Experiment C3, for details see tables 3.1 and 3.2.

3.3.2.3 The γ source

The γ source used in this work (figure 3.3) consisted of a lead shielded cylindrical chamber 15 cm in diameter and 16 cm in height with "pencils" of ^{60}Co set around the perimeter. The floor of the chamber (the stage) could be raised thereby removing the dilatometer from the γ source. Raising the stage took three seconds. Attached to the stage, and therefore moving up and down with the dilatometer, was a device (the Tracker) which monitored the height of the meniscus in the dilatometer. A low voltage induction stirrer was placed under the dilatometer to drive a magnetic stirrer bar. The dilatometer itself was water jacketed, the water being circulated by a peristaltic pump in suction mode.

Although this stirring and pumping arrangement was relatively inefficient it was necessary for safety reasons. (Rubber or plastic tubing and insulation are degraded rapidly in the γ source. Hence leaks and electrical shorts are inevitable. A two volt stirrer eliminates the risk of fire and using the pump in suction mode prevents water leaking into the radiation chamber in the event of a leak in the plumbing).

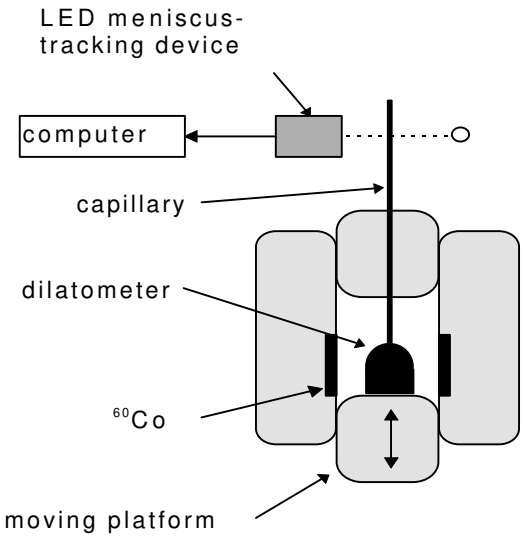

Figure 3.3: the γ source at Lucas Heights

The initial dose rate in the γ source was calibrated by Fricke dosimetry[98] and found to be 0.171 Gy s^{-1} in Oct 1991 (Gy = Gray and is one joule of absorbed energy per kilogram of irradiated material). Dose rates for later dates were then calculated according to the relation:

$$N_t = N_0 e^{-\lambda t} \qquad 3.18$$

where N_t is dose rate at time t, N_0 is the initial dose rate and λ is the decay constant for ^{60}Co. The half-life of ^{60}Co is 5.27 years which gives a decay of about 1.1% per month.

In order to allow some variation of the radiation dose rate in the reactor the radiation chamber was designed to accommodate up to 3 cm of lead shielding. 1 MeV (1.6×10^{-13} J) γ-radiation diminishes by 50% on passing through 1.06 cm of lead. The attenuation of radiation intensity may be calculated from the exponential attenuation law:

$$I = N_t e^{-\mu x} \qquad 3.19$$

where I is the intensity of the attenuated radiation, μ is the attenuation constant for lead (0.654 cm^{-1}) and x is the thickness of the lead shielding. However, because the lead shielding was not in perfectly overlapping sections, its effective thickness was somewhat reduced and the attenuation of the γ radiation intensity also had to be

determined by Fricke dosimetry. The attenuation factor was found to be 1.7 for the 1 cm nominal thickness shielding and 2.9 for the 2 cm nominal thickness shielding.

3.3.2.4 Purification of monomer

The general procedure for purifying monomer both for seed manufacture and for kinetics experiments was as follows.

VAc was obtained from Aldrich inhibited with 3-5 ppm hydroquinone. The inhibitor was removed on a column of basic alumina. The monomer was distilled under nitrogen at 72-73°C, with the first and last 20% being discarded. GC-MS conducted on the purified monomer showed no hydroquinone remaining. Bulk polymerizations performed with monomer purified in this way and degassed by multiple freeze thaw cycles had inhibition periods of just a few minutes indicating the satisfactory nature of the purification procedure. The monomer was either used immediately or stored overnight at 4°C.

3.3.2.5 Preparation of seed latexes

Many kinetic parameters are dependent on particle size and number so it is usually desirable in kinetic experiments to use a monodisperse seed. However, limit 1 and 2b kinetics are not very sensitive to particle size, (provided the particles are small enough to enforce zero-one behaviour) so a moderate degree of polydispersity is acceptable. The properties of the pVAc seeds used are listed in table 3.1.

Emulsifiers AMA-80 and AOT-75 were used as obtained from Cyanamid. The buffer used was sodium bicarbonate and the initiator used to prepare the seed was potassium persulfate. Both were obtained from Merck and used without further purification. Milli-Q water, 18.2 MΩ cm^{-1} was used throughout.

Seed C was prepared as a batch polymerization. Surfactant and buffer were dissolved in water, heated to 68°C and purged with nitrogen for 20 minutes. 9-vinyl anthracene was dissolved in VAc and emulsified in the surfactant solution. By the addition of 9-vinyl anthracene it was hoped to increase particle number concentration and reduce polydispersity by restricting polymerization in droplets and in particles formed at early times[13]. Potassium persulfate was dissolved in water before addition to the reaction mixture and a nitrogen atmosphere maintained throughout.

Unfortunately, VAc's propensity for secondary nucleation meant that it was only possible to approach monodispersity by preparing the seed as a starved feed batch. This has the drawback of increasing the degree of branching (section 2.3.1.2) which may affect the density of the polymer and non-ideality of mixing with monomer.

Uncertainty in densities affects the accuracy of dilatometry. However, termination rates extracted from γ relaxations depend only on relative rates immediately before and during the relaxation so the absolute densities are not critical.

Table 3.1: Seed recipes

		seed C	seed E	seed G	seed H
		batch	starved feed	starved feed	starved feed
temperature		68°C	60°C	60°C	60°C
water		521.5 g	472 g	602.5 g	589.17 g
AMA-80		5.36 g	3.762 g	5.22 g	5.44 g
OT-75		-	3.767 g	5.05 g	5.60 g
$NaHCO_3$		1.02 g	0.75 g	1.00 g	1.00 g
vinyl acetate	initial charge	101.5 g	29.7 g	40.0 g	32.3 g
	balance	-	164.6 g	221.6 g	194.3 g
	feed rate	-	0.5 ml/min	1.4 ml/min	1.0 ml/min
9-vinyl anthracene		0.0103 g	-	-	-
$K_2S_2O_8$ /		1.00 g	0.753 g	1.00 g	1.00 g
water		20.8 ml	29 ml	30 ml	30 ml
	initial charge	-	6 ml	6 ml	5 ml
	feed rate	-	0.1 ml/min	0.15 ml/min	0.1 ml/min
solids content	after dialysis	8.4%	18.67%	22.17%	18.64%
D_N		93 nm	76 nm	102 nm	104 nm
polydispersity		1.34	1.17	1.17	1.16

Seeds E, G & H were prepared at 60°C under nitrogen as starved-feed batches (see table 3.1 for more details). An initial charge of monomer was solubilised in water in which the emulsifiers and buffer had been previously dissolved. The potassium persulfate was dissolved in water and an initial charge of about 25% of the persulfate solution added to commence the reaction. The remaining monomer and initiator solution were added at rates of ~1 ml min^{-1} and ~0.1 ml min^{-1} respectively. The smaller particle size of seed E may be due to the lower monomer feed rate and differences in the stirrer design and stirring rate.

Because of concerns over the possible presence of a retardant in the latexes, seed H was made under more stringent conditions. Inhibitor was removed on basic alumina, monomer purged with nitrogen and distilled under 30 mm Hg at 38°C. The first and last 20% of monomer was discarded. Seed water and dialysis water were purged with

nitrogen, potassium persulfate was recrystallised and finally the dialysed seed was stored under nitrogen. No significant difference in overall polymerization rates or relaxation rates was observed between kinetic runs based on this seed and seeds C, E & G.

Total solids were determined by gravimetry and particle size distributions were determined by capillary hydrodynamic fractionation (CHDF) using a Matec Applied Sciences CHDF1100 fitted with a C570 high sensitivity column claimed to be suitable for particle diameters of 15-700 nm. The eluent used was GR500™ at a flow rate of 1.40 ml min^{-1}.

3.3.2.6 Typical procedure for γ relaxation

In a typical γ-relaxation experiment monomer (4 g) was solubilised in water (15 g) in which emulsifier (AMA-80: 0.14 g) and buffer (0.06 g) had been previously dissolved. Next, the seed (40 g) was added to the dilatometer and allowed to swell for one hour under a partial vacuum. The exact recipes are detailed in table 3.2.

Table 3.2: Recipes used for VAc γ relaxation experiments.

Expt. #	C1	C2	C3	H1	H2	H3	E1
temperature (°C)	50	50	2	2	2	50	2 – 40
dose rate (Gy s^{-1})	0.033	0.041	0.041	0.030	0.029	0.028	0.033
reactor vol. (ml)	53.5	53.5	60.0	60.0	60.0	60.0	60.0
AMA-80 (g)	-	0.0925	0.095	-	0.15	0.16	0.1385
$NaHCO_3$ (g)	-	0.0683	0.0825				0.060
H_2O (g)	42.8	44.3	53.1	48.8	45.6	45.4	49.4
vinyl acetate (g)	7.26	6.15	4.116	2.14	4.24	11.11	4.115
seed solids (g)	2.98	2.66	2.70	10.24	11.25	2.51	6.93

Finally, the capillary was fitted, the dilatometer was topped up with water and lowered into the γ-source (~0.03 Gy s^{-1}) where, after an inhibition period, polymerization commenced. When the reaction had reached a steady state the dilatometer was removed from the source and the meniscus height and reactor temperature monitored until a new (thermal initiation only) steady-state polymerization rate, $R_{p,th}$, was reached. This procedure was repeated several times per run.

3.3.2.7 Monitoring reaction temperature

Reaction temperature was measured in a dilatometer fitted with a 100 Ω platinum RTD probe. The probe had a "flattened" stainless steel sheath to maximise contact area with

the solution and obtain the fastest response time to the small temperature changes in this system. The specifications for the probe claim a response time of $0.63 \times \Delta T\ s^{-1}$. In other words, subsequent to a temperature change the output signal reaches 63% of its final value in 1 second, 86% in two seconds and 95% in 3 seconds. The probe's resistance was measured and converted to temperature (± 0.02°C) by a Moore Products Mycro XTC model 344 Temperature Controller Transmitter.

3.3.3 Acquisition of relaxation rate data

Relaxations were expected to be rapid so it was vital to have the minimum possible interval between rate measurements. A device called the Tracker, developed by David Sangster for similar work on styrene, was used. It is capable of accurate meniscus height measurements at intervals down to three seconds.

The Tracker comprised a platform that could be raised and lowered in 3.91 μm increments by a highly geared stepper motor. The platform carries a block with a light emitting diode and light sensitive resistor mounted on either side of a bore through which the dilatometer's capillary tube passed. The intensity of transmitted light varies dramatically as the Tracker descended to the meniscus. When the transmitted light intensity reaches a critical value it triggered a series of responses: (*i*) the Tracker stops, (*ii*) the time interval and distance travelled since the meniscus was last found is recorded on a PC and (*iii*) the Tracker is raised a small distance so that the next reading is taken with the drive mechanism in the same state as for the previous reading i.e. Tracker descending and any lash in the drive train taken up. The raw data so produced (meniscus height versus time) could then be converted to conversion versus time as detailed below.

3.3.4 Data treatment for water soluble monomers

For negligibly water soluble monomers there is an essentially linear relationship between volume contraction and conversion. Consequently, provided the capillary bore is of constant radius, there will be a linear relationship between meniscus height and conversion. The constant of proportionality for this relationship is calculated from the quantity and density of monomer and polymer and the dimensions of the reactor flask and capillary.

However, for significantly water soluble monomers it is necessary to take into account the amount of aqueous-phase monomer. This is because aqueous-phase monomer has a different density to organic phase monomer and the monomer partitions between the

two phases non-linearly with respect to monomer conversion. In the case of VAc the bulk monomer density at 60°C is 0.884 g cm^{-3} and the polymer density is 1.158 g cm^{-3} giving a 23.7% volume contraction for 100% conversion. Dunn and Taylor[96] found the contraction corresponding to complete polymerization of a 1% aqueous solution of VAc at 60°C to be 15.7% of the initial volume of monomer. This implies that the density of VAc in aqueous solution at 60°C is 0.999 g cm^{-3}.

Sarkar et al.[17] found the partition coefficient between the saturated polymer and aqueous phases for VAc at 50°C to be 21 ± 2. VAc has been found to partition between the aqueous and organic phases according to the empirical relation[13]:

$$\frac{C_{\mathrm{w}}}{C_{\mathrm{w}}^{\mathrm{sat}}} = \left[\frac{C_{\mathrm{p}}}{C_{\mathrm{p}}^{\mathrm{sat}}}\right]^{0.6} \qquad 3.20$$

where C_{w}, $C_{\mathrm{w}}^{\mathrm{sat}}$, C_{p} & $C_{\mathrm{p}}^{\mathrm{sat}}$ are the instantaneous and saturation concentrations of monomer in the aqueous and organic phases respectively. This rather simplified equation may break down at very low monomer concentrations but is adequate for the major portion of an emulsion polymerization. Calculation of conversion as a function of time is then undertaken by a simple program, which includes an iterative subroutine that determines C_{w}.

The program used actually outputs fractional conversion as a function of time, $x(t)$, so its derivative is fractional rate against time. Hence, the polymerization rate is given by:

$$R_{\mathrm{p}} = \frac{\mathrm{d}x}{\mathrm{d}t} \times n_{\mathrm{m}}^{0} \qquad 3.21$$

where n_{m}^{0} is the initial number of moles of monomer per litre of water in the system. $\bar{n}$ is then given by a rearranged equation 2.51 as:

$$\bar{n} = \frac{R_{\mathrm{p}} N_{\mathrm{A}}}{k_{\mathrm{p}} C_{\mathrm{p}} N_{\mathrm{c}}} \qquad 3.22$$

3.3.5 Effect of temperature variation on dilatometry

As dilatometry relies on measurement of the volume contraction that accompanies polymerization, it is desirable to avoid volume changes due to temperature variations during experiments intended to determine kinetic parameters. A slight variation about the desired temperature is acceptable for overall rate measurements, to determine, for instance, the dependence of polymerization rate on initiator concentration, particle

number, surfactant concentration etc. as these variations average out over the timescale of such an experiment.

A small increase in reaction temperature after the inhibition period is often found in dilatometry (and usually ignored) as the heat of reaction establishes a new (higher) steady state temperature due to the necessarily less than perfect heat transfer to the water jacket. This increase is typically of the order of 1°C for the more reactive monomers, though of course with careful design this can be reduced significantly. In any case rate determining parameters such as k_p and $k_{tr,M}$ change only slightly over a small temperature range and other factors in the determination of these parameters (such as MWDs from GPC) introduce far larger errors.

However, during relaxations even slight temperature changes can have a drastic effect. This is particularly so in the case of monomers with rapid relaxations such as VAc.

3.3.6 The mystery of slow relaxations of vinyl acetate

In γ-initiated experiments conducted at the beginning of this work it was observed that the half-life of relaxations (i.e. the time at which $\bar{n} = \bar{n}_0/2$) was much greater than one would expect from consideration of the known parameters. For instance, in experiment C1, $\bar{n}$ and ρ were determined from the insource steady-state rate of polymerization using the model independent equations 3.22 & 3.11. Values obtained at 50°C, with $N_c = 1.4\times10^{17}$and a dose rate of 0.033 Gy s^{-1} were $\bar{n} = 0.076$ and $\rho = 0.11$ s^{-1}. Rearranging equation 2.47 gives, for limit 1:

$$k = \rho(1-2\bar{n}) / \bar{n} \qquad 3.23$$

whence $k = 1.2$ s^{-1}. Rearranging equation 3.17 gives:

$$t = \frac{-\ln(\bar{n} / \bar{n}_0)}{k} \qquad 3.24$$

Thus, the relaxation half-life was predicted to be about 0.6 seconds in the case of limit 1 and half that for limit 2b. However, the raw conversion data (such as that plotted in figure 3.1) relaxed much more slowly, with a half-life of about 50 seconds. It was the investigation of this discrepancy which led to the observation of the "heat effect" described below.

In a typical emulsion polymerization at 50°C, a 1°C decrease in reaction temperature causes a decrease in volume of the reaction mixture equivalent to that accompanying

1 - 2% conversion. This is readily seen by applying the contraction factor due to polymerization (~25%) to the volume of monomer (5 ml) and comparing this to the contraction factors due to temperature change (figure 3.7) applied to the volumes of water, monomer and polymer respectively. In the experimental setup used in this work equilibration of reaction temperature on removal from the γ source took more than 200 seconds. This may also have occurred in previous γ relaxation studies on other monomers but probably to a much lesser extent because VAc has a very high k_p (which increases the rate of evolution of heat of reaction) and a very fast relaxation mechanism (which reduces the timescale over which the "heat effect" is spread).

This is also probably the explanation for Sunardi's results[92]. In that work, the dose rates were about seven times those used in this work and consequently, the "heat effect" may have been even larger. It took about five minutes for the temperature to equilibrate after "long" irradiation periods (i.e. more than one minute insource) in this work, and Sunardi's choice of a five minute reading interval would, therefore, tend to obscure this artefact.

This type of "heat effect" affecting relaxations has certainly been observed previously. Sack-Kouloumbris[99] found the same effect in photoinitiated relaxations of methyl methacrylate (MMA). In the relaxation of bulk MMA at 30% conversion, the apparent polymerization rate actually increased initially on removal of the (UV light) source. The subsequent relaxation had an apparent half-life of about 220 seconds. When corrections were made to account for the temperature changes the half-life dropped to about 70 seconds.

No mention of a "heat effect" could be found in the literature in relation to γ relaxation studies; however Scheren et al.[87] did observe a slight time lag (~one min) between "removal from the γ-source and commencement of relaxation kinetics proper" for which no satisfactory explanation was forthcoming. It seems likely that this could be due to the "heat effect".

Due to the limitations of the pumping and stirring arrangements in the γ facility, heat transfer to the water jacket was inefficient. As mentioned before (section 3.2.1.6) with the lead shielding in place the minimum dose rate available was equivalent to about 8×10^{-3} M potassium persulfate at 50°C. This leads to quite high polymerization rates and consequently high heat production. With the water bath at 50°C, the reaction temperature climbed as much as 2°C in the period from insertion into the γ source until a steady state was reached. On removal from the γ source the temperature dropped by ~1°C in 100 seconds.

It should be noted that there was no change in temperature when the experiment was repeated on a blank (a dilatometer fitted with a temperature probe and filled only with water).

Recognition of this experimental artefact, which we have called the "heat effect", has explained why VAc γ relaxations were yielding surprisingly low radical-loss rate coefficients in the past. Figure 3.4 shows the effect of this temperature drop on the measured relaxation rate at 50°C. The data (corrected by method 2, below) suggests a half-life of just a few seconds. As mentioned before, the data acquisition interval was about three seconds, as was the time taken to completely remove the dilatometer from the γ source. Consequently, the uncertainty in rates measured at early relaxation times is large; nevertheless, the data provided strong evidence for a rapid relaxation mechanism.

Clearly, without accounting for this "heat effect", completely erroneous conclusions concerning the relaxation mechanism and hence the overall kinetics of VAc emulsion polymerization will result.

3.3.7 Data correction for "heat effect"

A simple method was developed for correcting the raw data for the "heat effect". The change in meniscus height in the dilatometer is the sum of the contraction due to polymerization and contraction due to the reaction temperature dropping. During relaxations the reaction temperature was monitored as a function of time and converted to meniscus height as a function of time as detailed below (methods 1, 2 & 3). The change in meniscus height attributable to the measured temperature drop was subtracted from the raw data giving conversion (expressed as change of meniscus height) as a function of time.

The non-linearity of monomer partitioning between the aqueous and organic phases causes the proportionality between the rate of polymerization and the rate of change of meniscus height to decrease gradually with increasing conversion. However, during the brief period of a relaxation, a negligible amount of monomer is polymerized, the tiny change in the aqueous-phase concentration of monomer can be ignored and the polymerization rate is essentially proportional to the rate of change of the meniscus height.

Three methods were employed for estimating the change in meniscus height attributable to the temperature drop. The first (method 1) was to estimate the various amounts of monomer, polymer and water in the system at the time of the relaxation

and calculate the contribution of each component to the thermal contraction from temperature/density data (see figure 3.7)[54,100]. This procedure was questionable as it assumed ideal mixing of monomer/polymer and monomer/water. It also ignored effects of branching on density but at least to a first approximation it permitted analysis of relaxation data that was accompanied only by a relatively crude temperature profile.

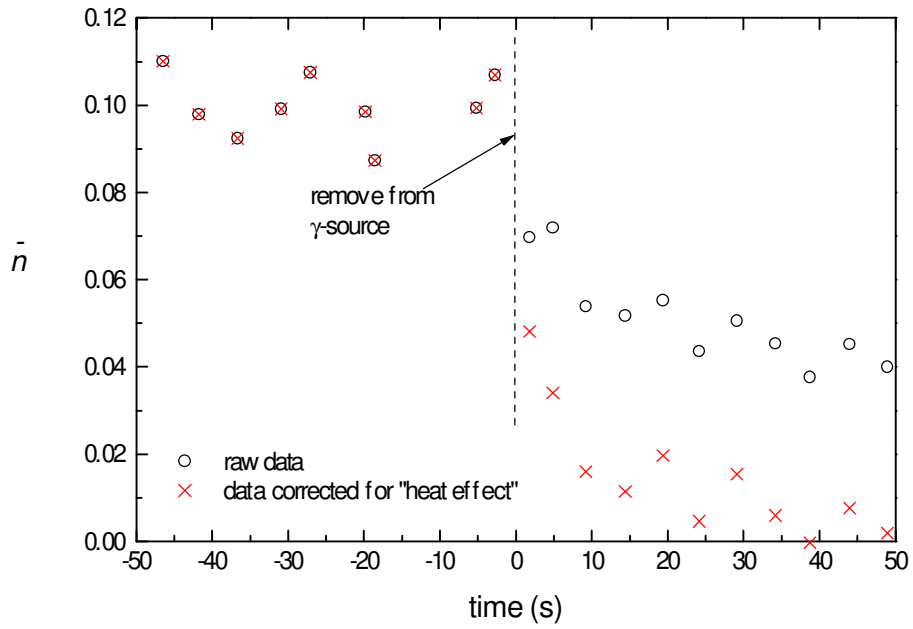

Figure 3.4: the "heat effect" in 50°C γ relaxations, expt. C1. Corrected by method 1 (see below).

Method 2 involved a direct calibration of the whole system thereby avoiding the shortcomings mentioned above for method 1. It consisted of briefly lowering the water bath temperature by about 1°C (with the dilatometer out of the γ source) then returning the water bath to its previous temperature. Meanwhile the Tracker monitored the change in meniscus height as a function of time and the operator monitored the temperature as a function of time. These data were then combined to produce a calibration curve of meniscus height as a function of temperature. This method was used except where otherwise stated.

It was found that the calibration cooling and heating curves exhibited a small hysteresis effect which was in fact due to underlying thermally initiated polymerization as the contraction due to $R_{p,th}$ adds to the cooling curve then subtracts from the heating curve. The contraction due to $R_{p,th}$ is much smaller than the

contraction due to the artificially induced temperature change, at least while the reactor temperature is changing relatively rapidly, i.e. immediately after changing the water jacket temperature. Thus, the effect of $R_{p,th}$ was small and the average of the heating and cooling curves at early times was used to estimate the "heat effect".

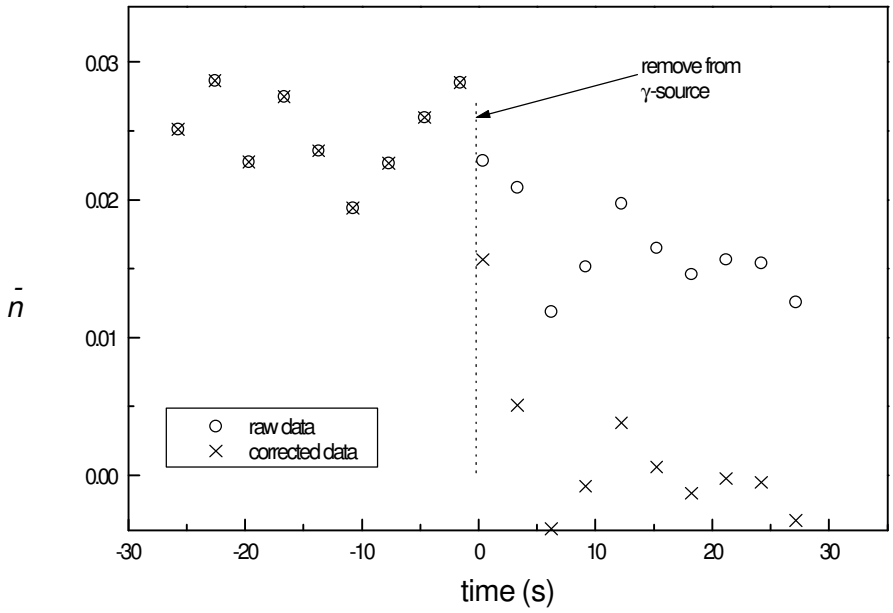

Figure 3.5: The "heat effect" in a 30°C γ relaxation, expt. E1. Corrected by method 2 (see above).

Method 3 was only used on data that was acquired before the "heat effect" was recognised. Consequently, data corrected with this method was only employed qualitatively. The method relied on the observation that the data treated by methods 1 & 2 showed that the relaxations were rapid. Hence the system should relax to the underlying thermally initiated polymerization rate within a few seconds at 50°C and within about 20 seconds at 0.5°C. As was shown in figure 3.2, thermally initiated polymerization of VAc is slow; consequently the heat it generates is negligible. Therefore, after the first few seconds of a rapid relaxation, polymerization is not generating significant amounts of heat and the system should begin cooling. Assuming that the rate limiting step for heat transfer out of the dilatometer is conduction through the glass walls to the water jacket, Fourier's Law gives the rate of heat loss ($\mathrm{d}Q/\mathrm{d}t$) as:

$$\frac{\mathrm{d}Q}{\mathrm{d}t} = -k_F \, \Delta T \qquad 3.25$$

where k_F is a system constant and ΔT is the difference between the reaction temperature and that of the water jacket. Hence the rate of heat loss will be proportional to ΔT which is at a maximum at early relaxation times and decreases gradually over about 200 seconds. So the difference between the "apparent" rate and the underlying thermally initiated rate after, say, 20 seconds of relaxation will be slightly less than the maximum contribution to the "apparent" rate attributable to the heat effect. If one extrapolates this difference back to early relaxation times a qualitative relaxation curve may be obtained (see figure 3.6).

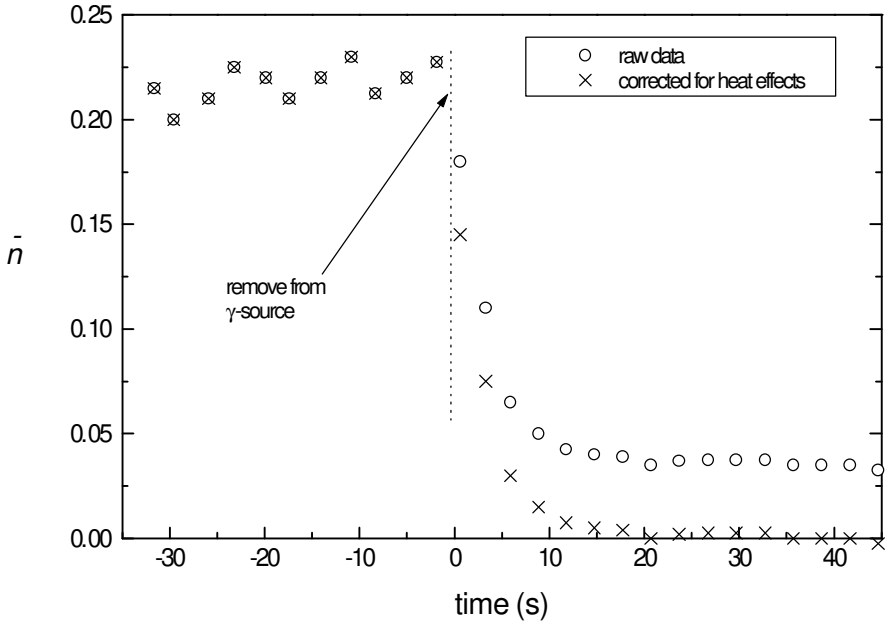

Figure 3.6: The "heat effect" in 2°C γ relaxations, expt C3. Corrected by method 3.

In figures 3.4 and 3.6 one can see that the correction required for the "heat effect" is much less at 2°C than at 50°C. This is partly because the temperature does not increase as much at 2°C as at 50°C. More importantly though, the thermal contraction of the main constituents of emulsion polymerizations decrease markedly at lower temperatures.

As one can see in figure 3.7, monomer contracts much more per degree of temperature decrease than polymer, especially at the higher temperatures. Hence, at a given temperature, contraction of the reaction mixture due to a temperature drop varies with conversion. For this reason, a "heat effect" calibration was required before each relaxation.

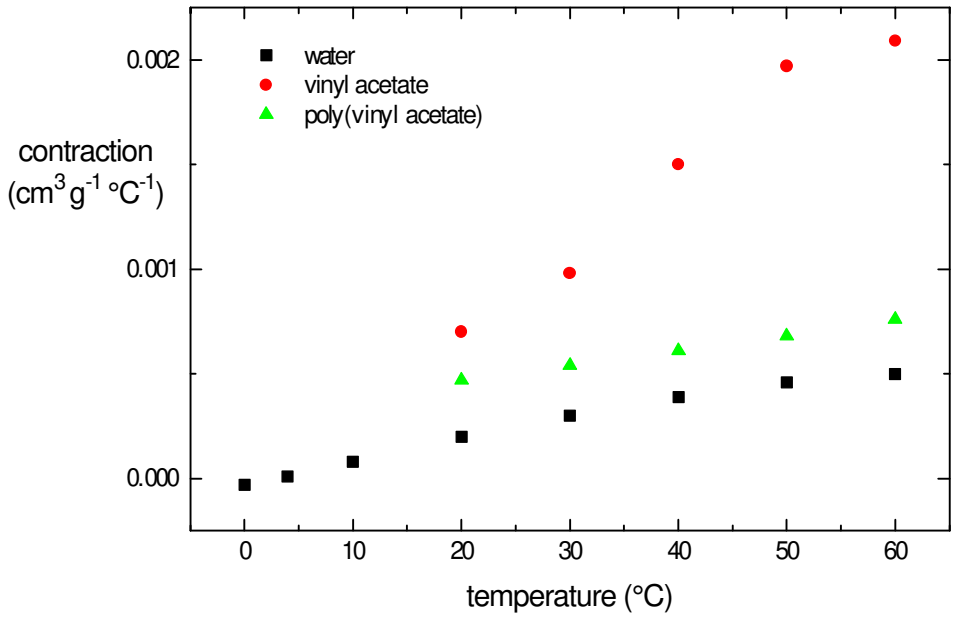

Figure 3.7: Contributions to the "heat effect" from the major constituents of VAc emulsion polymerizations[54,101].

It is also apparent from figure 3.7 that contraction as a function of temperature decreases at lower temperatures and so the magnitude of the "heat effect" is greatly diminished. This is particularly significant for water, which usually comprises at least 70% of the reaction mixture and whose thermal contraction is negligible from 0-5°C.

As can be seen in figure 3.8, the three methods described above for correcting for the "heat effect" were found to agree qualitatively and so corrected data from early experiments are included in the general discussion. However, it should be emphasised that the corrected relaxation data are only used to show that there was not a strong trend discernible in the dependence of radical-loss rates on temperature.

The methodology is sound but at elevated temperatures the "heat effect" is large and the uncertainties are too great to form any firm conclusions based on the corrected data. However, as is shown in the next section, an improved technique allowed for the acquisition of reliable data at 2°C.

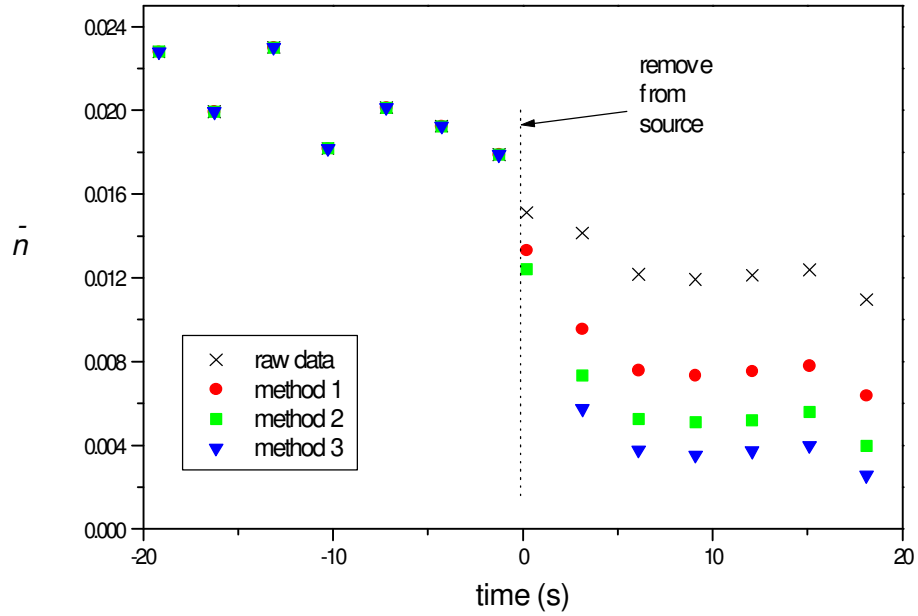

Figure 3.8: Comparison of methods for "heat effect" corrections, expt E1, 40°C.

3.3.8 Partial avoidance of "heat effect"

It was eventually realised, that to determine termination rates, it was not necessary to wait for the system to reach steady state before removing the dilatometer from the γ source. This allowed a rapid insertion/removal technique to be employed whereby, as the name suggests, the dilatometer was inserted into the γ source briefly (approximately 20 seconds) then removed. Under this regime it was found that at 2°C there was no significant temperature increase following insertion or temperature decrease during the subsequent relaxation. Hence no correction for "heat effect" was required (see figure 3.9).

Unfortunately at higher temperatures the rapid insertion/removal technique was found not to help as the reaction temperature began to increase immediately upon insertion into the γ source.

The fact that the termination rates determined at 2°C with this technique were in accord with those obtained from data corrected for the "heat effect" validated the previous experiments and allowed their incorporation in this work. Also, it supported the qualitative use of the corrected data obtained at higher temperatures.

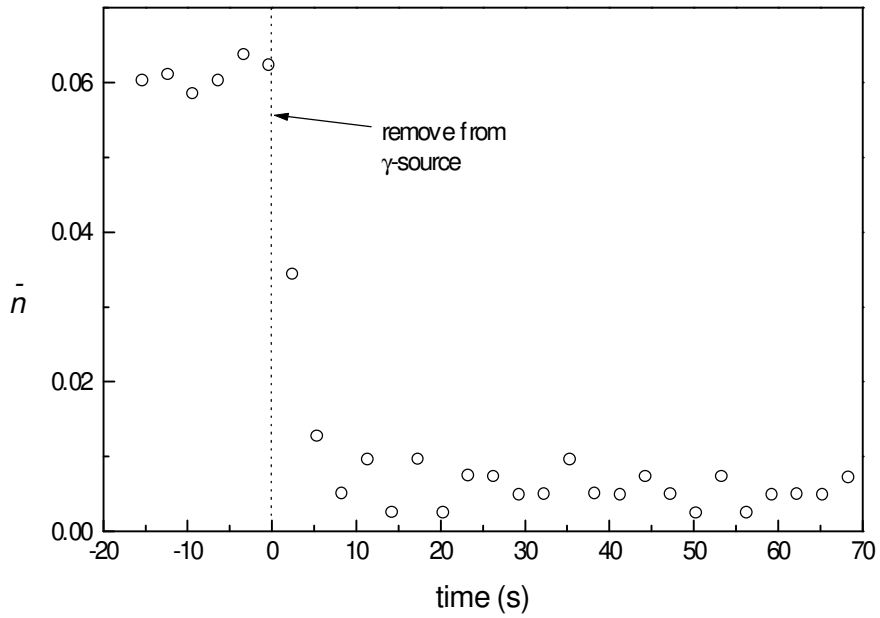

Figure 3.9: Rapid reinsertion γ relaxation, expt. H2, 2°C. This technique produces negligible "heat effect" so no correction required.

3.3.9 Results and Discussion

3.3.9.1 Gamma relaxations of seeded emulsion homopolymerization of vinyl acetate.

The first group of experiments in this part of the work were γ relaxations conducted on seeded VAc emulsions. The aim was to test the dependence of the polymerization rate, R_p, and the rate coefficient for radical loss, k_{rl}, on reaction temperature and monomer concentration in the latex particles.

The kinetic parameters and results relevant to these experiments are summarised in table 3.3. k_{rl} was determined over a range of temperatures and conversions and the results are presented in figures 3.10 and 3.11. From the foregoing discussion it should be clear that only relaxation rates obtained at low temperatures (2 - 10°C) can be considered quantitative.

If the radical loss mechanism involves transfer to monomer, then k_{rl} should be dependent on monomer concentration in the latex particles, C_p. The aim of experiment H2 was to test the dependence of k_{rl} on C_p. H2 was a seeded γ relaxation employing the "rapid reinsertion" technique as described in the preceding section. With this technique the system was only allowed to polymerize briefly between relaxations so it was possible to conduct many relaxations in the course of a single kinetic run. In the

case of experiment H2, 40 relaxations were monitored and k_{rl}, calculated as described in section 3.3.2.2 (equation 3.17), is plotted as a function of C_p in figure 3.10. It can be seen that the rate coefficient for radical loss decreased approximately linearly with monomer concentrations down to 1.1 M.

Table 3.3: Summary of γ relaxation experimental parameters and results. ρ_{init} calculated from radical production rate and radiation chemical yield (equation 3.11).

	C1	C2	C3	H1	H2	H3	E1	US1
Temperature (°C)	50	50	2	2	2	50	2-40	2
γ dose rate (Gy s^{-1})	0.033	0.041	0.041	0.030	0.029	0.028	0.033	0.083
$W_{p,initial}$	0.33	0.35	0.48	0.86	0.76	0.31	0.68	-
$W_{p,final}$	0.65	0.72	0.98	0.94	0.96	0.73	0.99	0.61
$N_{c,initial}$ ($\times 10^{17} dm^{-3}$)	1.4	1.2	1.0	3.1	3.6	0.81	5.3	0
$N_{c,final}$ ($\times 10^{17} dm^{-3}$)	1.3	1.3	1.35	3.1	4.0	4.0	5.4	2.1
$r_{initial}$ (nm)	47	47	47	52	52	52	38	-
r_{final} (nm)	56	55	57	55	55	55	44	55
ρ_{init} (insource, s^{-1})	0.069	0.10	0.17	0.057	0.041	0.045	0.037	0.24
$C_{p,initial}$ (M)	7.7	7.7	4	2	2	3	3	7.7
R_p,max ($\times 10^{-4}$ M s^{-1})	8.27	9.83	4.14	3.36	2.38	8.24	-	9.93

Interestingly, the radical-loss rates measured at 2°C were about the same as predicted by limits 1 and 2b (figure 3.11). Initially this was thought to support the proposed models. However, in the light of the rest of the data collected in this work, it seems that this agreement was coincidental.

Another consequence of the involvement of transfer to monomer in the radical loss mechanism is that the rate of radical loss should be dependent on reaction temperature. The aim of experiment E1 was to test the dependence of k_{rl} on T, and as C_p also changed during the experiment it is included in the presentation of the data.

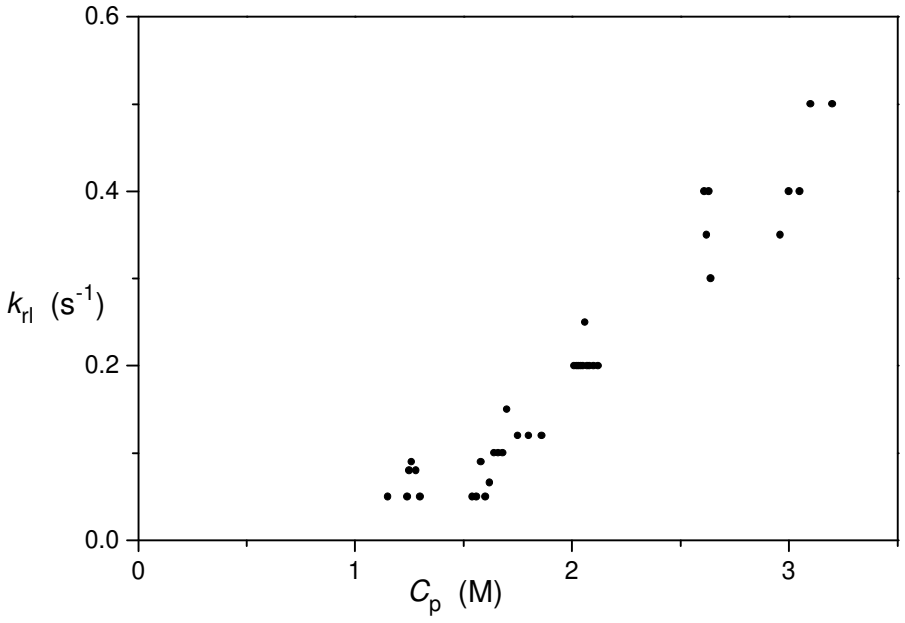

Figure 3.10: Rate coefficient for radical loss, k_{rl}, in VAc emulsion polymerization determined as function of C_p, expt. H2 (2°C, no correction for "heat effect" required).

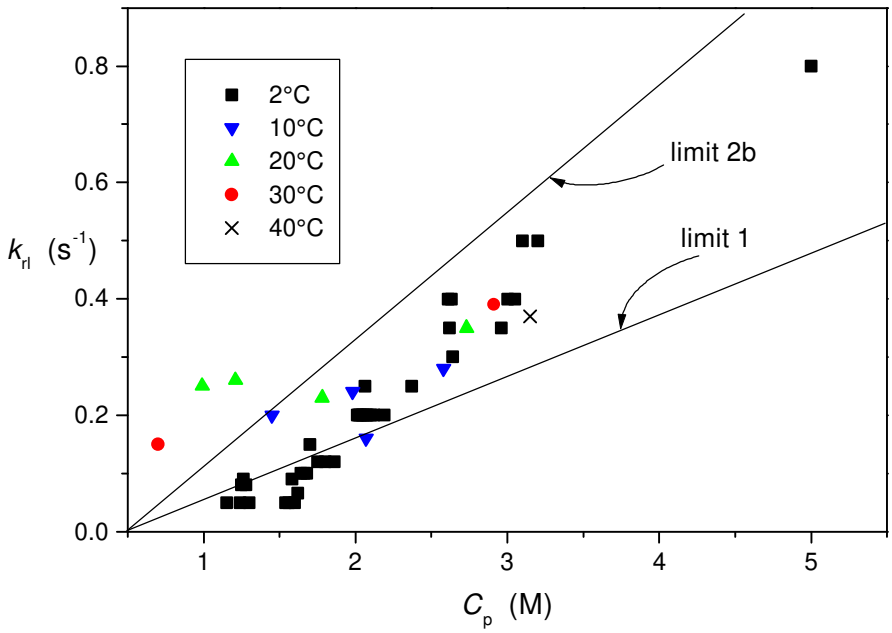

Figure 3.11: k_{rl} as function of C_p and temperature, points: expt. E1, details: table 3.3, lines: model predictions for conditions of expt. E1, 2°C.

As discussed previously (sections 3.3.6, 3.3.7, 3.3.8) termination rates obtained in this work above about 10°C can only be considered qualitative. There may be a slight trend towards higher termination rates with increasing temperature in the data presented in figure 3.11. However, it is not nearly as strong as one would expect if transfer to monomer was the rate determining step for termination. From the literature and the molecular weight distributions discussed in chapter 5, the activation energy for transfer to monomer is about 35-40 kJ mol^{-3}, so $k_{tr,M}$ should nearly double for each 10°C temperature increase; however, this is not apparent in the relaxation rates. There does appear to be an approximately linear dependence on C_p as observed in experiment H2 (figure 3.10).

3.3.9.2 Dependence of polymerization rates on temperature and gamma dose rates.

The maximum polymerization rates for seven γ-initiated emulsion polymerizations, six seeded and one unseeded, are presented in figure 3.13. For the experiments conducted at 2°C the polymerization rate is approximately proportional to the radical production rate as calculated from equation 3.10. As can be seen in figure 3.12, polymerization rates increased throughout the polymerizations so the maximum rates attained have been used in figure 3.13.

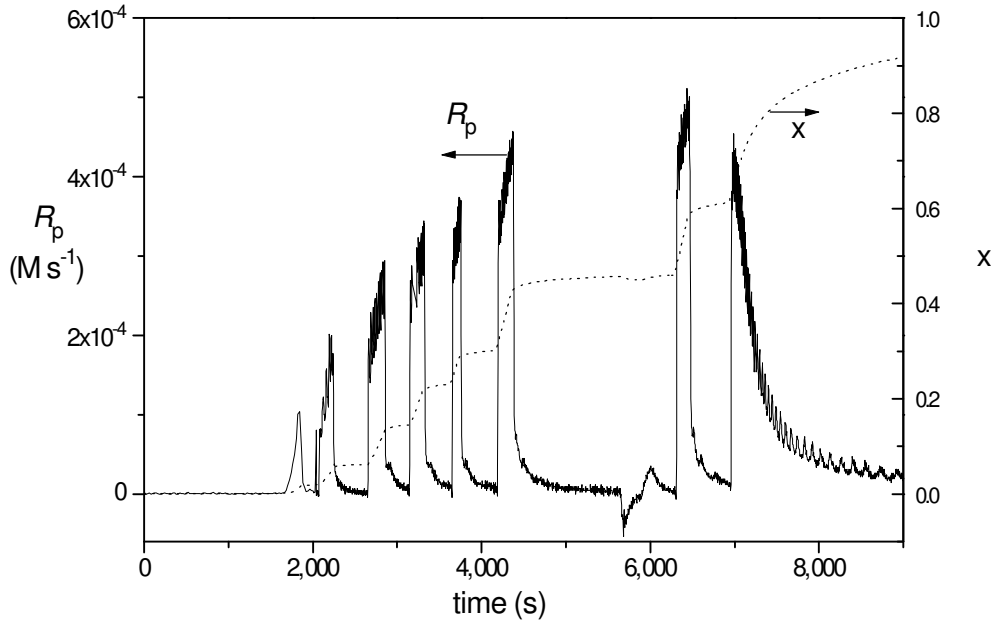

Figure 3.12: Polymerization rate, R_p, and conversion, x, as functions of time for a seeded, γ-initiated, interval III, VAc γ relaxation run, showing the insource rate increasing with time, expt. C3, 2°C, details: table 3.3.

A similar effect was observed in persulfate-initiated polymerizations at high initiator concentrations (figure 4.2). Hence, comparisons of rate data between polymerizations commenced at differing W_p, must be treated with a degree of caution.

Challa et al.[68] found that the dependence of R_p on dose rate was 1.03±0.49 at 20°C. The dose rates employed were 4-8 times the maximum γ dose rates used in this work. Stannett[94] reported an order of dependence of 0.79 at 30°C over a similar range of γ dose rates to that used in this work.

Unfortunately, there is not a large enough spread of data to establish a rate dependence on radiation dose rates at 50°C, although there would appear to be an approximately first order dependence in the 2°C data. Clearly there is a significant temperature dependence. Challa et al.[68] found an "activation energy for γ initiated polymerization", based on the dependency of polymerization rate on temperature, of about 22 kJ mol^{-1}. This is remarkably close to the current value for the activation energy of propagation[33], though it is not clear how this relates to the system kinetics, particularly as their experiments were conducted in a flow type reactor.

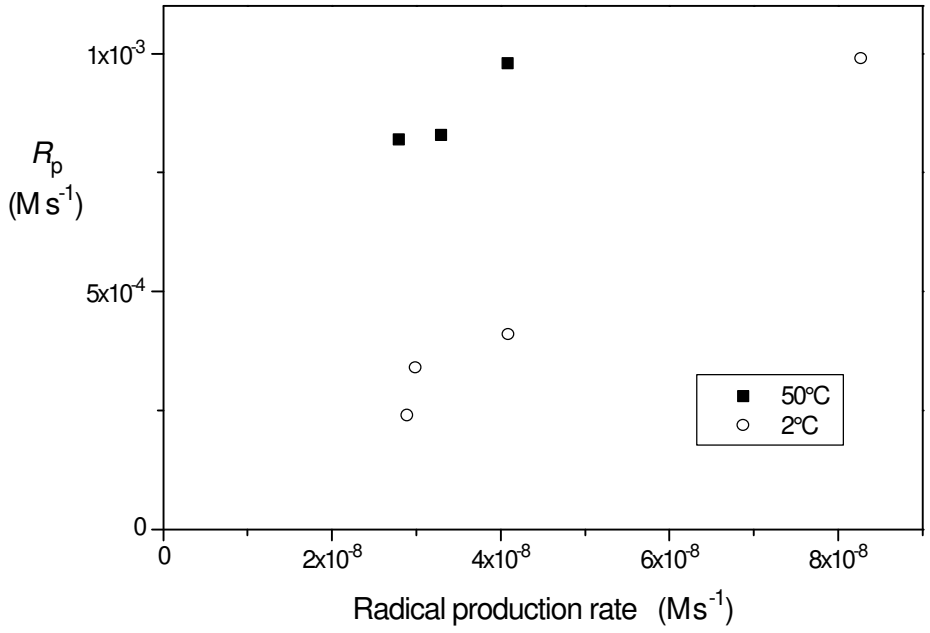

Figure 3.13: Polymerization rates of γ-initiated, VAc emulsion polymerizations as function of temperature and radical production rate. Radical production rate calculated from radiation chemical yield (equation 3.10, experiments C1-3, H1-3, US1; details: table 3.3).

3.4 Experimental II - vinyl acetate copolymerization

VAc was copolymerized with VnD in an attempt to reduce relaxation rates and thereby obtain more reliable data for higher temperatures. The reasoning behind this was as follows.

VnD is expected to have similar reactivity to VAc (except perhaps for a higher rate coefficient for transfer to monomer due to the greater number of alkyl hydrogens). However, transfer to VnD is not likely to lead to exit, due to its very low water solubility (figure 2.2). Dilution of the VAc with VnD was expected to reduce the relaxation rate as radical loss in the former was presumed to depend on exit of transferred radicals and subsequent termination.

3.4.1 Materials and methods

Choice of seed - measurement of C_p^{sat}

In order to choose an appropriate seed for the copolymerization (i.e. one which was swollen by both monomers), C_p^{sat} was determined for VAc and VnD in both pVnD and pVAc seeds. Latex particle sizes were measured by photon correlation spectroscopy (PCS) in pure water and in water saturated with monomer. The instrument used was a Malvern Instruments System 4700c (25°C, 15 mW, 488 nm).

It was found that a 127 nm diameter poly(vinyl neo-decanoate), pVnD, seed latex was swelled to 139 nm by VAc. However, 113 nm diameter pVAc seed latex was only swelled to 117 nm by VnD. Hence, C_p^{sat} for VAc in pVnD was 2.5 M while C_p^{sat} for VnD in pVAc was negligible. Therefore, a pVnD seed was used for the emulsion copolymerization.

It may be noted that this method is considered to be only approximate as C_p^{sat} calculated in this manner has a 3rd order dependence on the swollen particle diameters determined by PCS. However, it was found to be adequate for the purpose of selecting a suitable seed.

Experimental methods were the same as for the previous section except that VnD was distilled under partial vacuum. The recipe for experiment J1 is given in table 3.4.

Seed J was prepared by R. Balic, University of Sydney, in two stages, a nucleation stage and a particle growth stage. To Milli-Q water (800 ml) was added Dowfax surfactant 2A1 (1.25 g) and distilled VnD (30.4 g). This was emulsified and heated to 85°C. Next was added potassium persulfate (0.5 g), potassium hydrogencarbonate

(0.2 g) and sodium bisulfite (0.05 g) dissolved in water (30 ml). The mixture was kept at 85°C for one hour then at 60°C for four hours.

Second stage monomer was added (130 g) and the reaction mixture held at 55°C for 66 hours with potassium persulfate (0.1 g) added after 18 hours and again after a further 24 hours. Finally, the reaction mixture was held at 75°C for 24 hours. The solids content was 7.4% and particle size was 127 nm diameter measured by PCS as described below.

Table 3.4: Recipes for VnD γ copolymerization and homopolymerization relaxation experiments

Expt. #	J1	J2
temperature (°C)	2	2 – 20
γ dose rate (Gy s^{-1})	0.089	0.089
reactor vol. (ml)	60.0	60.0
AMA-80 (g)	0.125	0.156
CH_3COONa (g)	0.1059	0.114
H_2O (g)	54.2	53.4
vinyl acetate (g)	0.20	-
vinyl neo-decanoate (g)	2.01	2.44
seed solids (g)	3.32	3.70

3.4.2 Results and Discussion

Figure 3.14 shows a typical relaxation for the VnD/VAc copolymerization. Comparison with figure 3.9, shows that the radical-loss rate has not been changed significantly by the substitution of 90% of the VAc with VnD.

This is difficult to reconcile with the physical properties of VnD and the known parameters of the emulsion polymerization. VnD must have a low exit rate and VAc should provide high entry efficiency, $\bar{n}$ is low, (which mitigates against intra-particle termination) yet the radical-loss rate is high. This is suggestive of an artefact affecting the experiment. Whether this was due to VAc or vinyl esters generally was tested in the next section.

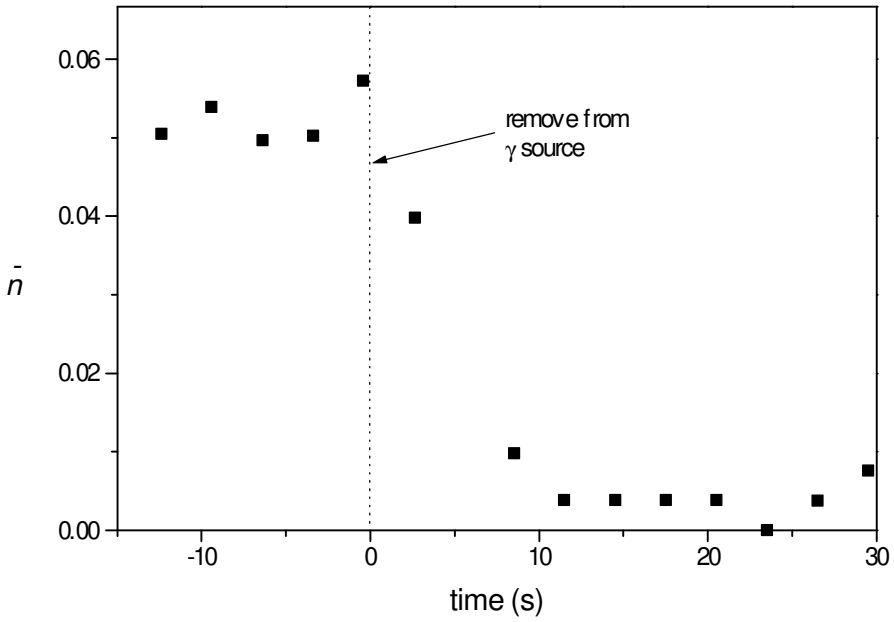

Figure 3.14: VnD / VAc emulsion copolymerization γ relaxation at 2°C, expt. J1, no correction for "heat effect" required.

3.5 Experimental III - vinyl neo-decanoate polymerization

In order to remove any possibility that the unexpected results of the previous section could be due in some way to the presence of VAc, γ relaxations were conducted on a VnD homopolymerization.

3.5.1 Materials and methods

Experimental methods were the same as for the previous section. The same pVnD seed was used and the recipe for the polymerization can be found in table 3.4, expt. J2.

C_p^{sat} for VnD in pVnD was determined by the PCS method (section 3.4.1) and found to be 1.8 M. A more accurate determination was undertaken by Balic[31] who obtained a value of 2.2 M using the creaming/GC method. This reasonable agreement supported the use of the PCS method in the previous experimental section.

3.5.2 Results and Discussion

In figure 3.15 it is evident that VnD relaxes on the same timescale as VAc (compare with figure 3.9).

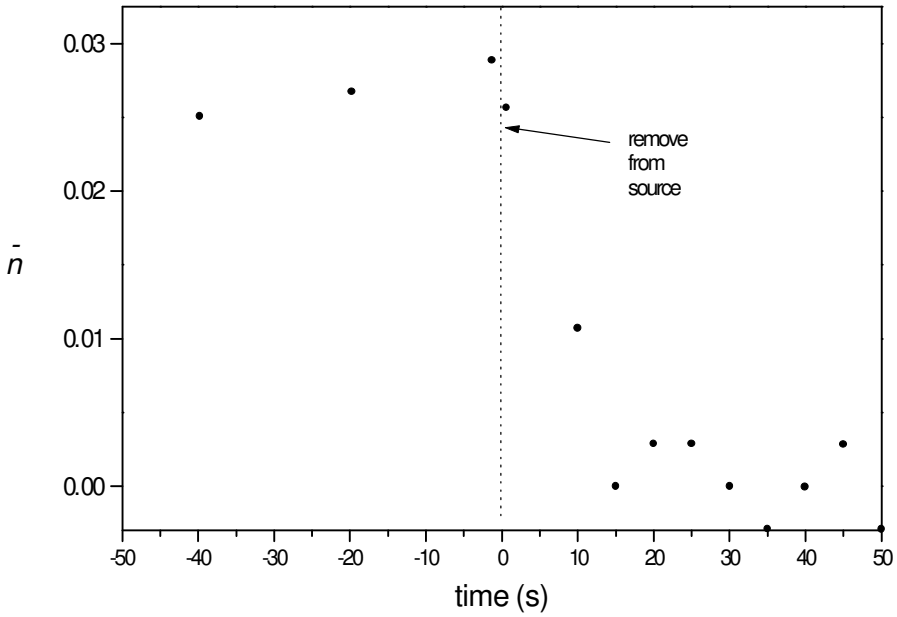

Figure 3.15: Vinyl neo-decanoate γ relaxation at 2°C, expt. J2, no correction for "heat effect" required. Noise magnified by differentiation of conversion data.

Figure 3.16 shows that, in the γ-initiated emulsion polymerization of VnD, the polymerization rate is independent of monomer concentration and temperature, at least over the range 2-20°C.

The rapid relaxation observed for VnD is difficult to explain without invoking the possibility that an experimental artefact, not observed in previous γ relaxation studies on styrene and MMA, may be responsible for the rapid relaxations observed in this work.

One can only speculate as to the nature of the artefact. It may be that an unreactive radical produced directly by interaction with a γ photon behaves as a spin trap. Recall the discussion of the reactivity of the radicals formed by chain transfer towards VAc monomer (section 2.3.1.7).

Similarly, hydrogen abstraction by one of the extremely reactive primary radicals created by the γ radiation may create unreactive radicals, possibly at the particle-water

interface. Rate coefficients for some possibly relevant hydrogen abstraction reactions are given below (M^{-1} s^{-1})[95]:

$OH\bullet + CH_3CO_2CH_2CH_3 \rightarrow CH_3CO_2\dot{C}HCH_3 + H_2O$ $\quad k = 4.0\times10^{8}$ 3.26

$OH\bullet + CH_3CH_2OH \rightarrow CH_3\dot{C}HOH + H_2O$ $\quad k = 1.9\times10^{9}$ 3.27

$OH\bullet + pVOH \rightarrow (CH_2\text{-}CH_2OH)_n\text{-}CH_2\dot{C}HOH\text{-}(CH_2\text{-}CH_2OH)_m$ $\quad k = 9.2\times10^{10}$ 3.28

$OH\bullet + HOCH_2CH_2OH \rightarrow HO\dot{C}HCH_2OH + H_2O$ $\quad k = 1.8\times10^{9}$ 3.29

As pVOH (reaction 3.27) is likely to be found at the particle-water interface, the extremely high rate coefficient for this reaction is of particular interest. Furthermore, the principle that readily formed radicals tend to be relatively stable suggests that the radical so formed might be quite stable and therefore, potentially unreactive.

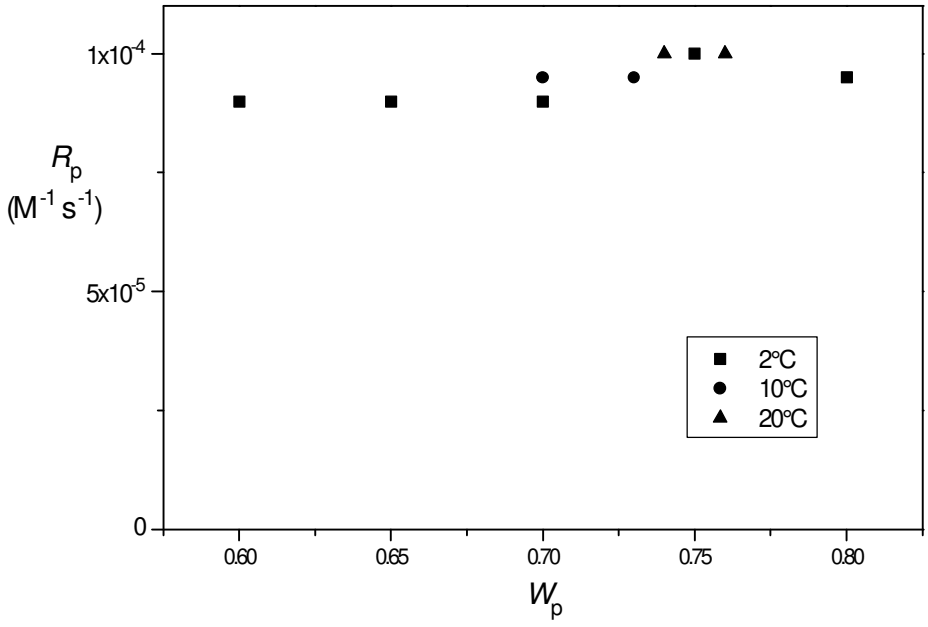

Figure 3.16: Vinyl neo-decanoate interval III γ-initiated polymerization showing rate as a function of W_p and temperature, expt. J2.

3.6 Conclusions

The rapid relaxations observed for VAc did not exhibit the dependence on temperature predicted by the proposed model. The large uncertainties in the data obtained at higher temperatures prevent any more quantitative assessment than this.

The rapid relaxations observed for VnD are very surprising, as they suggest that the termination mechanism, which is probably the same for VAc, involves transfer but not exit and may include an artifact of the γ radiolysis.

The next step may be photolysis relaxations which, even though they suffer from problems of inhomogeneous aqueous-phase radical distribution, may avoid some of the problems associated with γ irradiation of vinyl esters.

-oOo-

4 Persulfate-Initiated Emulsion Polymerization of Vinyl Acetate

4.1 Introduction

This section of the work combines the insource rate data from the γ radiolysis experiments of the preceding chapter with data from experiments described below to clarify some aspects of the persulfate-initiated emulsion polymerization of VAc. Specifically examined are (a) the order of dependence of rate of polymerization on initiator concentration, (b) the mechanism of the induced decomposition of persulfate by VAc and quantification of the rate coefficient for same, (c) kinetics of retardation by traces of dissolved oxygen and (d) the effect of acetaldehyde.

The original aim of the γ-radiolysis experiments of the preceding chapter was to determine the kinetics of radical loss in the emulsion polymerization of VAc. This was then to be applied to a study of the industrially important persulfate-initiated system. In order to reconcile the high radical-loss rates measured in the γ relaxation experiments with the rate of polymerization measured in persulfate-initiated experiments, it was necessary to quantify the rate of radical production in the persulfate-initiated system. This, then, was the primary aim of the work discussed in the present chapter.

Unfortunately, it was found as a result of these studies that the radical loss rates determined by γ radiolysis of vinyl esters cannot be applied to chemically initiated systems, for reasons discussed in the previous chapter. However, some useful insights may be gained by comparison of the γ-initiated rate data with those from persulfate-initiated experiments (section 4.3). Of particular interest in this regard is the possibility of elucidating the mechanism of the induced decomposition of persulfate by VAc.

As with nearly every aspect of the literature on VAc emulsion polymerization kinetics, the values reported for the order of dependence on initiator concentration vary widely. For example, at 50°C some reported values are 0.5[102], 0.72 [8] and at 60°C they range from 0.6[103] to 1.0[9]. It seems unlikely that this variation could be due to widespread poor experimental practice. Such a variation is normal in many systems: e.g., in styrene, entry efficiency varies with N_c, and so the order of dependence on initiator concentration also depends on N_c. However, under normal emulsion polymerization

conditions, it is expected that VAc should exhibit 100% entry efficiency and so R_p should be independent of N_c.

The total lack of agreement between the reported values of the order of dependence on various system parameters extends to dependence on surfactant type and concentration, particle number concentration and even initial monomer concentration. This suggests that a process is occurring which affects the system's kinetics and which is sensitive to experimental conditions. Three possibilities were investigated in this work: (a) retardation by oxygen (section 4.3.3.2), (b) induced decomposition of persulfate (section 4.4) and (c) hydrolysis of VAc to produce acetaldehyde, which may act as a chain transfer agent or retardant (section 4.5).

4.2 The induced decomposition of potassium persulfate.

Morris and Parts[14] showed that 5×10^{-2} M VAc caused a fifty-fold increase in the decomposition rate of 0.1 M persulfate in aqueous solution at 50°C compared to the thermal decomposition rate in pure water. They offered no suggestions as to the mechanism of the induced decomposition or for the products formed. They did observe, however, that although all the monomer was consumed, no insoluble pVAc was formed, thereby supporting the notion of solubilised oligomers.

Dunn and Taylor[96] showed that, in the surfactant-free polymerization of an aqueous solution of VAc, a latex formed and its final particle number increased with persulfate concentration. Their explanation was the generally accepted notion that the charged end group derived from the initiator confers sufficient colloidal stability to form a stable latex. It is possible, however, that a subtle variation of this mechanism contributes to the formation of the latex. It seems likely that the formation of surface active aqueous-phase oligomers could be a much bigger factor in VAc emulsion polymerizations than is the case for most other monomers.

There are two reasons for this. One is that because of the high k_p and C_w^{sat} for VAc, aqueous-phase oligomers grow to a surface-active size quickly and efficiently. This might be expected to produce a significant number of surface active oligomers that may facilitate particle formation which, in turn, may contribute to the variability of the reported dependence of polymerization rate on persulfate concentration.

The other significant feature of VAc in this regard is that the induced decomposition of persulfate by VAc may produce many more aqueous-phase oligomers than is the case for other common monomers. This proposal is examined in section 4.4.3 where a

model is developed that estimates the increase in the rate of production of aqueous-phase oligomers due to induced decomposition of persulfate.

Uncertainty as to the mechanism of induced decomposition of persulfate also raises the possibility of a potentially large increase in the rate of radical production. Induced decomposition of persulfate has been observed for many monomers; however the effect is greatest for the more water-soluble monomers. Morris and Parts[14] gave pseudo-first-order rate constants for the induced decomposition of persulfate at 50°C by 0.05 M monomer in aqueous solution, for acrylonitrile, methyl acrylate and VAc as 6.8×10^{-6} s^{-1}, 7.8×10^{-6} s^{-1} and 7.0×10^{-5} s^{-1} respectively, compared to 1.4×10^{-6} s^{-1} for persulfate in pure water, an increase by a factor of fifty in the case of VAc. Patsiga[104] found an increase by a factor of ten in the emulsion polymerization of VAc at 60°C. Subsequently, Litt and Chang[105] found the increase to be about a factor of four in the emulsion polymerization of VAc. The rates of induced decomposition in solution and emulsion polymerization can not be compared directly as many of the aqueous phase oligomeric radicals may be swept up by particles. Finally, Henton et al.[15] found a factor of two to seven, depending on the degree of neutralisation, for acrylic acid.

The other chemical process that has been considered as a potential source of "bad" behaviour is the hydrolysis of VAc. This is taken up in section 4.5.

4.3 Experimental I – dependence of polymerization rate on persulfate concentration

4.3.1 Aim

The aim of this section of the work was to determine whether the induced decomposition of persulfate proceeds by a radical-producing pathway. The first set of experiments was to establish the order of dependence of polymerization rate on persulfate concentration. This was necessary, not to provide the literature with yet another set of contradictory rate-dependence data, but to establish the rate dependence for a system employing the same ingredients and methodology as for the γ relaxation experiments of the previous chapter. A comparison of polymerization rates of the persulfate-initiated system with the rates in the γ-initiated system, for which the rate of production of radicals is known (section 3.2.1.6) may indicate the rate of production of radicals in the persulfate system. A simple model for retardation by dissolved oxygen is also developed.

4.3.2 Materials and methods – experiments G1 – G5.

The experiments in this part of the work were seeded homopolymerizations carried out at 50°C varying the persulfate concentration over nearly two orders of magnitude. As was the case for the γ-initiated experiments of the previous chapter, these polymerizations were commenced in interval III.

The seed latex was prepared as described in section 3.3.2.5, seed G being used for this set of experiments (see table 3.1 for seed recipe). Monomer was purified as described in section 3.3.2.4. The emulsifier was AMA-80, used as obtained from Cyanamid. Sodium acetate (Aldrich) was used as buffer because the more common choice of buffer, sodium bicarbonate, was found to evolve bubbles in the presence of VAc and persulfate. As the polymerization rate was to be measured by dilatometry, bubbles could not be tolerated.

One experiment (H4) was run using hydrogenphosphate/dihydrogenphosphate buffer (Aldrich, molar ratio HPO_4^{2-}:$H_2PO_4^-$ 0.63:1 - pH=7.0) to check that there was no peculiar behaviour related to the use of acetate buffer. Milli-Q water (18.2 M Ω cm^{-1}) degassed by boiling under a partial vacuum was used throughout. The initiator was potassium persulfate (Aldrich) recrystallised from a saturated aqueous solution at 30°C to which was added ethanol and the solution cooled in an ice bath.

The procedure was as follows: a thermostatted 62.6 ml dilatometer was charged with sodium acetate (0.12 g) and AMA-80 (0.12 g) dissolved in water (12 g). To this was added VAc (7.5 g), the mixture was then emulsified under partial vacuum by stirring with a magnetic bar. pVAc seed (40 g – 7.2 g solids) was added and the mixture allowed to swell under partial vacuum at 50°C for 30 minutes. The seed used (seed G, table 3.1) had a number average particle diameter of 102 nm (determined by CHDF as described in section 3.3.2.5) giving a particle number concentration of 2.3×10^{17} dm^{-3}. In order to prevent loss of monomer, the vacuum line was attached to the dilatometer via a valve, which was closed after a few seconds and remained closed during the emulsifying period. This process was repeated for the swelling period. Potassium persulfate (~0.1-2 g) was dissolved in water (~20 ml) and 1.00 ml injected into the dilatometer. The capillary was then fitted and water added to the appropriate meniscus height.

Meniscus height was monitored automatically as described in section 3.3.3 and converted to conversion as a function of time by the software described in section 3.3.4.

4.3.3 Results and discussion

Polymerizations were monitored to about 95% conversion. Some polymerizations were allowed to run for a further 20 hours during which time the polymerization rate was about 0.1% h^{-1}, ultimately reaching conversions of over 98% (figure 4.1).

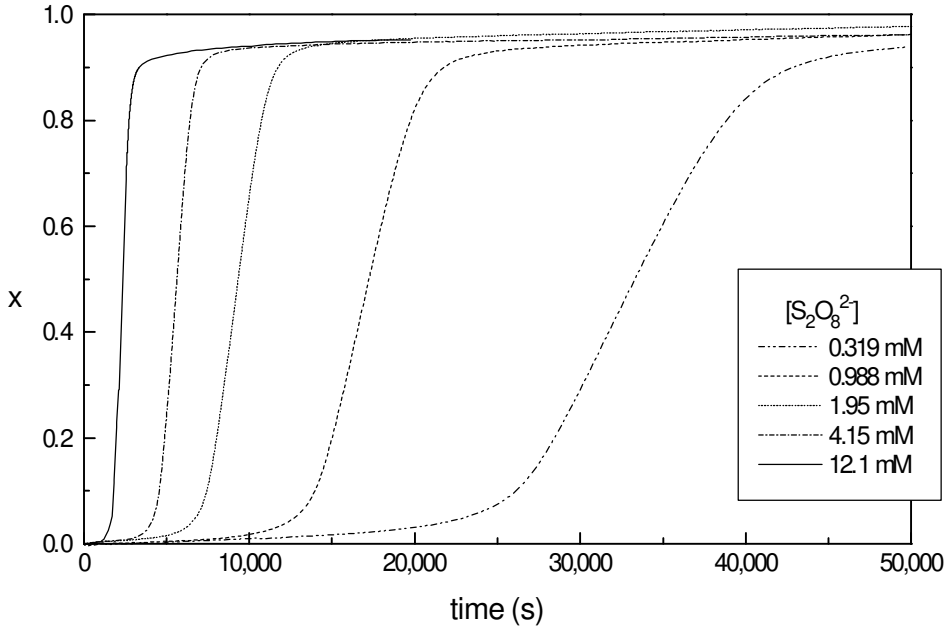

Figure 4.1: Conversion, x, as function of time and persulfate concentration for series of interval III, seeded homopolymerizations. Experiments G1-5, 50°C, details: section 4.3.2.

The main features of VAc emulsion polymerizations are clearly seen in figure 4.1. These are: an induction period that was approximately inversely proportional to the initiator concentration, a retardation period which also decreased with increasing initiator concentration and a steady-state rate which was nearly constant until the rate decreased abruptly at high conversions. The steady-state rate will be considered first, the induction and retardation periods are discussed in section 4.3.3.1 and the decreasing rate at high conversions is discussed in section 4.3.3.3.

In figure 4.2 it is clear that R_p is nearly constant up to high conversions (except, perhaps, at the highest initiator concentration) despite the fact that the entire polymerization was conducted in interval III with a decreasing monomer concentration throughout.

The 95% confidence limits of the order of dependence of R_p on [I] (figure 4.3) is 0.80 ± 0.09. As the same R_p was observed for the experiment with phosphate buffer, it seems that acetate buffer has no undue effect on R_p.

The most useful result that can be claimed from this group of experiments is the comparison of the rate of polymerization in persulfate-initiated and γ-initiated emulsion polymerizations. It can be seen (figure 4.4) that the rates of polymerization are comparable for a γ-initiated emulsion polymerization with the same primary radical production rate as calculated for the thermal decomposition of persulfate.

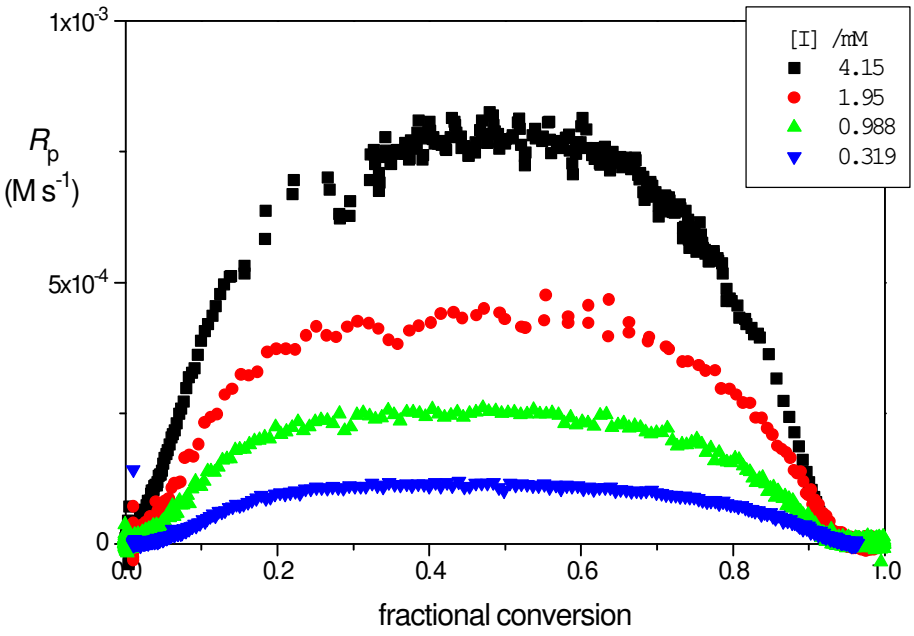

Figure 4.2: Polymerization rate, R_p as function of conversion and initiator concentration, [I], for VAc emulsion polymerizations initiated by potassium persulfate and commenced in interval III. Experiments G1-G4, 50°C (experimental details: section 4.3.2).

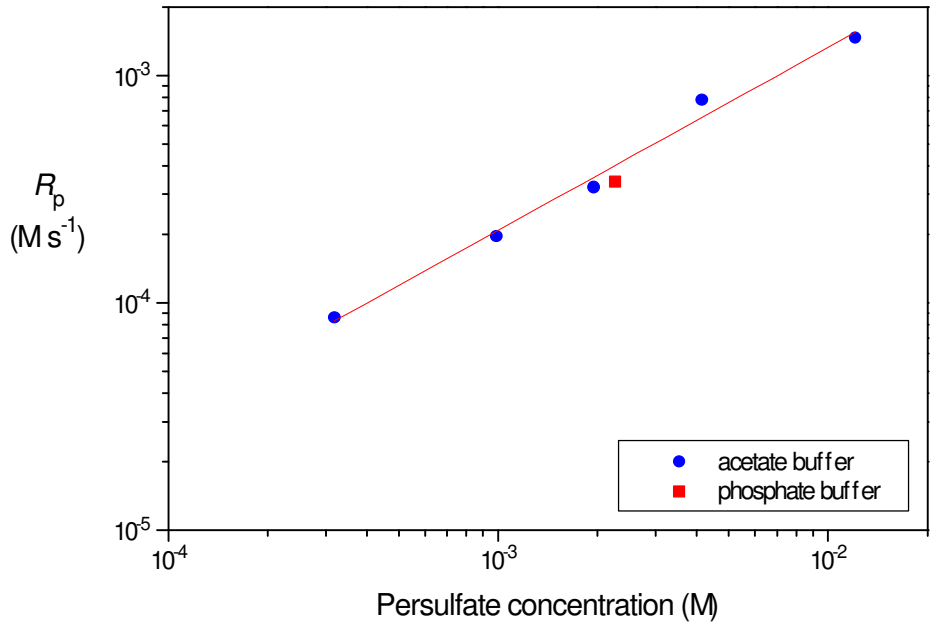

Figure 4.3: Steady-state, interval III polymerization rate of VAc emulsion polymerizations as function of potassium persulfate concentration at 50°C, experiments G1 – G5 (1), H4 (4), details: section 4.3.2.

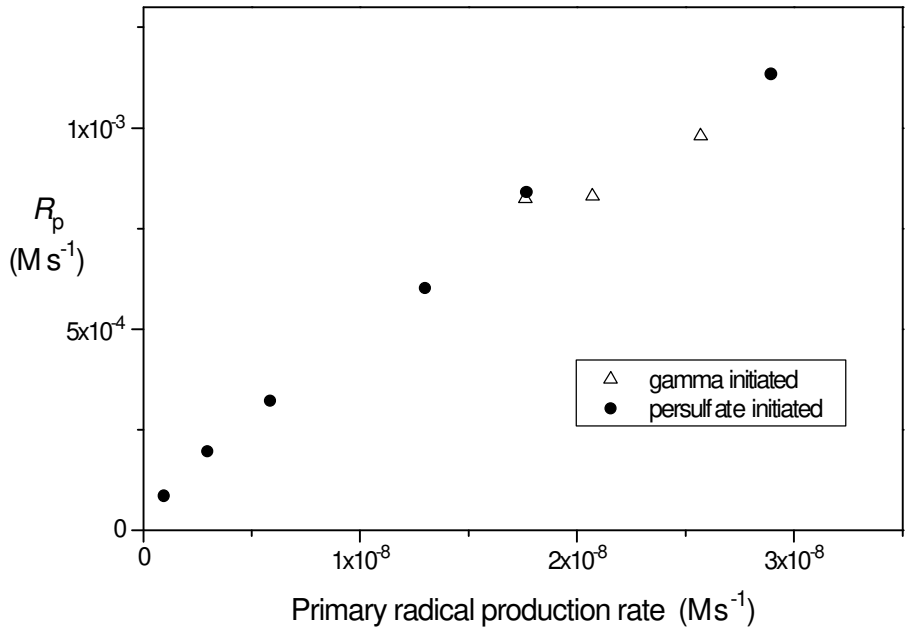

Figure 4.4: Comparison of R_p initiated by γ and persulfate at 50°C. Primary radical production rate calculated for γ by equation 3.10 and for persulfate using k_d = 1.4×10^{-6} s^{-1}.

This strongly supports a non-radical-producing mechanism for the induced decomposition of persulfate by VAc, which implies that the cage-complex mechanism is not significant. The most likely non-radical-producing mechanism is transfer to initiator and this is discussed in section 4.4. It also suggests that aqueous-phase bimolecular termination is a rare event at the aqueous-phase radical concentrations found under normal VAc emulsion polymerization conditions, in accord with equation 2.11. Otherwise, one would expect that the rate of polymerization for a persulfate-initiated emulsion polymerization would be less than that for a γ-initiated emulsion polymerization under conditions of equal rate of production of primary radicals. This is because the aqueous-phase radical concentration in the persulfate system should be much greater than that in the γ system, for two reasons. The first is that induced decomposition of persulfate by the transfer mechanism increases the time the initiator-derived oligomeric radicals spend in the aqueous phase as they may transfer many times before growing to *z*-mers. Secondly, z should be greater for the persulfate system than for the γ system because of the increased solubility conferred on the oligomers by the anionic sulfate end group.

4.3.3.1 Inhibition and retardation – elimination of the usual suspects

• *Persulfate*

As mentioned in section 4.3.3, an inhibition period was observed that was approximately inversely proportional to the initiator concentration. In the γ-initiated emulsion polymerizations of this work (see figure 3.1) and those reported by Stannett et al.[106], Sunardi[92] and Challa et al.[68] a similar retardation to that seen in persulfate-initiated emulsion polymerizations was observed during the initial irradiation period. This would seem to remove persulfate-related effects from consideration as the possible cause of retardation.

• *Kinetics – barrier to entry?*

In the γ relaxations carried out in this work the subsequent insertions (figure 4.5) show virtually no retardation which suggests that the *initial retardation is not due to any kinetic effects such as a barrier to entry*. The rate data presented in figure 4.5 were acquired at 2°C. At this temperature the "heat effect" was minimal and it can be seen that a steady-state rate was attained in about 10 seconds.

The slight initial curvature evident in the subsequent insertions of figure 3.1 is due to the heat effect described in section 3.3.6. In this case it has the opposite effect to that during relaxations in that the onset of polymerization releases heat of reaction that raises the temperature and causes the reaction mixture to expand until a new steady-state temperature is reached. This was unavoidable at 50°C.

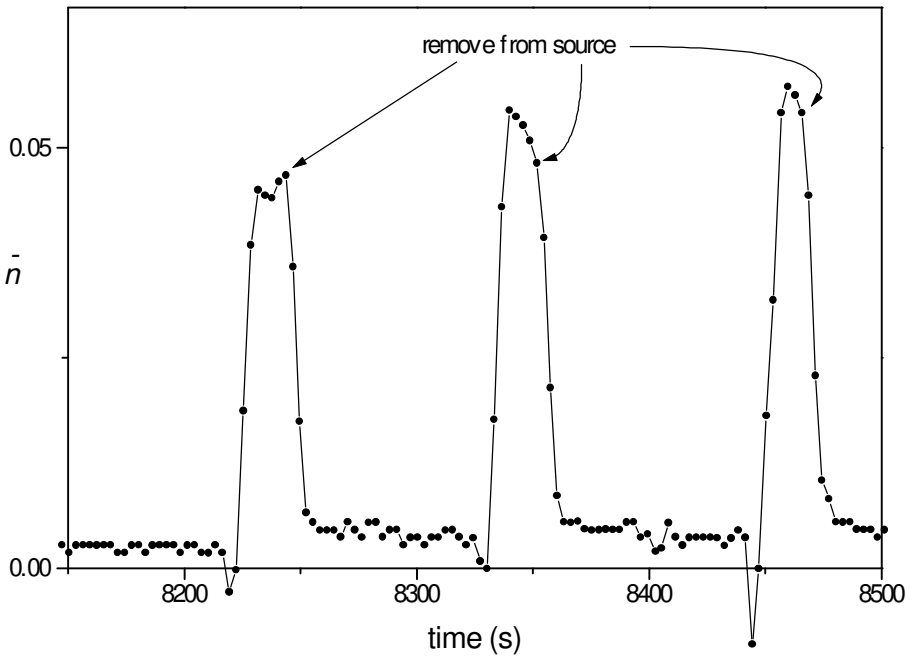

Figure 4.5: $\bar{n}$ as function of time for typical VAc emulsion polymerization initiated by γ radiolysis showing absence of retardative kinetic processes. Experiment H2, 2°C, Dose rate = 0.029 Gy s^{-1} (experimental details: table 3.2).

• *Acetaldehyde*

It is well known that VAc hydrolyses readily to produce acetic acid and acetaldehyde. Acetaldehyde may be susceptible to transfer reactions and/or co-polymerization. Presumably the co-polymerization is the addition reaction of the pVAc macroradical with the enol form of acetaldehyde, vinyl alcohol, although the enol is only present as a minute fraction of the aldehyde concentration (reaction 4.1)[107] and acetaldehyde itself is only likely to form in small quantities.

$$CH_3CHO \quad CH_2{=}CHOH \qquad K_{eq}=2\times10^{-5} \qquad 4.1$$

However, as has been argued by Gilbert[13], reactive impurities existing at very low concentrations (of the order of particle concentrations, i.e. $<10^{-6}$ M or even of the order of aqueous-phase radical concentrations $<10^{-7}$ M) may impart significant kinetic effects and affect particle formation. Stickler and Meyerhoff[108] found that k_{tr} for MMA decreased by a factor of eight when extreme care was taken with purification procedures. The role of acetaldehyde is considered in detail in section 4.5.

4.3.3.2 Inhibition and retardation by oxygen

Dunn and Taylor[96] showed that the inhibition period was primarily due to dissolved oxygen. Furthermore, they showed that, apart from the length of the inhibition period, exclusion of oxygen had no other effect on the progress of VAc emulsion polymerization. In experiments G1 – G5 of this work the water was degassed and monomer distilled under nitrogen but oxygen was not rigorously excluded from the seed latex. It is also possible that oxygen may have dissolved in the emulsion while filling the dilatometer.

The inhibition period was followed by a retardation period that also decreased with increasing initiator concentration. There are several likely mechanisms of retardation in emulsion polymerizations, more than one of which may operate simultaneously. These include retardation by oxygen, which is generally considered to be an inhibitor but may, as is shown below, behave as a retardant. Polymerization may also be retarded by adventitious chain transfer agents that are very slow to reinitiate.

Dunn and Taylor[96] reported similar retardation behaviour to that shown in figure 4.1. They showed that the retardation was the same for polymerizations where oxygen had been rigorously excluded (by repeated freeze/thawing of the solution) as for polymerizations where no special effort was made to exclude oxygen.

Inhibition and retardation by oxygen is complicated by the possibility of reinitiation by hydrogen transfer or addition reactions as outlined by Moad and Solomon[60] who also state that oxygen facilitates chain transfer in VAc polymerization:

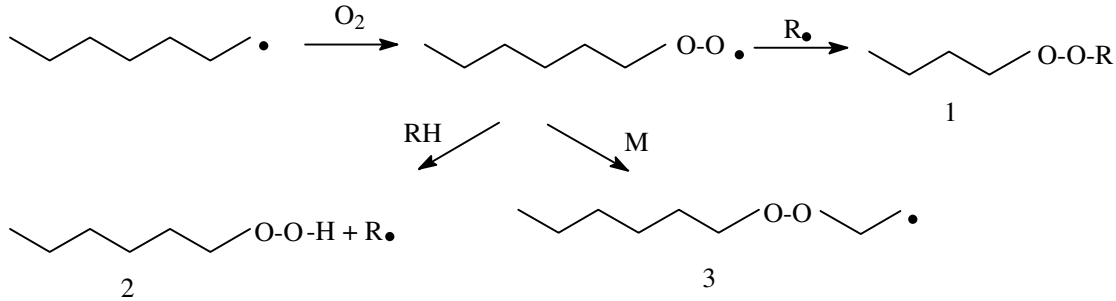

Figure 4.6: Retardation by oxygen.

However, as the rate of polymerization during the inhibition period was always very much smaller than after the retardation period, it seems reasonable to assume that during the inhibition period the vast majority of sulfato radicals are terminated before growing to *z*-mers. This is most likely to occur by reaction with oxygen followed by a bimolecular termination with another aqueous-phase oligomeric radical. Hence, it also seems likely that each oxygen molecule is responsible for the termination of two initiator-derived radicals.

As can be seen in figure 4.1, some polymerization occurs during the inhibition period. This suggests that oxygen is not a 100%-efficient inhibitor in VAc emulsion polymerizations. This may be due to either of the processes shown in figure 4.6. The hydroperoxide (1) produced in the hydrogen abstraction mechanism and the alkylperoxide (2) produced in the addition reaction may even generate extra radicals.

However, it is most likely that the main factor in the retardation of the emulsion polymerization of monomers with a high entry efficiency, such as VAc, is that a very small amount of residual oxygen may result in a situation where the formation of z-mers competes with aqueous-phase termination.

Ignoring the possible reinitiation processes, the competing reactions and rate coefficients at 50°C are:

$$^{-}SO_4M_i\bullet + T\bullet \xrightarrow{k_{t,aq}} {}^{-}SO_4M_iT \quad \ldots\ldots\ldots k_{t,aq} \approx 10^9\ M^{-1}\ s^{-1} \qquad 4.2$$

$$^{-}SO_4M_i\bullet + O_2 \xrightarrow{k_{t,O_2}} {}^{-}SO_4M_iO\text{-}O\bullet \quad \ldots\ldots\ldots k_{t,O_2} \approx 10^9\ M^{-1}\ s^{-1} \qquad 4.3$$

$$\downarrow T\bullet$$

$$^{-}SO_4M_iO\text{-}OT$$

$$^{-}SO_4M_i\bullet + M \xrightarrow{k_p^i} {}^{-}SO_4M_{i+1}\bullet \quad \ldots\ldots\ldots k_p^i \approx 6.7\times10^3\ M^{-1}\ s^{-1} \qquad 4.4$$

For a range of normal VAc emulsion polymerization conditions a simulation based on detailed aqueous phase kinetics (see equations 4.9-4.17 below) gave $[T\bullet] < 10^{-9}$ M. Hence, $k_{t,O_2}[O_2] >> k_{t,aq}[T\bullet]$, so the main aqueous-phase radical loss mechanism will be via reaction 4.3. The probability of an aqueous-phase sulfato radical growing to a z-mer, f_{entry}, is then given by:

$$f_{entry} \cong \left\{\frac{k_{p,aq}[M_{aq}][M_i^\bullet]}{k_{t,O_2}[O_2][M_i^\bullet] + k_{p,aq}[M_{aq}][M_i^\bullet]}\right\}^{z-1} \qquad 4.5$$

$$\cong \left\{\frac{k_{p,aq}[M_{aq}]}{k_{t,O_2}[O_2] + k_{p,aq}[M_{aq}]}\right\}^{z-1} \qquad 4.6$$

Using values given above for these coefficients f_{entry} may be plotted as a function of $[O_2]$ and z (see figure 4.7 below).

Thus, at dissolved oxygen concentrations below about 10^{-6} M, inhibition ceases and the polymerization is retarded until $[O_2]$ drops below about 10^{-8} M. As O_2 is

consumed, f_{entry} increases and the rate of consumption of oxygen by initiator-derived radicals decreases according to:

$$\frac{d[O_2]}{dt} = - k_d \times [I] \times (1 - f_{entry}) \qquad 4.7$$

As discussed in section 2.3.1.7, radicals formed by transfer within the particles may exit occasionally. However, during the retardation period $N_c/N_A \approx [O_2]$ and as the particles are so much larger than oxygen molecules most exiting $M_{tr}^{\bullet}$ will re-enter and propagate. Hence, for the purposes of this discussion exiting $M_{tr}^{\bullet}$ can be ignored. Combining equations 4.6 and 4.7 gives the rate of depletion of $[O_2]$ as:

$$\frac{d[O_2]}{dt} = - k_d \times [I] \times \left\{ 1 - \left[\frac{k_{p,aq}[M_{aq}]}{k_{t,O_2}[O_2] + k_{p,aq}[M_{aq}]} \right]^{z-1} \right\} \qquad 4.8$$

Equation 4.8 was solved numerically for the range of initiator concentrations used in experiments G1 – G5 and also for a range of initial $[O_2]$. The results for f_{entry} so obtained (equations 4.6 and 4.8) are presented in figures 4.8 and 4.9.

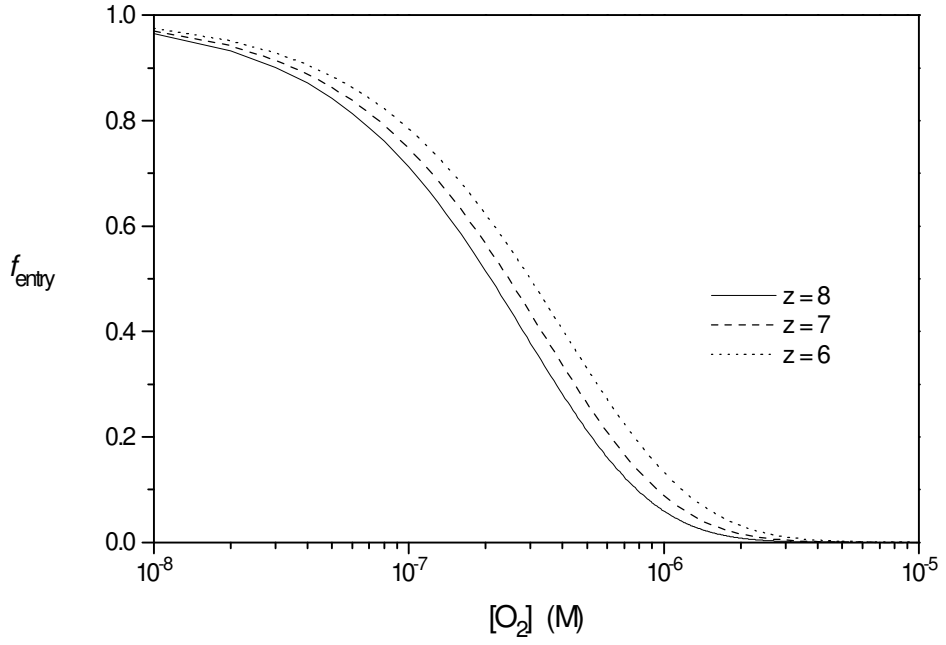

Figure 4.7: f_{entry} calculated as function of $[O_2]$ and z (equation 4.6) for VAc emulsion polymerization in interval II at 50°C, $k_p = 6.7 \times 10^{-3}$ M^{-1} s^{-1}, $[M_{aq}] = 0.3$ M, $k_{t,O_2} = 10^9$ M^{-1} s^{-1}.

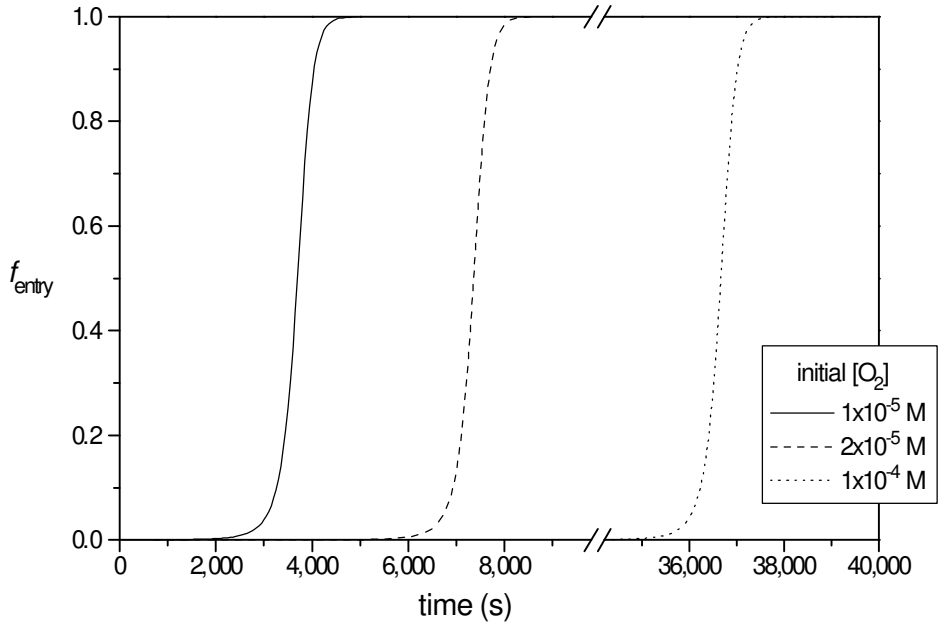

Figure 4.8: f_{entry} calculated as function of time and initial [O_2] for [I] = 1.95×10^{-3} M and $z = 6$ (equations 4.6 and 4.8). VAc emulsion polymerization, interval II, 50°C, $k_p = 6.7\times10^3$ M^{-1} s^{-1}, $[M_{aq}] = 0.3$ M, $k_{t,O_2} = 10^9$ M^{-1} s^{-1}.

The first thing to notice (figure 4.8), is that the entry efficiency is practically zero for a period proportional to initial [O_2] which corresponds to the inhibition period. Secondly, if the retardation period is defined as the period from the end of the inhibition period to a time at which R_p is close to its steady-state value, then it can be seen that the time taken for f_{entry} to increase from 0-100% (figure 4.8) is similar to the retardation period (figure 4.1, [I] = 1.95×10^{-3} M, expt. G3). Furthermore, it can be seen in figure 4.8 that the retardation behaviour is independent of initial [O_2], as expected, which is consistent with the observations of Dunn and Taylor[96].

If one relates f_{entry} to retardation then, from figure 4.9, the expected retardation due to dissolved oxygen can be estimated and compared to that observed in experiments G1-G5 (figure 4.1). These estimates are presented in table 4.1 where it can be seen that, given the uncertainty in the termination rate coefficients and the efficiency of termination by oxygen, the agreement is reasonable.

This may be only a lower limit for the retardation period as the reinitiation mechanisms of figure 4.6 and retardation by other species such as acetaldehyde have been ignored. More importantly, it shows that even if inhibition by oxygen is nearly 100% at moderate to high concentrations, eventually [O_2] will become low enough for

entry of z-mers to compete with termination. Furthermore, if formation of z-mers is efficient (high C_w and k_p) the oxygen retardation period can be quite long.

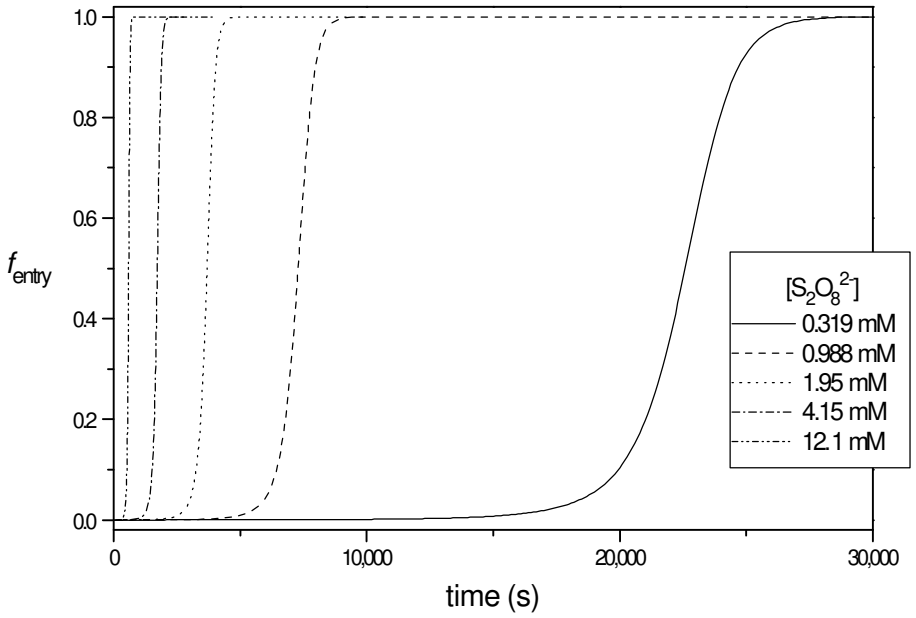

Figure 4.9: f_{entry} calculated as function of time and [I] for initial $[O_2] = 10^{-5}$ M and $z = 6$. VAc emulsion polymerization, interval II, 50°C, $k_p = 6.7\times10^3$ M^{-1} s^{-1}, $[M_{aq}] = 0.3$ M, $k_{t,O_2} = 10^9$ M^{-1} s^{-1}.

Table 4.1: Retardation of VAc emulsion polymerization by dissolved oxygen. 50°C, data from experiments G1-G5, details in section 4.3.2. Initial $[O_2]$ for calculations 10^{-5} M.

$[S_2O_8^{2-}]$ (M)	retardation period* (s)	
	experimental	calculated
3.19×10^{-4}	17,000	15,000
9.88×10^{-4}	6,000	5,000
1.95×10^{-3}	3,000	2,300
4.15×10^{-3}	2,000	1,300
1.21×10^{-2}	700	500

*retardation period as defined above, p97.

4.3.3.3 The decreasing polymerization rate at high conversions

Given that the rate of polymerization is independent of monomer concentration up to high conversion, the question arises as to why the rate decreases while there is still a substantial amount of monomer in the system. There are several possibilities to consider, two of which can be eliminated immediately; (a) limiting behaviour as $\bar{n}$ approaches 0.5, (b) decreased entry efficiency as C_w decreases.

(a) *limiting behaviour as $\bar{n}$ approaches 0.5*

It is clear from figure 4.10 that even though $\bar{n}$ increased throughout interval III, up to high conversion, it never approached the Smith-Ewart limiting case of $\bar{n} = 0.5$. Calculation of $\bar{n}$ from equation 2.16 requires the assumption that k_p is independent of C_p and hence of W_p. From the discussion in section 2.2.1.2 it is clear that in a rubbery system, such as VAc at 50°C, propagation does not become diffusion controlled until well beyond the conversions at which the decrease in both R_p and $\bar{n}$ are observed (figure 4.10). Thus, *the limiting behaviour of $\bar{n}$ can not be held to account for the decreasing polymerization rate observed at high conversions*.

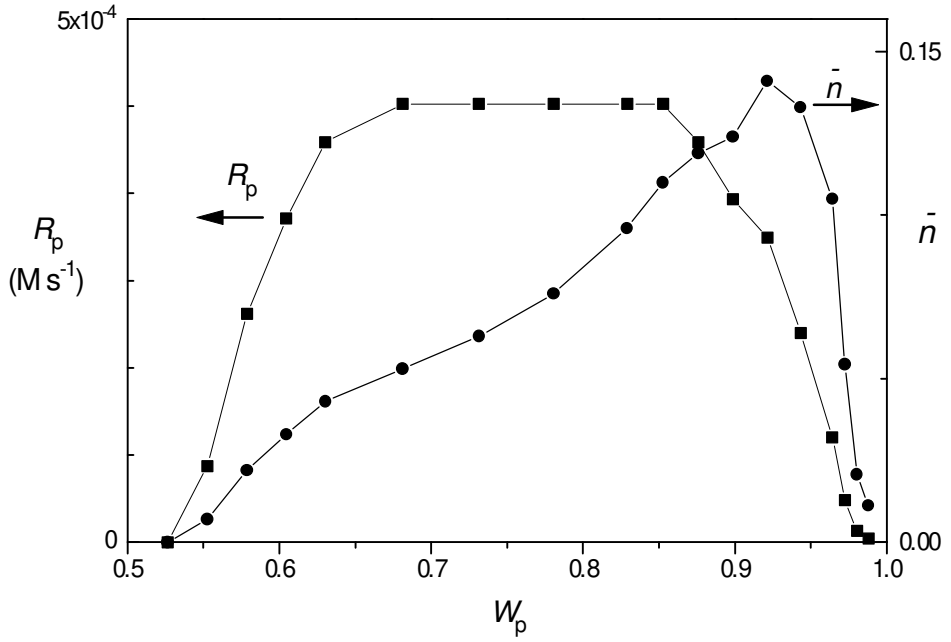

Figure 4.10: (4) - Polymerization rate, R_p, and (1) - average number of radicals per particle, $\bar{n}$, as function of weight fraction of polymer, W_p, for typical VAc emulsion polymerization initiated by potassium persulfate and commenced in interval III. Experiment G3, 50°C, $[K_2S_2O_8] = 1.95 \times 10^{-3}$ M. $\bar{n}$ calculated from equation 2.16 assuming k_p unaffected by W_p.

(b) *decreased entry efficiency as C_w decreases*

The entry efficiency, f_{entry}, is the proportion of initiator fragments produced by thermal decomposition of initiator that eventually, perhaps after many induced decomposition steps, grow to z-mers and enter particles.

As the entry efficiency, f_{entry}, is approximately z^{th} order in aqueous-phase monomer concentration, depletion of aqueous-phase monomer may contribute to the abrupt decrease in R_p at high conversion. This effect could be compounded in the VAc/persulfate system by the higher aqueous-phase oligomeric radical concentration resulting from the induced decomposition mechanism described in section 4.4.3. However, the simulation developed in section 4.4.3 shows that, at the persulfate concentrations used in normal emulsion polymerizations, the increase in the total aqueous-phase radical concentration due to induced decomposition is small. Furthermore, the amount of induced decomposition decreases with decreasing C_w and hence has a negligible effect on f_{entry} at high conversions.

The dependence of the experimentally determined R_p on C_w and the dependence of the calculated f_{entry} on C_w and z are shown in figure 4.11. (The dependence of f_{entry} on z is included as z is not accurately known. However, varying z over the range 6-12 has little effect on f_{entry}). It is clear that, for VAc emulsion polymerization at typical initiator concentrations (2×10^{-3} M in the case of figure 4.11), the experimental R_p begins to decrease well before the calculated f_{entry} decreases. C_w was calculated as a function of conversion from mass balance and the monomer partition equation 3.20. f_{entry} is given by equation 2.11.

For all persulfate-initiated emulsion polymerizations R_p began to decrease at a C_w of about 0.15 M and had decreased significantly before C_w decreased to 0.1 M. The calculated initiator efficiency is close to 100% when R_p is less than 10% of its maximum value. Hence, it is clear that the calculated decrease in f_{entry} due to the *decrease in C_w at high conversions is not responsible for the decrease in R_p at high conversion unless z is much higher than indicated by current theories and data.*

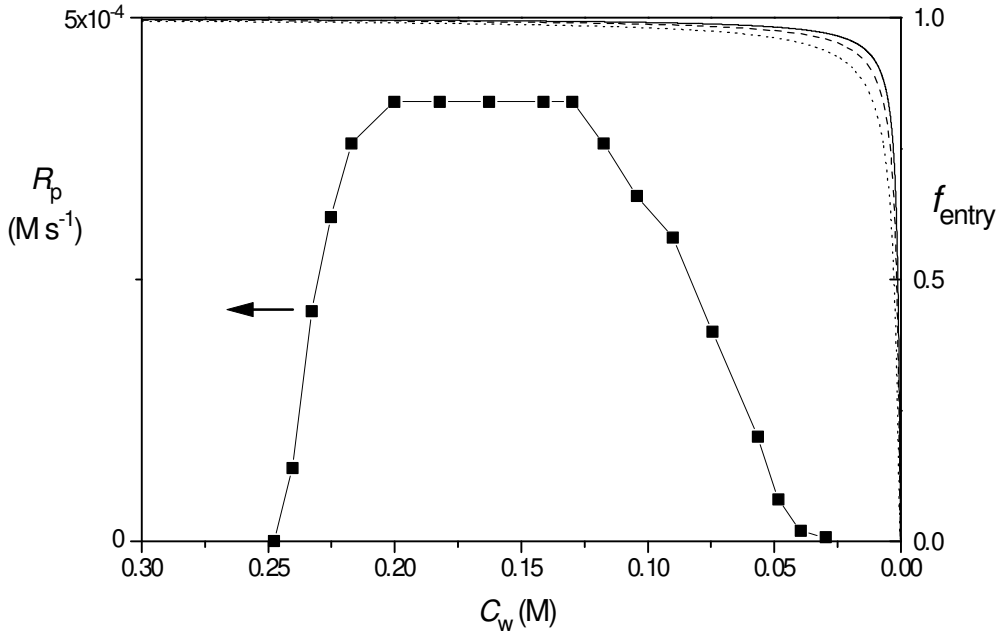

Figure 4.11: Experimental R_p (-4-) as function of C_w and calculated f_{entry} as function of C_w and z (—— z = 6, - - - z = 8, ····· z = 12) showing that decreasing f_{entry} is not the main cause of decreasing R_p at high conversion in VAc emulsion polymerization. R_p from experiment G3, Interval III, 50°C, $[S_2O_8^{2-}]$ = 1.95×10^{-3} M, f_{entry} calculated from equation 2.11 using k_d = 1.4×10^{-6} M^{-1} s^{-1} and $k_{t,aq}$ = 5×10^8 M^{-1} s^{-1}.

4.4 Experimental II – The role of aqueous-phase oligomers in the induced decomposition of persulfate.

4.4.1 Introduction

Many researchers have reported a high rate of induced decomposition of persulfate by VAc[14,59,105]. Two mechanisms have been proposed to account for the observed decomposition rates. They are: reduction by aqueous-phase oligomeric radicals, (which is essentially the "normal" mode of transfer to initiator) and the "cage-complex mechanism" whereby a polar scavenger such as VAc monomer may form a cage around a charged species such as the persulfate anion. It has been argued[17] that the high local concentration of scavenger due to a cage complex may result in the scavenging of sulfato radicals which would otherwise have undergone geminate recombination.

Sarkar[17] argued that a cage complex should give a radical production rate proportional to $[M_{aq}]^{1.5}[S_2O_8^{2-}]^{0.5}$. If radical production were dependent on $[M_{aq}]$ then the cage-complex mechanism predicts decreasing R_p in interval III. It can be seen in figure 4.2 (and the VAc literature) that this is clearly not the case.

The cage complex mechanism proposed by Sarkar[17] produces two "extra" radicals for each induced decomposition (equation 4.9).

$$S_2O_8^{2-} + M_{cage} \rightarrow {}^{-}SO_4M\bullet + SO_4^{\bullet-} \qquad 4.9$$

If this were the primary mechanism of induced decomposition of persulfate one might expect the rate of production of primary radicals to be about fifty times that calculated for the normal thermal decomposition of persulfate in order to account for the fifty-fold increase in the decomposition rate reported by Morris and Parts.

In the case of the cage complex mechanism most aqueous-phase termination must be "head-to-head" bimolecular termination of the aqueous-phase oligomeric radicals. This is easily seen by considering the following:

$$SO_4^{\bullet-} + M \xrightarrow{k_{p,I}} {}^{-}SO_4M\bullet \qquad k_{p,I} \approx 10^9\ M^{-1}\ s^{-1}\ [20]\ \text{at } 50°C. \qquad 4.10$$

$${}^{-}SO_4M\bullet + M \xrightarrow{k_p^1} {}^{-}SO_4M_2\bullet \qquad k_p^1 \approx 10^4\ M^{-1}\ s^{-1}\ \text{at } 50°C. \qquad 4.11$$

This value of k_p^1 is estimated from the long chain k_p and arguments based on transition state quantum calculations[109] that propose that k_p^1 is expected to be several times the long-chain k_p. There is also indirect evidence from model compounds[40] and empirical fits to experimental data (initiator efficiency in the persulfate/styrene system[110] and MWDs in PLP experiments[111]) that support this view.

$${}^{-}SO_4M_i\bullet + M \xrightarrow{k_p^i} {}^{-}SO_4M_{i+1}\bullet \qquad k_p^i = 6.7\times10^3\ M^{-1}\ s^{-1}\ \text{at } 50°C[33]. \qquad 4.12$$

As $k_{p,I} >> k_p^1 > k_p^i$ one can see that $[{}^{-}SO_4M_i\bullet] >> [SO_4^{\bullet-}]$ and, as there are no particles for the aqueous-phase oligomeric radicals to enter under the experimental conditions of Morris and Parts, the cage complex mechanism implies most radical loss is by head-to-head bimolecular termination of aqueous-phase oligomeric radicals. This was tested in experiment A4 and is discussed in section 4.4.3.2 where it is shown that no significant amount of head-to-head bimolecular termination occurred.

The reductive transfer mechanism is:

$$^{-}SO_4M_n\bullet + S_2O_8^{2-} \xrightarrow{k_{tr,I}} {}^{-}SO_4M_nSO_4^{-} + SO_4^{\bullet-} \qquad 4.13$$

$$M_{aq} \downarrow k_{p,I}$$

$$^{-}SO_4M\bullet$$

As can be seen from equation 4.13, the reductive transfer mechanism consumes persulfate but generates no "extra" radicals. Rather, it produces a large number of surface-active aqueous-phase oligomers. Recalling that under the conditions of Morris and Parts' experiment (50°C, $[S_2O_8^{2-}] = 0.1$ M) no insoluble polymer was formed, it follows that the aqueous-phase oligomers terminated before reaching j_{crit} and thereby remained in solution. In the case of the reductive transfer mechanism they would be expected to have propagated almost exclusively by the "normal" head–to–tail addition mechanism until they terminated by transfer to persulfate.

It was hoped to characterise the oligomers presumed to be formed in the aqueous phase by MALDI-TOF MS (Matrix Assisted Laser Desorption Ionisation – Time of Flight Mass Spectrometry) or electrospray MS. Unfortunately, the molecular weights of the oligomers formed by both of the proposed induced decomposition mechanisms are identical, so mass spectrometry can not distinguish between them. However, as little is known with any certainty regarding the composition of the aqueous-phase oligomers in the normal persulfate-initiated emulsion polymerization of VAc, it was hoped that some insight would be gained from mass spectrometric analyses. Finally, it was hoped that the molecular weight distribution of the aqueous-phase oligomers would be of use in determining the kinetics of the Morris and Parts induced decomposition experiment.

In experiment A1 and A3 samples of oligomers were prepared under the experimental conditions of Morris and Parts (very high persulfate concentrations) to investigate the induced decomposition of persulfate. Experiment A2 repeated A1 but at a lower persulfate concentration more akin to the conditions of a "normal" VAc emulsion polymerization. It was found that at lower persulfate concentrations latexes were formed (also seen by Dunn[96]) and subsequently oligomeric radicals must have entered particles and propagated. This was of interest in its own right, and is discussed further in section 4.4.3.1, but is of little use in the direct analysis of aqueous-phase oligomers. The mass spectra of the oligomers prepared in experiment A3 were obtained by electrospray MS.

In order to prevent the oligomeric radicals growing to a surface-active size at lower persulfate concentrations, experiment A4 incorporated a small amount of styrene that, because of its extremely unfavourable reactivity ratios with VAc, effectively "capped" the oligomeric radicals. The aqueous-phase oligomers were characterised by MALDI.

4.4.2 Materials and methods

Experiment A1:

Sodium persulfate (72.2 g) used as obtained from Aldrich (AR grade) was dissolved in Milli-Q water (3 dm^3, 18.2 M Ω cm^{-1}) at 50°C to give $[S_2O_8^{2-}]$ = 0.1 M and pH = 3.5. The water had been previously de-oxygenated by bubbling high purity nitrogen through for one hour. To this solution was added sodium hydrogencarbonate (4.8 g) dissolved in water (40 ml) to give pH = 7.4. VAc, purified as described in section 3.3.2.4, was added (12.3 g) and the solution held at 50°C under nitrogen with stirring for 160 minutes, during which time the pH decreased steadily to 6.3 and the smell of monomer disappeared.

Experiment A2:

Repeat of experiment A1 except that only 16.2 g sodium persulfate was used to give [I] = 0.022 M. In this experiment a latex formed, presumably stabilised by the large number of surface active oligomers produced under these conditions.

Experiment A3:

The aim of this experiment was to repeat experiment A1 except that ammonium persulfate was to be used as this would allow the subsequent removal of most of the inorganic material as follows: (1) Addition of a quantitative amount of iron(II) to reduce unreacted persulfate to sulfate followed by a quantitative amount of barium hydroxide to precipitate iron hydroxides and barium sulfate; (2) the remaining excess inorganic material, NH_4OH, is expected come off in the freeze-drier as NH_3 and H_2O leaving just the ammonium salts of the oligomers for analysis by mass spectroscopy.

Ammonium persulfate (6.83 g) used as obtained from Aldrich (AR grade) was dissolved in Milli-Q water (250 ml, 18.2 M Ω cm^{-1}) at 50°C to give $[S_2O_8^{2-}]$ = 0.12 M. The water had been previously de-oxygenated by bubbling high purity nitrogen through for one hour. VAc, purified as described in section 3.3.2.4, was added (2.2 g) and the solution held at 50°C under nitrogen with stirring for 160 minutes.

To this solution was added a solution of iron(II) sulfate ($FeSO_4.7H_2O$-16.68 g in 100 ml H_2O) to reduce unreacted persulfate to sulfate. To half of the resulting solution was added barium oxide (9.18 g in 100 ml H_2O) and the heavy precipitate consolidated by centrifugation. The supernatant was a pale yellow colour with a pH of 9.5. This was freeze dried to remove NH_4^+ and OH^- as NH_3 and H_2O. The resulting oily/resinous material redissolved readily in water.

Experiment A4:

Vinyl acetate (5.60 g), purified as described in section 3.3.2.4, and styrene (0.20 g) purified in the same way except under reduced pressure (53°C, 40 mmHg) were dissolved in Milli-Q water (280 ml, 18.2 M Ω cm^{-1}) at 70°C. The water had been previously de-oxygenated by bubbling high purity nitrogen through for one hour. To this solution was added a solution of sodium persulfate (2.70 g, used as obtained from Aldrich) in Milli-Q water (31.5 ml) to give $[S_2O_8^{2-}]$ = 0.036 M. The solution was held at 70°C under nitrogen with stirring for 10 minutes then cooled in an ice bath. Lead nitrate (3.755 g) dissolved in water (26 ml) was then added (this had previously been found to precipitate persulfate quantitatively) and the remaining monomer evaporated off under vacuum at 40°C. The final pH was 1.6. This was raised to 7 by the addition of sodium hydroxide (0.5 g) dissolved in Milli-Q water (10 ml).

The resulting solution foamed on shaking, the foam persisting for several minutes. This was presumed to be due to the formation of significant amounts of surface-active oligomers. Although many attempts were made to extract the oligomers prepared in experiments A1, A3 and A4 into organic solvents (chloromethane, toluene, ethyl acetate), none gave satisfactory results.

An extract of the crude oligomer solution (experiment A3) obtained by HPLC and submitted to MALDI-TOF MS analysis produced no useful spectra. A sample of the crude oligomer solution from experiment A4 was analysed by MALDI, the spectrum obtained is discussed in section 4.4.3.

4.4.3 Results and Discussion

Experiment A1 was a repeat of Morris and Parts' experiment. The kinetics of this system were modelled with the intention of explaining the absence of polymer in the solution polymerization of VAc at high persulfate concentrations and estimating a value for the rate coefficient for the induced decomposition of persulfate, assuming the reductive transfer mechanism for induced decomposition.

• S*imulation of oligomer distributions*

z is generally the degree of polymerization at which aqueous-phase oligomeric radicals attain sufficient surface activity such that they irreversibly enter a particle and so are lost from the aqueous phase. However, at high initiator concentrations, such as the conditions of Morris and Parts' experiment, there may be no particle formation and aqueous-phase oligomeric radicals are lost via bimolecular termination and via transfer to initiator. Hence, for the purpose of the following discussion, the definition of z will be broadened slightly to "the degree of polymerization above which a negligible proportion of aqueous-phase oligomeric radicals grow, either because they terminate in the aqueous phase or enter a particle".

The model was based on the following set of differential equations:

$$\frac{d[M_1^\bullet]}{dt} = 2k_d[S_2O_8^{2-}] + k_{tr,I}\sum_{i=2}^{z-1}[M_i^\bullet][S_2O_8^{2-}] - k_p^1[M_{aq}][M_1^\bullet] - k_{t,aq}[M_1^\bullet][T\bullet] \qquad 4.14$$

where k_p^1 is the propagation rate coefficient for one-mers, $k_{tr,I}$ is the rate coefficient for transfer to initiator, $[M_1^\bullet]$ is the concentration of aqueous-phase oligomeric radicals with degree of polymerization of one and $[M_i^\bullet]$ is the concentration of aqueous-phase oligomeric radicals with degree of polymerization i.

There is no term in equation 4.14 for radical loss resulting from induced decomposition by one-mers. One-mers lost in step one of reaction 4.13 (with n = 1) are immediately replaced in step two, as $k_{p,I} \approx 10^9$ M^{-1} s^{-1} [20] and $[M_{aq}]$ is typically greater than, say, 0.05 M for VAc.

$$\frac{d[M_i^\bullet]}{dt} = k_p[M_{aq}][M_{i-1}^\bullet] - k_p[M_{aq}][M_i^\bullet] - k_{t,aq}[M_i^\bullet][T\bullet] - k_{tr,I}[M_i^\bullet][S_2O_8^{2-}] \quad i = 2,..,z-1 \qquad 4.15$$

No allowance was made in the simulation for solvent effects on k_p or chain length dependence of k_p as these variables have not been quantified and, though they may have a significant effect on the average degree of polymerization of the oligomers, they have a negligible effect on the rate of induced decomposition. As a first approximation then, applying the steady-state assumption (and ignoring the effect of the solvent and chain-length dependence of some of the rate coefficients) yields the following:

$$[M_1^\bullet] = (2k_d[S_2O_8^{2-}] + k_{tr,I}\sum_{i=2}^{z-1}[M_i^\bullet][S_2O_8^{2-}]) / (k_p[M_{aq}] + k_{t,aq}[T\bullet]) \qquad 4.16$$

$$[M_i^\bullet] = k_p[M_{aq}][M_{i-1}^\bullet] / (k_p[M_{aq}] + k_{t,aq}[T\bullet] + k_{tr,I}[S_2O_8^{2-}]) \qquad i = 2,..., z-1 \qquad 4.17$$

Equations 4.16 – 4.17 were solved numerically (by iteration from an initial guess) for the conditions of experiment A1 and comparing with Morris and Parts' decomposition rate data. Considering that aqueous-phase termination in this system is between small species, an average value for $\langle k_{t,aq} \rangle = 5\times10^{8}$ M^{-1} s^{-1} seems reasonable. Adjusting $k_{tr,I}$ to give accord with the results of Morris and Parts gives a value of 3×10^{3} M^{-1} s^{-1} for $k_{tr,I}$ (figure 4.12) which is comparable to the value of 5×10^{3} M^{-1} s^{-1} reported for the acrylonitrile/persulfate system[112].

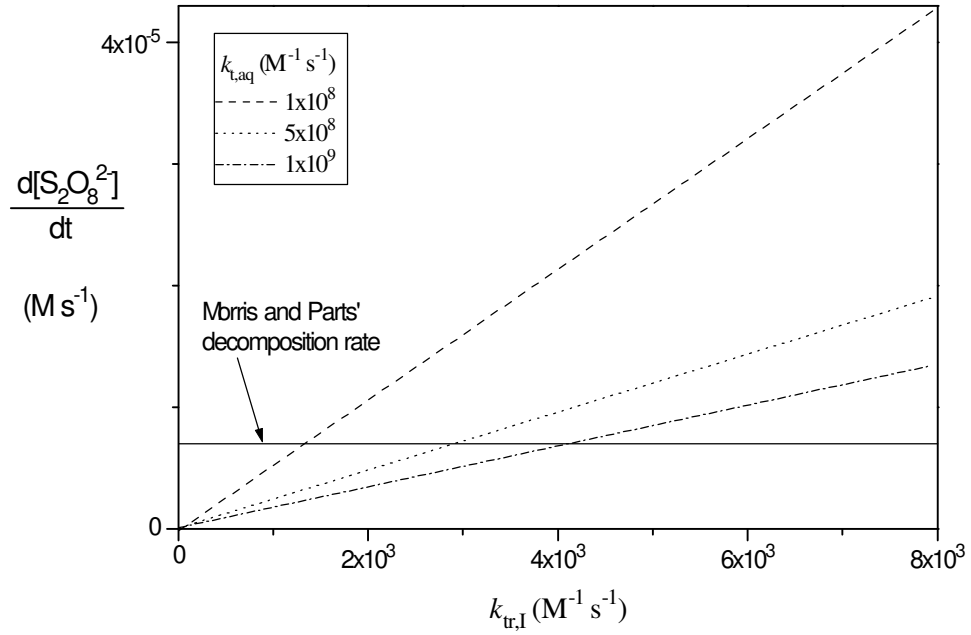

Figure 4.12: Calculated rate of consumption of persulfate as function of the rate coefficient for transfer to initiator, $k_{tr,I}$, compared with Morris and Parts' data[14]. Simulation based on equations 4.9 – 4.17. $[S_2O_8^{2-}]$ = 0.1 M, 50°C, [VAc] = 0.05 M.

The only adjustable input parameter is $k_{t,aq}$ and, as can be seen in figure 4.13, the order of dependence of the calculated value of $k_{tr,I}$ on $k_{t,aq}$ is approximately 0.49.

Under Morris and Parts' conditions, $k_{tr,I}[M_i^{\bullet}] \approx 50\times k_d = 7\times10^{-5}$ s^{-1}. The calculations thus yield $[SO_4^{\bullet-}] = 2.6\times10^{-14}$ M. At lower concentrations of initiator one would expect even lower concentrations of sulfato radicals. Calculated total radical concentrations are shown in figure 4.14 and range from 1×10^{-8} - 5×10^{-8} M. As this is more than five orders of magnitude greater than $[SO_4^{\bullet-}]$, the sulfato radicals will make a negligible contribution to bimolecular termination. This is as expected from the argument put forward in section 4.4.1.

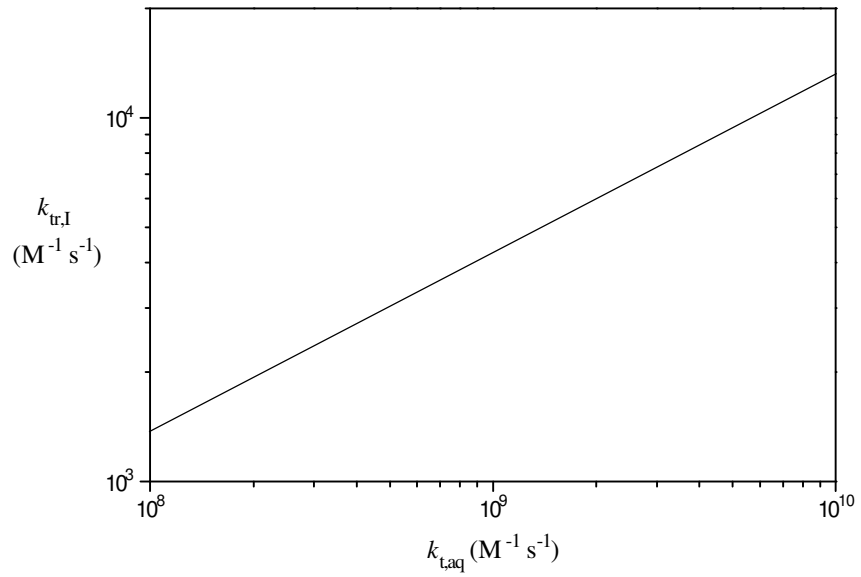

Figure 4.13: The dependence of the calculated rate coefficient for transfer to initiator, $k_{tr,I}$, on the assumed aqueous-phase termination rate coefficient, $k_{t,aq}$, slope = 0.49.

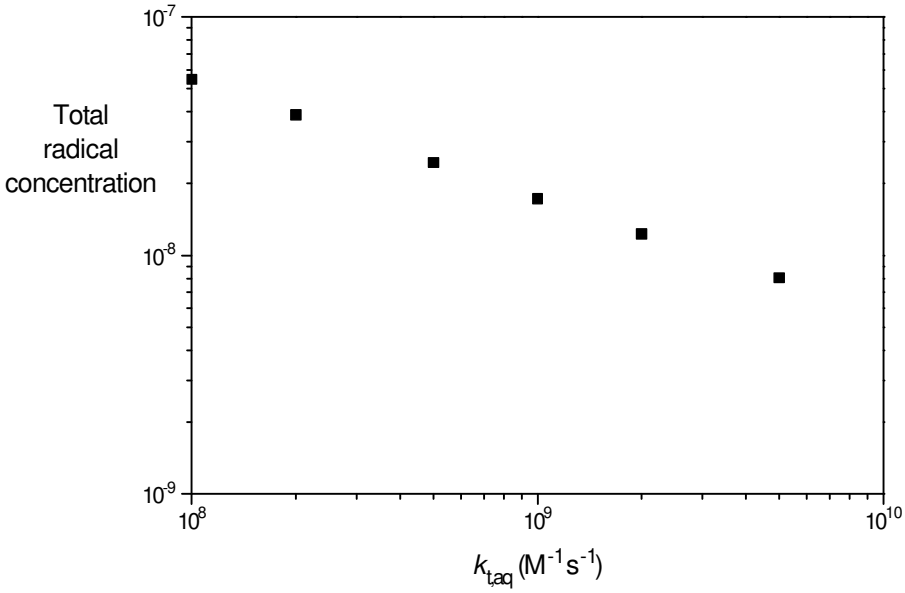

Figure 4.14: Calculated total radical concentration for solution polymerization of VAc (expt. A1) as function of $k_{t,aq}$. Simulation based on equations 4.9 – 4.17. [$S_2O_8^{2-}$] = 0.1 M, 50°C, [VAc] = 0.05 M.

The probability of an *i*-meric aqueous-phase radical terminating is given by:

$$P_{\text{term}}^{\,i} = \frac{k_{t,aq}[M_i^\bullet][T\bullet] + k_{tr,I}[M_i^\bullet][S_2O_8^{2-}]}{k_{t,aq}[M_i^\bullet][T\bullet] + k_{tr,I}[M_i^\bullet][S_2O_8^{2-}] + k_{p,aq}^{\,i}[M_i^\bullet][M_{aq}]} \qquad 4.18$$

where $k_{p,aq}^{\,i}$ is the propagation rate coefficient for an aqueous-phase i-mer. For the high persulfate concentrations (>0.02 M) of this part of the work $[T\bullet] < 2\times10^{-9}$ M and so, for any reasonable value of $k_{t,aq}$:

$$k_{tr,I}[M_i^\bullet][S_2O_8^{2-}] >> k_{t,aq}[M_i^\bullet][T\bullet] \qquad 4.19$$

Hence, equation 4.18 simplifies to:

$$P_{\text{term}}^{\,i} \cong \frac{k_{tr,I}[S_2O_8^{2-}]}{k_{tr,I}[S_2O_8^{2-}] + k_{p,aq}^{\,i}[M_{aq}]} \qquad 4.20$$

Equation 4.20 presents a more comprehensible physical picture of the important events that determine whether aqueous-phase oligomeric radicals will grow to a length that will confer sufficient surface activity to induce particle formation.

Results of the simulation are presented in figure 4.15 which shows the degree of polymerization below which more than 95% of aqueous-phase oligomeric radicals terminate, as a function of the assumed value of $k_{t,aq}$. As discussed in section 4.4.1, most termination is by transfer to initiator resulting in aqueous-phase oligomers with two sulfato end groups.

If it is assumed that sufficient surface activity to guarantee entry of a singly anionically charged oligomeric radical is only attained with a degree of polymerization greater than about eight (as predicted by equation 2.10), then it seems reasonable to suggest that the aqueous-phase oligomers terminated by transfer to initiator will remain soluble with degrees of polymerization up to about 16, as they will include two anionic groups. Clearly, over a large range of values of $k_{t,aq}$ (figure 4.15), not many surface active aqueous-phase oligomers would be expected to form under the experimental conditions of Morris and Parts, which explains why no latex formed under their conditions.

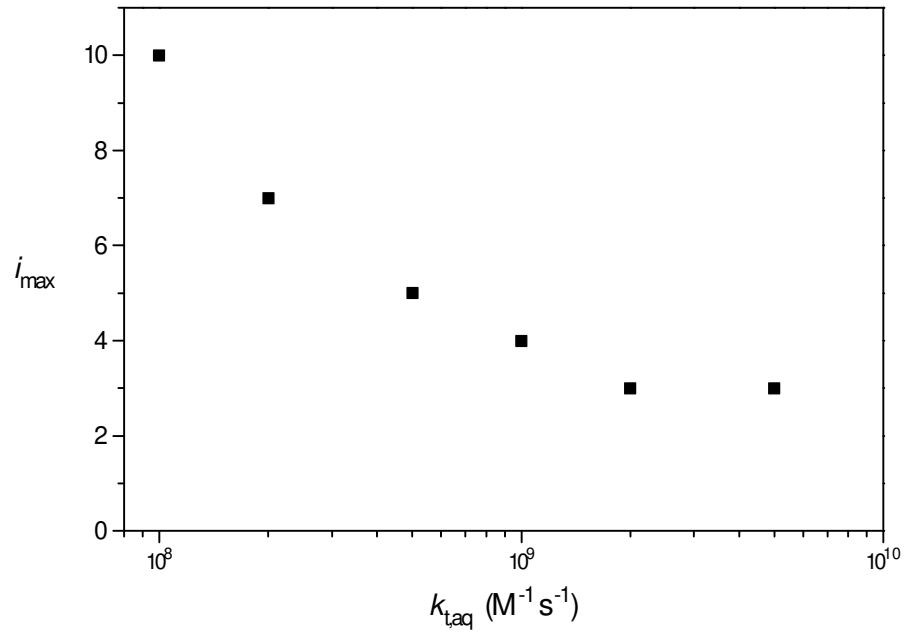

Figure 4.15: Degree of polymerization, i_{max}, below which more than 95% of aqueous-phase oligomeric radicals terminate (i.e. value of i where $P^{i}_{term} > 0.05$, equation 4.20) as function of $k_{t,aq}$. Simulation based on equations 4.9 – 4.17, termination calculated from equation 4.18. $[S_2O_8^{2-}] = 0.1$ M, 50°C, [VAc] = 0.05 M.

4.4.3.1 Electrospray Mass Spectroscopy Results

The expectation of a high incidence of termination of relatively small oligomers from the foregoing theoretical discussion was supported by the lack of polymer formed in experiments A1 and A3. The results of electrospray mass spectrometry on the crude oligomer solutions and the freeze-dried oligomer sample from experiment A3, figures 4.16 – 4.21, confirm this.

A sample of the oligomer solution from experiment A3 was dissolved in 50:50 MeOH/H_2O and fed into the electrospray ionisation unit at 10 µL/min. The negative ion spectra (figures 4.16- 4.21) were obtained on a Finnigan Mat LCQ MS Detector with Finnigan LCQ Data Processing and Instrument Control Software, ESI spray voltage was 5 kV, the sheathing gas was nitrogen at 60 psi and the heated capillary temperature was 200°C.

The spectrum of the freeze-dried sample (figure 4.16) exhibits major peaks at 355, 399, 441, 485, 527, 571, 613, 657, 699, 743 and 785 daltons. From table 4.2 it can be seen that these peaks correspond to oligomers with three or four vinyl alcohol units and two to seven VAc units.

When a crude oligomer solution was analysed after it had been stored at room temperature for one week, some hydrolysis of the acetate side groups had evidently occurred. This is shown by the enhancement of peaks in figures 4.18 and 4.19 at 183, 227, 271, 359, 445, 489, 659, 701 and 787 daltons, which correspond to oligomers with three to eight vinyl alcohol units and zero to six VAc units.

When the same crude oligomer solution was analysed after it had been stored at room temperature for five weeks, more hydrolysis of the acetate side groups was evident. This is shown by the further enhancement of peaks in figure 4.20 at 227, 271, 315, 359, 533, 579,621 and 665 daltons, which correspond to oligomers with four to twelve vinyl alcohol units and zero to two VAc units.

Peak assignments from the electrospray mass spectra of the oligomers produced in experiment A3 (figures 4.16- 4.20) are listed in table 4.2. The isotope peak spacing of one unit (figure 4.21) shows that the charge on the ionic species being detected is unity, hence the aqueous-phase oligomers appear in the spectrum at their actual molecular weight. It is also clear from figure 4.21 that there is substantial improvement in resolution when the electrospray scans a narrow window.

Uncertainty as to the exact nature of the end groups prevents an unequivocal determination of the oligomer structure. The expected structure of the freeze-dried oligomer is the diammonium salt of the partially hydrolysed pVAc-disulfate. It seems likely that the sulfate end groups have been hydrolysed as, for any reasonable combination of sulfate, VAc and vinyl alcohol, the calculated molecular weights do not correspond to peaks of any significance. For example the peak at 183 daltons (figures 4.18 and 4.20) can not be reconciled with two sulfates (MW = 192), neither can the peak at 227 (figure 4.21) be reconciled with two sulfates plus even one vinyl alcohol group. Hence, the freeze-dried oligomers are likely to be a mixture of $NH_4O(CH_2CHOH)_m(CH_2CHOCOCH_3)_nONH_4$ for m+n less than about twelve.

Figure 4.16: Mass spectrum of oligomers produced in experiment A3; freeze-dried and redissolved one day before electrospray analysis.

Figure 4.17: Expanded scale of spectrum of figure 4.16.

Figure 4.18: Mass spectrum of oligomers produced in experiment A3; crude oligomer solution stored at room temperature for one week prior to electrospray analysis.

Figure 4.19: Expanded scale of spectrum of figure 4.18.

Figure 4.20: Mass spectrum of oligomers produced in experiment A3; crude oligomer solution stored at room temperature for five weeks prior to electrospray analysis.

Figure 4.21: High resolution window from figure 4.20 showing isotope peaks occur at unit intervals.

In the electrospray ionization process very small droplets are produced with a net charge, negative in the case of the spectra presented in this work. As the solvent evaporates, the droplets contract, the concentration of charged species increases and charged species are ejected from the droplets. As there is a deficit of positive counterions and the isotope peaks (figure 4.21) show that the detected species were singly charged it seems most probable that the species present in the electrospray ionization chamber are $NH_4O(CH_2CHOH)_m(CH_2CHOCOCH_3)_nO^-$.

Table 4.2: Calculated peak assignments for the mass spectrum of partially hydrolysed aqueous-phase oligomers produced in the solution polymerization of VAc. Bold numbers are peaks identified in the electrospray spectra (figures 4.16- 4.20).

$NH_4O(CH_2CHOH)_m(CH_2CHOCOCH_3)_nO^-$											
m	n=0	n=1	n=2	n=3	n=4	n=5	n=6	n=7	n=8	n=9	n=10
1	95	181	267	353	439	525	611	697	783	869	955
2	139	225	311	397	483	569	655	741	827	913	999
3	**183**	**269**	**355**	**441**	**527**	**613**	**699**	**785**	871	957	1043
4	**227**	**313**	**399**	**485**	**571**	**657**	**743**	**829**	915	1001	1087
5	**271**	**357**	**443**	**529**	**615**	**701**	**787**	**873**	**959**	1045	1131
6	**315**	**401**	**487**	**573**	**659**	**745**	831	917	1003	1089	1175
7	**359**	**445**	**531**	**617**	703	789	875	961	1047	1133	1219
8	**403**	**489**	**575**	661	747	833	919	1005	1091	1177	1263
9	**447**	**533**	**619**	705	791	877	963	1049	1135	1221	1307
10	**491**	**577**	663	749	835	921	1007	1093	1179	1265	1351
11	**535**	**621**	707	793	879	965	1051	1137	1223	1309	1395
12	**579**	**665**	751	837	923	1009	1095	1181	1267	1353	1439
13	623	709	795	881	967	1053	1139	1225	1311	1397	1483

The most important features of the mass spectra are the progressions by 44 and 86 dalton increments, corresponding to homologous series of oligomers of partially hydrolysed pVAc. A second series is shifted to higher molecular weights by 17 daltons and may be due to either some change in the end groups, replacement of an alcoholic hydrogen by an ammonium ion or an adduct with NH_3 forming in the electrospray unit. The breadth of the peaks is due to oligomers which have lost more than one acetate group by hydrolysis, as the loss of two acetate groups produces oligomers of molecular weight only two daltons higher than the corresponding non-hydrolysed series of one less monomer unit. Also, the yellow colouration of the solution is probably due to the presence of conjugated ketones produced by oxidation

of the aqueous-phase oligomers[113] and these may contribute to the broadening of the peaks and the noisy baseline.

Most of the oligomers are of degree of polymerization of less than twelve monomer units, in accord with the expectations of the theoretical discussion above.

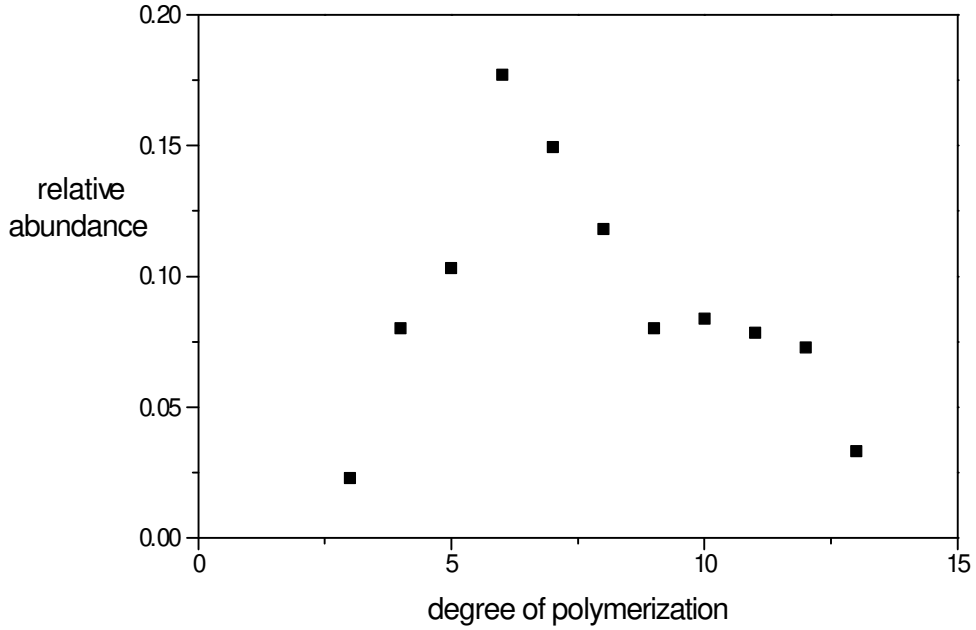

Figure 4.22: Distribution of degree of polymerization of partially hydrolysed oligomers produced under similar conditions to those of Morris and Parts, $[S_2O_8^{2-}]$ = 0.12 M, 50°C, [VAc] = 0.05 M, experiment A3.

The average degree of polymerization of the oligomers, as determined by electrospray MS, is about six. This is higher than the average degree of polymerization predicted by the simulation. Given the assumed value of $k_{t,aq} = 5\times10^8$ M^{-1} s^{-1}, the simulation predicts an average degree of polymerization of three.

This discrepancy might partly be due to the simulation not taking into account the higher values of k_p^i for small i, or the decrease in [I] during the experiment, both of which will tend to increase the degree of polymerization. Furthermore, a smaller assumed value of $k_{t,aq}$ (and hence a smaller calculated $k_{tr,I}$) will also increase the expected degree of polymerization of the aqueous-phase oligomers. Finally, the anionic end group on the aqueous-phase oligomeric radicals will repel persulfate ions, thereby reducing $k_{tr,I}$ for smaller oligomers, thus increasing the average degree of polymerization.

When the persulfate concentration was reduced to 0.022 M (experiment A2) a latex formed. As can be seen in figure 4.23 at initiator concentrations less than about 0.05 M (depending on the actual degree of polymerization at which surface activity is attained) a significant number of surface active aqueous-phase oligomers can be expected. As each aqueous-phase oligomer has two sulfato groups, and as this is the fate of virtually all sulfato groups, the production rate of aqueous-phase oligomers equals the consumption rate of persulfate which is given by:

$$\frac{d[S_2O_8^{2-}]}{dt} = -k_d[S_2O_8^{2-}] - k_{tr,I}[M_i^\bullet][S_2O_8^{2-}] \qquad 4.21$$

Hence, the rate of production of aqueous-phase oligomers, $d(IM_nI)/dt$, is given by:

$$\frac{d(IM_nI)}{dt} = (k_d + k_{tr,I}[M_i^\bullet])[S_2O_8^{2-}] \qquad 4.22$$

Modelling the conditions of experiment A2 gives $[M_i^\bullet] = 9.3\times10^{-9}$ M and the production rate of aqueous-phase oligomers is $6\text{x}10^{-7}$ mol s^{-1}. Hence, the production rate of surface-active oligomers can be estimated, once again depending on the degree of polymerization at which surface activity is attained.

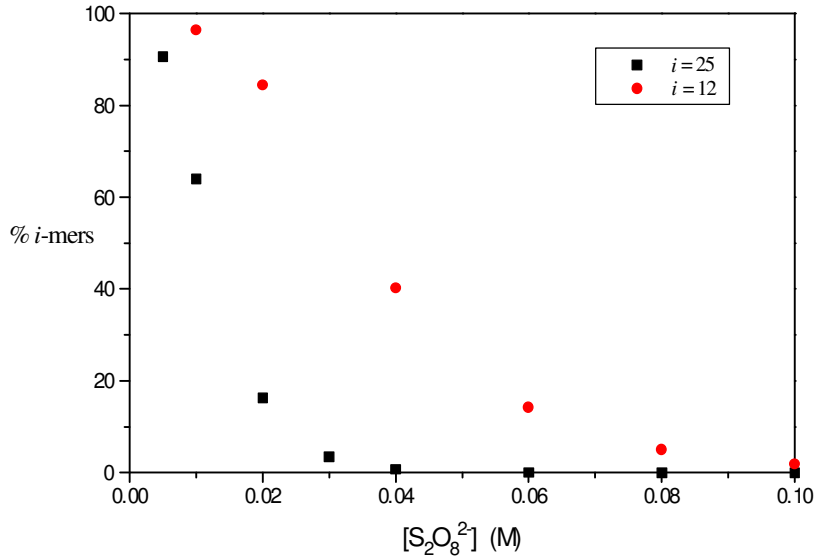

Figure 4.23: Proportion of aqueous-phase oligomers that grow to *i*-mers, or greater, as a function of initiator concentration and *i*, the degree of polymerization. Simulation based on equations 4.9 – 4.17 using $k_{tr,I} = 3\times10^3$ M^{-1} s^{-1}, termination calculated from equation 4.18. 50°C, [VAc] = 0.05 M .

From figure 4.23 it can be seen that more than 50% of the aqueous-phase oligomers formed in the presence of 0.02 M persulfate (~2×10^{17} s^{-1}) would be expected to be

surface active (i.e. with degree of polymerization greater than about 16) and this explains the appearance of latexes at this initiator concentration.

4.4.3.2 Styrene "capped" aqueous-phase oligomeric radicals

The rationale behind this experiment was that, due to the unfavourable reactivity ratios for VAc and styrene copolymerization, styrene would behave as a spin trap thereby preventing the formation of latex. It was hoped that analysis of the molecular weight of the aqueous-phase oligomers so formed would provide an insight into the mechanism of the induced decomposition of persulfate.

The solution prepared in experiment A4 was analysed by MALDI in a 2,5-dihydrobenzoic acid matrix on a PerSeptive Biosystems Voyager DE STR. The positive ion spectrum is shown in figure 4.24. As the oligomers were expected to be doubly negatively charged and there was an excess of sodium cations present, it is possible that the species detected were tri-sodiated. That is to say, one sodium cation is required to neutralise each of the two negatively charged sulfate end groups and one more to give the oligomer the requisite positive charge to enable detection in the MALDI-TOF-MS. In that case the assignments made in table 4.3 should be valid. However, even if the assumed end groups and counter ion assignments are incorrect the main conclusions regarding the number of styrene units and general size of the oligomers still hold.

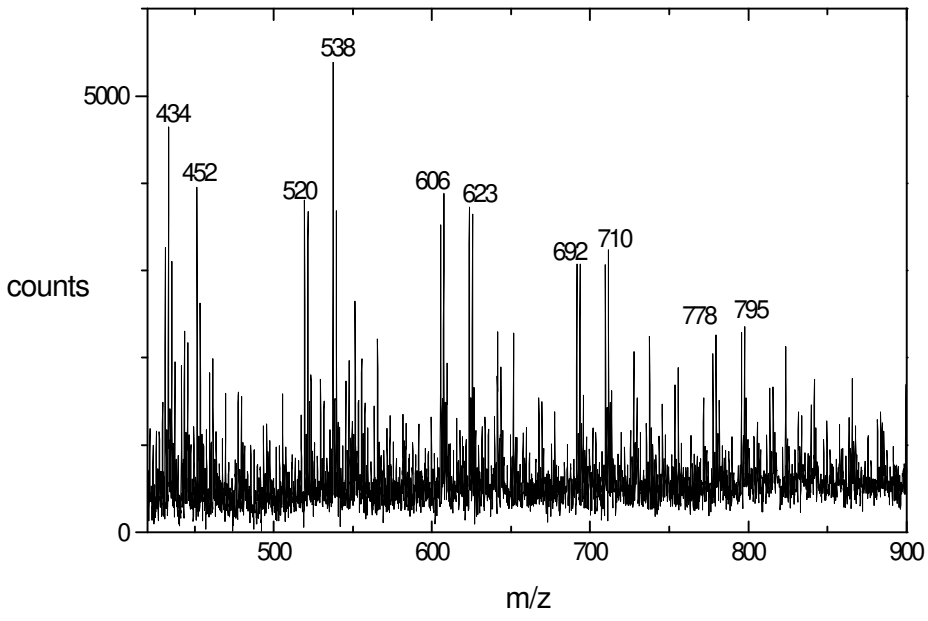

Figure 4.24: MALDI spectra of styrene/vinyl acetate aqueous-phase co-oligomers initiated by persulfate. 50°C, $[S_2O_8^{2-}]$ = 0.1 M.

This spectrum raises more questions than it answers; however, some tentative conclusions are indicated. If the cage-complex mechanism were significant one would expect most radical loss to be via bimolecular termination. As the longest lived radical species in this system are the "styrene-capped" oligomeric radicals one would further expect the major proportion of aqueous-phase oligomers to incorporate two styrene units. The absence of major peaks corresponding to aqueous-phase oligomers with two styrene units, though not conclusive, argues against the cage-complex mechanism.

The composition of the oligomers as indicated by the MALDI spectrum is also consistent with the aqueous-phase oligomeric radical entry model of Maxwell and Morrison[21] and the model and experimental results of Chern and Poehlein[35,114] in that sulfato radical anions initiate polymerization and grow in the aqueous phase until they become surface active and enter a particle. In the absence of particles entry is simulated approximately by "capping" with styrene, though of course the oligomers do not have to grow to a surface active length and so the "surface-active" constraint is lifted.

Table 4.3: Assignment of MALDI peaks to oligomers from experiment A4.

species	calculated MW	peak assignment
$Na_3(SO_4)_2VAc_2^+$	434	434
$Na_3(SO_4)_2VAcSty^+$	452	452
$Na_3(SO_4)_2VAc_3^+$	520	520
$Na_3(SO_4)_2VAc_2Sty^+$	538	538
$Na_3(SO_4)_2VAc_4)$	606	606
$Na_3(SO_4)_2VAc_3Sty^+$	624	623
$Na_3(SO_4)_2VAc_5^+$	692	692
$Na_3(SO_4)_2VAc_4Sty^+$	710	710
$Na_3(SO_4)_2VAc_6^+$	778	778
$Na_3(SO_4)_2VAc_5Sty^+$	796	795

4.5 Experimental III – retardation by acetaldehyde

Acetaldehyde, which is formed by the hydrolysis of VAc, is a known transfer agent. Clarke et al.[58] have shown that the chain transfer constant for transfer from pVAc to acetaldehyde is 6.6×10^{-2} at 60°C compared to 2.5×10^{-4} for transfer to VAc monomer. Furthermore, they argue that acetaldehyde is only mildly degradative.

It has been reported that the addition of a small amount of acetaldehyde (8×10^{-3} M) at the beginning of an emulsion polymerization had no effect on R_p[9]. This also suggests that acetaldehyde is not acting as a degradative chain transfer agent. However, prolonged storage, especially in industrial applications, and/or inadequate distillation techniques may cause the accumulation of significant amounts of acetaldehyde. The effect of a relatively high concentration of acetaldehyde was tested with the following experiment.

4.5.1 Materials and methods

A single kinetic experiment was conducted to examine the effect of the enol form of acetaldehyde, vinyl alcohol. A poly(butyl methacrylate) seed was used because, like pVAc, it is a rubbery polymer and is swollen by VAc but is not subject to the extensive branching found in pVAc. This simplifies interpretation of the molecular weight distributions of the polymer produced.

The seed latex was prepared with the following ingredients: the emulsifier was AMA-80 used as obtained from Cyanamid. The buffer used was sodium bicarbonate and the initiator used to prepare the seed was potassium persulfate. Both the latter were obtained from Merck and used without further purification

Seed B was prepared as a batch polymerization. Milli-Q water, 18.2 M Ω cm^{-1} was used throughout. AMA-80, used as obtained from Cyanamid (11.51 g) was dissolved in water (220 ml) and heated to 84°C. The solution was buffered with sodium bicarbonate, obtained from Merck and used without further purification (1.683 g in 15 ml water). To this solution was added butyl methacrylate (187.1 g) obtained from Aldrich and purified by distillation at 56°C under reduced pressure (18 mmHg) then a further 187 ml of water. The emulsion was purged with nitrogen for 40 minutes then pre-dissolved potassium persulfate was added (0.6624 g in 14 ml water). Heat-of-reaction increased the reaction temperature to 96°C in the ten minutes following the addition of initiator. Over the subsequent 50 minutes the reaction temperature gradually decreased to 85°C. The latex was kept at 50°C overnight to complete the polymerization and dialysed for seven days with daily changes of the dialysis water. The particle radius, measured by PCS, was 56 nm with a polydispersity of 1.12.

The heteroseeded emulsion polymerization was prepared in the same manner as those described in section 4.3.2 except that the poly(butyl methacrylate) seed B was used. Sodium acetate trihydrate (0.1940 g) and surfactant (AMA-80, 0.2032 g) were dissolved in 50 ml of Milli-Q water (18.2 M Ω cm^{-1}) under argon in an 83.3 ml water-

jacketed dilatometer. To this was added VAc (7.41 g) which had been extracted with 5% NaOH three times, washed with Milli-Q water, dried over calcium chloride and distilled under nitrogen at 72°C and 760 mm Hg, the first and last 20% being discarded. The mixture stirred under a partial vacuum to form an emulsion. The poly(butyl methacrylate) seed was added (2.426 g, 24% solids) and the latex allowed to swell under partial vacuum for two hours at 50°C. Recrystallised potassium persulphate (0.2197 g) was dissolved in Milli-Q water (10.5257 g) and 1.0 ml injected giving $[S_2O_8^{2-}] = 1.03\times10^{-3}$ M. The dilatometer was then filled to the appropriate meniscus height.

Acetaldehyde (Aldrich) was distilled under nitrogen at 20°C and stored at –30°C until needed. When the polymerizing mixture had reached a steady-state rate, acetaldehyde (1.0 ml) was injected into the dilatometer (which was fitted with a sidearm and septum). After 3,400 seconds a sample was taken for GPC analysis.

4.5.2 Results and Discussion

The experiment was repeated at 30°C with and without acetaldehyde, and the molecular weights then compared. The peak molecular weight, $\langle M_p \rangle$, was reduced in the presence of acetaldehyde from 6.7×10^5 to 4.3×10^5. The MWDs were obtained on the GPC system described in detail in section 5.3.1.3. Unfortunately, at this stage in the work the problems with column selection had not been identified and so the absolute values of $\langle M_p \rangle$ may be incorrect. However, the significant reduction observed in $\langle M_p \rangle$ is unlikely to be seriously affected.

The rate data are presented in figure 4.25. It was found in this experiment that the addition of a large amount of acetaldehyde reduced the polymerization rate by about 50% and the rate remained at this level up to high conversion. This was consistent with the acetaldehyde acting as a reservoir of vinyl alcohol, which then co-polymerises to produce an unreactive radical end-group that promotes bimolecular termination. This can not be taken as proof that acetaldehyde is responsible for the retardation so often seen in VAc emulsion polymerizations; however it is a possibility which might warrant further investigation. Clearly, *acetaldehyde is not responsible for the inhibition period,* as even at this relatively high concentration of acetaldehyde, R_p is only halved.

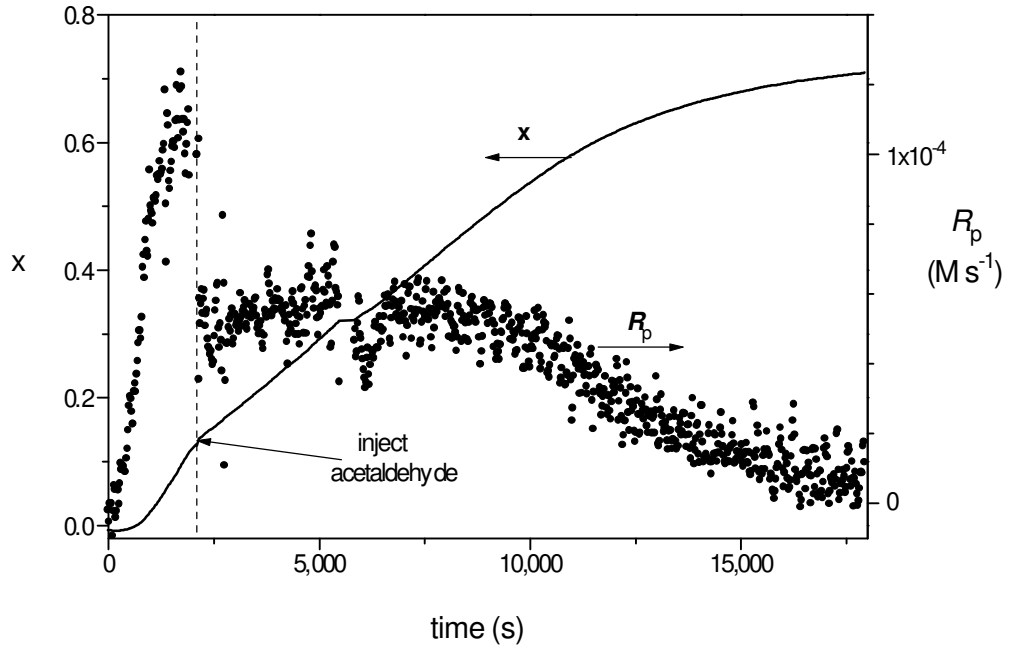

Figure 4.25: Effect of acetaldehyde on conversion, x, and the polymerization rate, R_p, of VAc emulsion polymerization initiated by potassium persulfate. Experiment B1, 30°C, $[K_2S_2O_8] = 1.03 \times 10^{-3}$ M. The "flat spot" at ~5,500 seconds is due to extracting the sample for GPC analysis.

4.6 Conclusions

Comparisons of R_p for chemical and radiation induced emulsion polymerizations have shown that induced decomposition of persulfate by VAc produces no more radicals than that calculated for the thermal decomposition of persulfate. Therefore, it seems likely that the mechanism for induced decomposition is simply transfer to initiator.

Modelling of the system based on this premise and the data of Morris and Parts semi-quantitatively predicts the formation of surfactant-free latexes from aqueous solutions of VAc at persulfate concentrations below about 0.02 M and also the absence of polymer at higher persulfate concentrations. The rate coefficient for the induced decomposition of persulfate by VAc aqueous-phase oligomeric radicals, $k_{tr,I}$ was calculated from an empirical fit to the data of Morris and Parts[14] as 3×10^3 M^{-1} s^{-1}.

The inhibition period is due to dissolved oxygen. Acetaldehyde, even when present in significant quantities, plays a minor role in inhibition and retardation of VAc emulsion polymerizations. However, it is an effective chain transfer agent and may be responsible for a significant reduction in molecular weights.

The retardation period following the inhibition period in VAc emulsion polymerizations can be attributed to dissolved oxygen at concentrations below about 10^{-6} M. This is also likely to apply to other systems with high k_p and/or C_w.

It has been shown that the decrease in R_p reported by many researchers as W_p exceeds about 0.85, can not be attributed to the concomitant decrease in C_w effecting a decrease in entry efficiency. Neither can the decreasing rate at high conversion be due to a "Smith-Ewart" $\bar{n} = 0.5$ type of limiting behaviour.

-oOo-

5 Determination of the Rate Coefficient for Transfer to Monomer

5.1 Introduction

In order to interpret the γ relaxation data of chapter 3 it was desirable to know, as accurately as possible, the rate coefficients relevant to the system's kinetics. Chief among these are the propagation rate coefficient, k_p, and the rate coefficient for transfer to monomer, $k_{tr,M}$ (often represented simply by k_{tr} when transfer to other entities is not being considered).

The value of k_p for VAc has been established by Hutchinson et al.[33] using PLP (pulsed laser polymerization). Although this technique is difficult to apply to monomers with high k_{tr}, such as VAc, the availability of faster lasers has now made this possible. When suitable conditions are achieved, PLP provides an unambiguous, direct measurement of k_p. However, determination of the molecular weight of the species produced by PLP still depends on SEC (size exclusion chromatography), and an error margin of about 10% should probably be exercised.

Until quite recently, values of $k_{tr,M}$ were always obtained using the Mayo method[65]. This actually produces the ratio $C_M = k_{tr,M}/k_p$. Before the advent of PLP, the uncertainty in k_p meant that results were usually quoted as C_M, as discussed in section 2.3.1.4. Even so, the literature values of C_M are widely scattered (see figure 2.3). To remedy this situation $k_{tr,M}$ was determined using the ln$P(M)$ method described below combined with Hutchinson's PLP-derived k_p[33].

Due to the unforeseeable difficulties encountered in obtaining good MWD's for pVAc, detailed below, and a lack of time to complete a thorough determination, the following treatment must be considered to be a preliminary investigation only. However, the main obstacles have been overcome and hopefully this work will be completed at a later date.

5.2 The ln$P(M)$ method for determination of transfer coefficients

It has been shown by Clay and Gilbert[115] that, where chain stoppage is completely dominated by transfer to monomer, the rate coefficient for transfer to monomer, $k_{tr,M}$, is readily obtained from the following:

$$\lim_{i\to\infty,[I]\to 0} P(M) = \exp\left\{\frac{-k_{tr,M}}{k_p}\frac{M}{M_0}\right\} \qquad 5.1$$

where $P(M)$ is the instantaneous number molecular weight distribution and $i = M/M_0$ is the degree of polymerization. $P(M)$ is obtained from the difference between the cumulative number molecular weight distributions, $\bar{P}(M)$, of successive samples taken at increasing conversions. $\bar{P}(M)$ is obtained from the GPC distribution corrected for non-linear calibration, $G(V)$, where V is the elution volume, using the following equation:

$$\bar{P}(M) = \left\{\frac{G(V)}{M^2}\right\} \qquad 5.2$$

For the appropriate experimental conditions, if $\ln P(M)$ is plotted against M, the region extending from $<M_w>$ to high molecular weights should be a straight line with slope, Λ, equal to $k_{tr,M}/k_p M_0$. Hence:

$$k_{tr,M} = \Lambda\, k_p M_0 \qquad 5.3$$

The region immediately to the high side of $<M_w>$ is the optimal region for the determination of the transfer rate coefficient. Two factors mitigate strongly for the use of this portion of the GPC distribution. (1) It includes a large proportion of the polymer being measured, hence the signal to noise ratio is optimised[116]. (2) Although the derivation of equation 5.1 suggests that linearity should be best observed in the limit of high MW, (to minimise the complications arising from termination by combination and the chain-length dependence of termination rate coefficients[115]) this region is most sensitive to experimental artefacts such as exclusion limits and baseline subtraction[117]. Moad[116] argues that, as bimolecular termination is most likely to occur between a long and a short radical, it will have little effect on the chain-length distribution. Furthermore, based on the same short-long termination argument, the mode of bimolecular termination (disproportionation or combination) can be seen not to matter either[116]. Therefore, it is not necessary to restrict measurement to the very high MW tail of the $\ln P(M)$ plot.

Appropriate experimental conditions include low initiator concentrations and low conversion samples to minimise branching, an important consideration in VAc polymerization. Consistency checks include independence of Λ on initiator concentration (provided [I] is low enough for the system to be in the transfer dominated limit) and independence of Λ on conversion (for low conversions). Linearity of the $\ln P(M)$ plot over a large portion of the molecular weight distribution

indicates that the GPC has been set up correctly as the plot is unlikely to be linear unless everything is working well.

5.3 Experimental

Vinyl acetate was polymerized in bulk and emulsion over a range of temperatures and low initiator concentrations. Molecular weight distributions of low conversion samples were determined by GPC and analysed by the ln$P(M)$ method described above.

5.3.1 Materials and methods

5.3.1.1 Bulk polymerizations

Vinyl acetate (Aldrich) was stripped of inhibitor on a basic alumina column and distilled at one atmosphere under nitrogen at 72.5-73°C, the first and last 20% of the distillate being discarded. The monomer (about 50 g) was deoxygenated in a round bottomed reaction vessel with several freeze-thaw cycles, then heated to the desired reaction temperature in a water bath. 2,2'-azobisisobutyronitrile (AIBN – Wako) was recrystallised from ethanol at 45°C, dissolved in a small portion of the purified monomer and added to the contents of the reaction vessel. The mixture was stirred under argon by a small magnetic stirrer bar. Polymerization commenced within a few minutes, as indicated by a small but significant temperature increase, which was monitored throughout the reaction.

Samples (~1.5 g) were extracted every few minutes up to about ten percent conversion, which could be estimated by visual inspection of the increasing viscosity of the polymer solution. They were then added to pre-weighed, chilled sample jars, weighed again and quenched with a small amount (~0.4 g) of a 1% solution of hydroquinone (HQ) in tetrahydrofuran (THF). Samples were allowed to evaporate at room temperature for 24-48 hours, then in a vacuum oven at 40°C for two hours. Conversion was determined gravimetrically. As can be seen in figure 5.1, the inhibition period was minimal and there was no indication of any retardation. This suggests that the procedures employed in monomer purification and sample preparation for gravimetry and GPC were adequate.

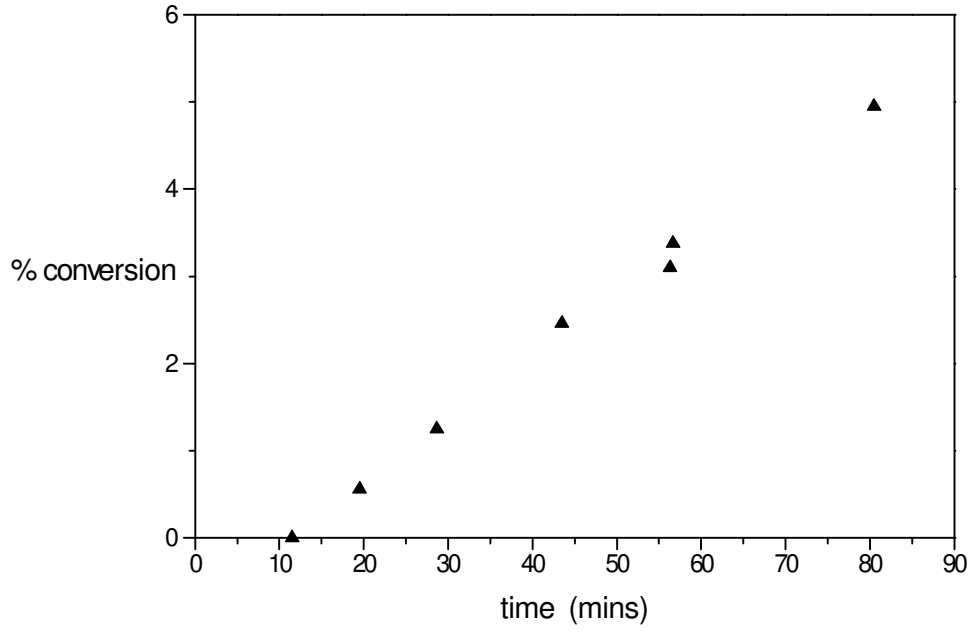

Figure 5.1: Typical plot of conversion as function of time for bulk polymerization of VAc, 64°C, [AIBN] = 6.4×10^{-5} M.

As many of the γ radiolysis experiments of chapter 3 were conducted at 2°C, it was desirable to also measure k_{tr} at this temperature. For this purpose a photoinitiator was employed, 2,2-dimethoxy-1,2-diphenylethan-1-one (Irgacure 651), obtained from Ciba-Geigy and used without further purification. VAc was purified as described above for the bulk polymerizations. Initiator (0.0037 g) was dissolved in monomer (11.90 g) to give an initiator concentration of 1.08×10^{-3} M, and aliquots (~1 ml) were added to ampoules fitted with Teflon® taps and wrapped in alfoil to protect the mixture from light during degassing. These were then degassed by repeated freeze-thaw cycles under argon. The sealed ampoules were placed in drills in a brass block with thermostatted water flowing through the block. U.V. light was directed up through the ampoules from the base of the block. The ampoules were inspected periodically and when the viscosity indicated about 10% conversion the polymer solution was removed and added to a pre-weighed pan, followed by ~1 ml of the 1% HQ/THF quenching solution. Conversion was determined gravimetrically as in the previous bulk experiments.

5.3.1.2 Emulsion polymerization MWDs

Vinyl acetate emulsion polymerization does not lend itself well to the ln$P(M)$ method. There are several reasons for this and these are discussed in section 5.3.2.2. However,

as a methodology had been found to obtain reasonable ln$P(M)$ plots for bulk polymerizations, it seemed logical to attempt the same for emulsion polymerizations.

An emulsion was prepared using the same ingredients and purification procedures as for the seeds prepared as described in section 3.3.2.5. Surfactants (AMA-80 : 5.02 g, OT-75 : 4.95 g) and buffer ($NaHCO_3$: 1.20 g) were dissolved in de-oxygenated Milli-Q water (595.14 g) and heated to 60°C. Purified VAc was added and the mixture emulsified by stirring with a magnetic stirrer bar under nitrogen. Sodium persulfate (0.1026 g) was dissolved in water (14.57 g) and added to the emulsion giving a persulfate concentration of 7×10^{-4} M and rate of polymerization of about 1% min^{-1}. Weighed samples (~3 g) were taken throughout interval II and these were quenched with a 1% solution of hydroquinone in water and dried in a vacuum oven at 40°C overnight for gravimetric analysis.

A portion (72 g) of the resulting latex was adjusted to pH=7.0 with NaOH solution, buffered with phosphate solution (3.0 ml, 0.213 M, molar ratio HPO_4^{2-}:$H_2PO_4^-$ 0.63:1 - pH=7.0, as described in section 4.3.2) and used as a seed latex for a 40°C emulsion polymerization. Particle size (determined by CHDF) was D_W/D_N = 106/88 nm and the solids content was 22.1%.

To 50 g of the buffered latex was added 7.5 g of VAc, purified as described previously, and the mixture allowed to swell for one hour at 40°C. Recrystallised potassium persulfate (0.0231 g) dissolved in water (1 ml) was injected to give a persulfate concentration of 1.9×10^{-3} M and rate of polymerization of about 0.1% min^{-1}. The same sampling procedure was followed as in the 60°C emulsion polymerization above.

5.3.1.3 GPC analysis – the importance of correct column selection

GPC analysis was conducted on a Waters system, using Ajax Unichrom HPLC grade THF as eluent delivered by a Waters 510 HPLC pump at a flow rate of 0.8 ml min^{-1}. The pump was fitted with a pressure reduction unit to minimise pressure fluctuations due to cross-over of the pump heads. The detector was an Erma Optical Works ERC-7510 Refractive Index detector, the RI cell being maintained at 35°C. Data were collected by a Waters System Interface Module and Millenium version 2.10 software.

The dried polymer samples and the polystyrene standards were dissolved in HPLC grade THF to make up solutions of ~0.4% polymer for injection into the GPC.

Universal calibration was used as pVAc standards were not available. Narrow molecular weight polystyrene standards were obtained from Polymer Labs and Waters.

The peak molecular weights ranged from 4×10^3 to 6.85×10^6 daltons. Mark-Houwink parameters used were, for polystyrene in THF at 30°C: $K = 11.4\times10^{-5}$ dl g^{-1}, $\alpha = 0.716$, for pVAc in THF at 30°C: $K = 22.4\times10^{-5}$ dl g^{-1}, $\alpha = 0.674$[33].

Initially a series of monodisperse pore size columns (Waters 10^6, 10^5, 10^4, and 10^3 Å) was used, thermostatted to 30°C. This arrangement produced curved ln$P(M)$ plots for polymer produced under a range of conditions of temperature, initiator concentration, and conversion. Varying the sample concentration made no appreciable difference. A set of samples was run on a different machine (Polymer Laboratories) also running a set of monodisperse pore size columns with similar results.

Replacement of the monodisperse pore size columns with a series of three mixed bed columns (Waters Styragel HT 6E, 7.8×300 mm) resulted in a dramatic improvement in the ln$P(M)$ plots. An example of the difference is shown in figure 5.2. The old data, obtained so painstakingly on the monodisperse pore size columns, were discarded and the data presented herein (apart from the example in figure 5.2) were obtained from samples re-run on the new mixed bed columns.

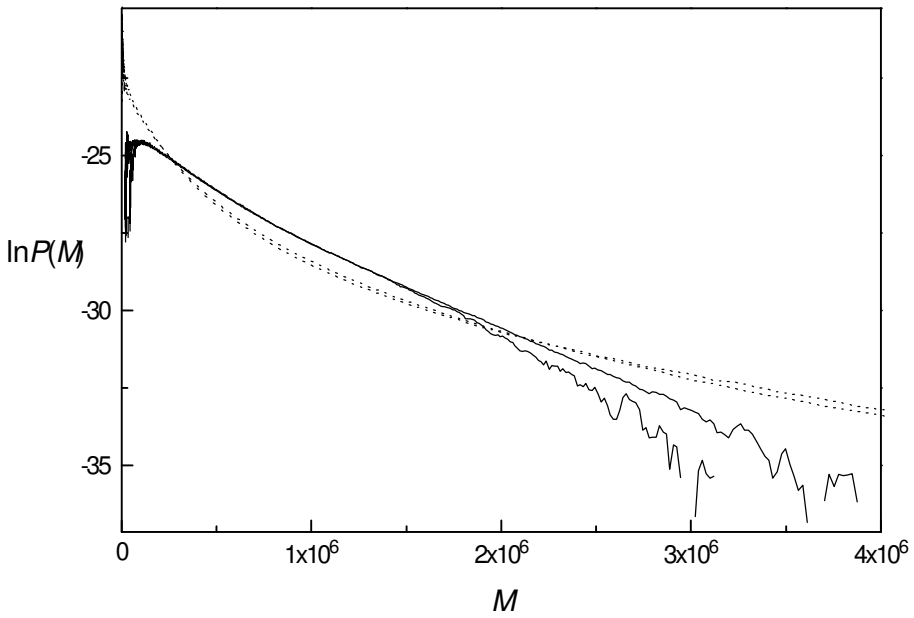

Figure 5.2: Instantaneous ln$P(M)$ plots, (·····) Waters 10^6, 10^5, 10^4, and 10^3 Å monodisperse pore size columns, (——) Waters Styragel mixed bed columns. VAc bulk polymerization, 64°C, [AIBN] = 6.4×10^{-5} M.

5.3.2 Results and Discussion

Unfortunately, most of the polymer samples collected were consumed in fruitless runs on the monodisperse pore size columns. Hence, only a limited number of samples remained for analysis on the new columns and there was insufficient time to repeat the polymerizations required to obtain a new set of samples. However, such data as could be collected are presented in figures 5.3 to 5.11.

5.3.2.1 Bulk polymerizations

Because of the lack of samples, instantaneous ln$P(M)$ plots for bulk polymerizations were only able to be determined at 64°C. The ln$P(M)$ plots for 50°C and 2°C were, of necessity, only determined from cumulative MWDs.

The ln$P(M)$ plots for the 2°C data were consistent with each other, within the errors normally associated with GPC, giving Λ as -7.06×10^{-7} and -6.93×10^{-7}. Furthermore, the values of $\ln(k_{tr})$ determined therefrom, when plotted on an Arrhenius plot, are consistent with the higher temperature data.

Figure 5.3 shows the cumulative MWDs of three polymer samples obtained at low conversion (2.46, 3.38 and 4.95%), very nearly superposed, and the "instantaneous" MWDs of the two higher conversion samples. Figure 5.4 shows the ln$P(M)$ distribution of the same samples.

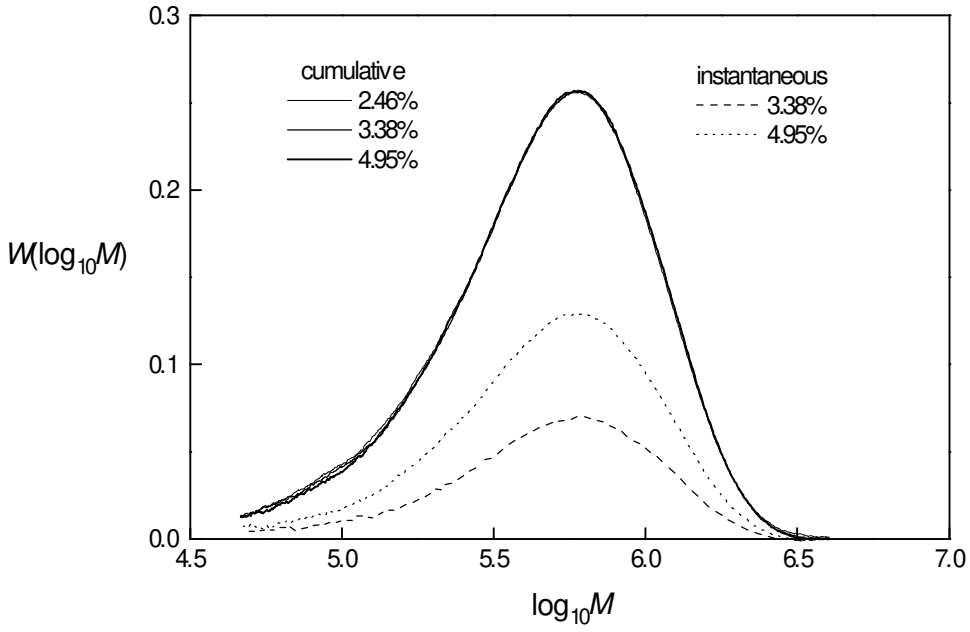

Figure 5.3: MWDs for bulk VAc polymerization, 64°C, [AIBN] = 6.4×10^{-5} M.

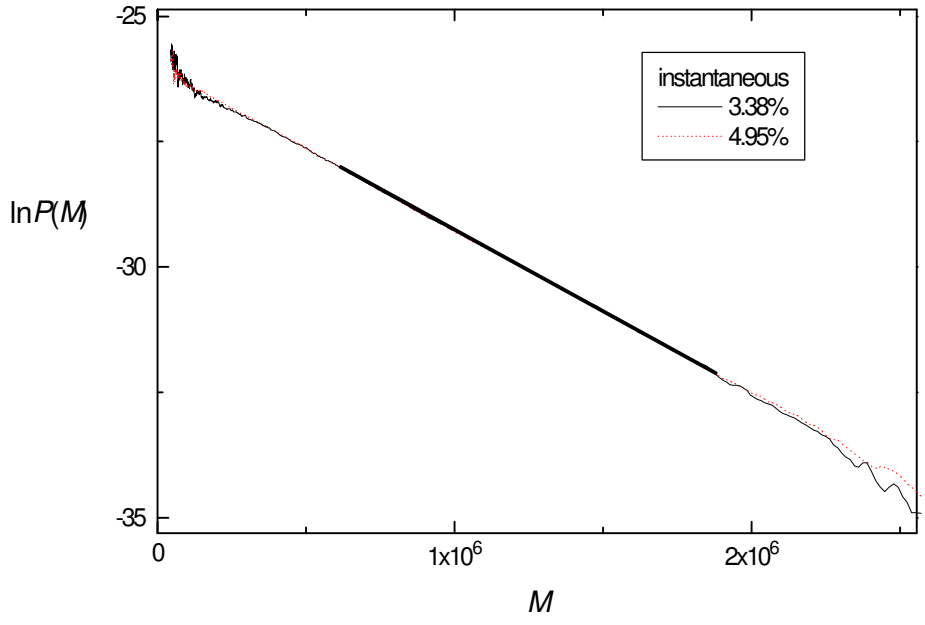

Figure 5.4: ln$P(M)$ plot for bulk VAc polymerization, 64°C, [AIBN] = 6.4×10^{-5} M. The region of the plot used in equation 5.3 is shown in bold.

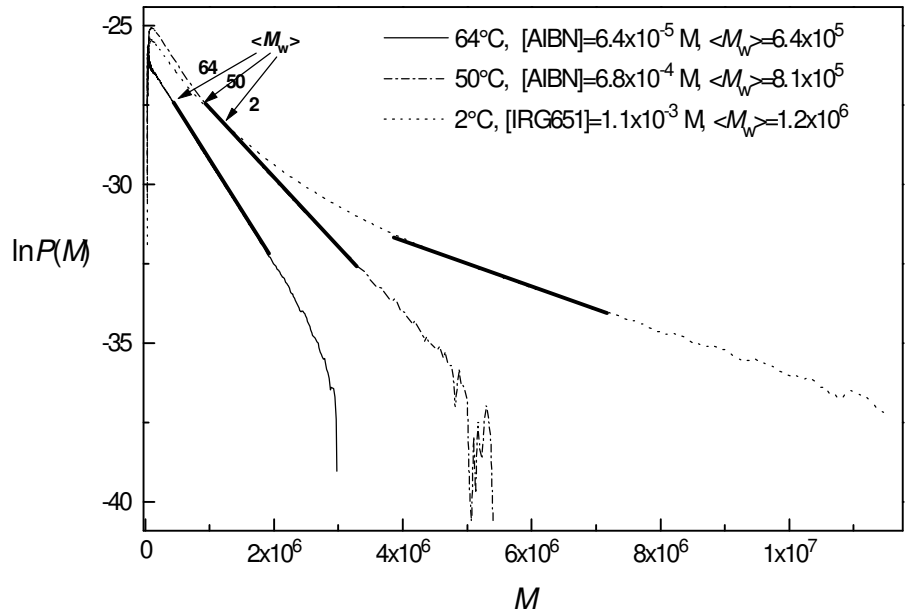

Figure 5.5: ln*P*(*M*) plots for bulk VAc polymerizations at 64°C, 50°C and 2°C. The regions of the plots used in equation 5.3 are shown in bold.

In figure 5.5, the linear portions of the ln*P*(*M*) distributions over the region extending from $<M_w>$ to high molecular weights give values of Λ for the temperature range 64°C – 2°C, from which k_{tr} was calculated using equation 5.3.

The curvature at the low molecular weight end of the ln*P*(*M*) distribution for the bulk polymerizations at 2°C is unexplained and may be an experimental artefact. The ampoules in which the polymerizations were conducted had rounded ends through which the U.V. light, required for photolysis, entered. This may have had a lensing effect, which in turn may have markedly increased the local rate of primary radical production. Alternatively, the curvature may be a GPC artefact. In any case, the high molecular weight region is linear and the slope of this part of the ln*P*(*M*) plot was used to calculate k_{tr} at 2°C.

The fit to the data of figure 5.6 gives a pre-exponential factor for transfer to monomer of $10^{6.38}$ M^{-1} s^{-1} and activation energy of 38.8 kJ mol^{-1}. These results are consistent with the (widely scattered) data of the literature when that data is reprocessed using Hutchinson's PLP results for k_p (figure 5.12).

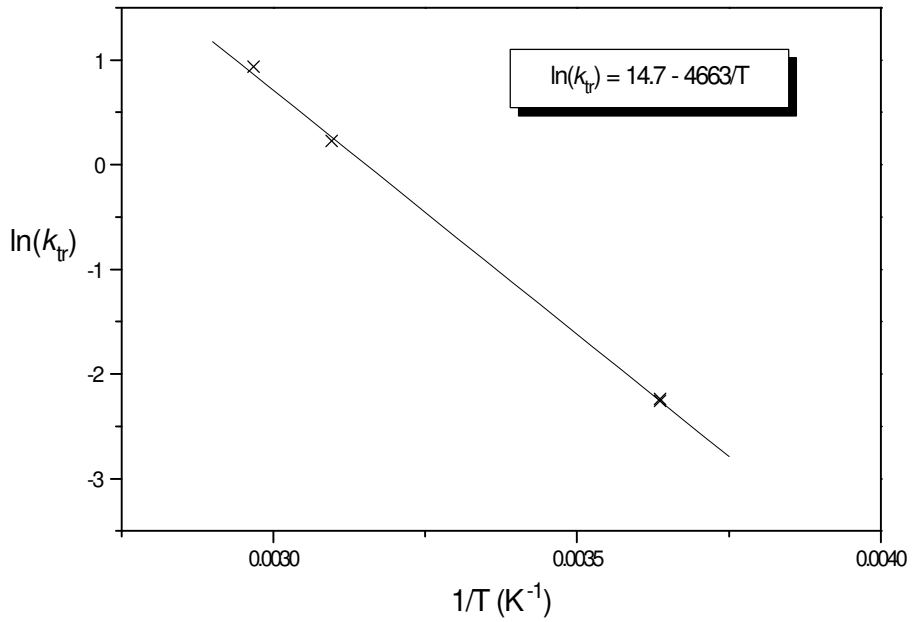

Figure 5.6: Arrhenius plot for bulk VAc polymerizations at 64°C, 50°C and 2°C.

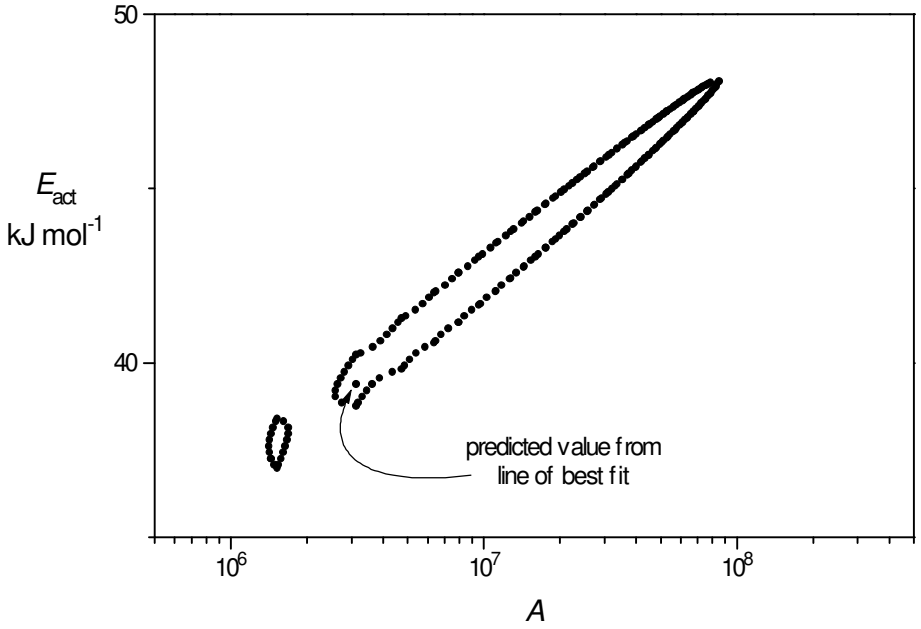

Figure 5.7: 95% confidence interval for the Arrhenius parameters of figure 5.6. Calculated with a least squares fitting program written by van Herk[118] and allowing a 20% error in the slopes of the ln$P(M)$ plots.

The results of similar work conducted on butyl acrylate have been reported by Maeder and Gilbert[117]. They found a pre-exponential factor for transfer to monomer of $10^{5.46}$ M^{-1} s^{-1} and activation energy of 32.6 kJ mol^{-1}.

Table 5.1: GPC results for low conversion pVAc.

system	Temp. (°C)	[I] (M)	conversion	$<M_w>$	Λ	k_{tr} (M^{-1} s^{-1})	figure
bulk	64	6.4×10^{-5}[a]	3.38%[d]	6.46×10^{5}	-3.21×10^{-6}	2.55	5.4
bulk	64	6.4×10^{-5}[a]	4.95%[d]	6.43×10^{5}	-3.21×10^{-6}	2.55	5.4
bulk	50	6.8×10^{-4}[a]	3.1%[e]	8.13×10^{5}	-2.17×10^{-6}	1.26	5.5
bulk	2	1.1×10^{-3}[b]	9.2%[e]	1.21×10^{6}	-7.06×10^{-5}	0.11	5.5
bulk	2	6.4×10^{-5}[b]	11.1%[e]	1.34×10^{6}	-6.93×10^{-5}	0.10	5.5
e. pol.	62	7.1×10^{-4}[c]	23%[d]	5.3×10^{5}	-2.51×10^{-6}	1.90	5.8
e. pol.	40	1.9×10^{-3}[c]	5.3%[f]	$\sim1.2\times10^{6}$	-1.06×10^{-6}	0.48	5.10

[a]AIBN; [b]Irgcure 651; [c]persulfate; [d]instantaneous; [e]cumulative; [f]seed subtracted.

5.3.2.2 Emulsion polymerizations

In the case of seeded polymerizations, even at low conversions, the weight fraction of polymer within the particles is greater than 30%, the remaining monomer being in droplets, away from the locus of polymerization. VAc branches readily (see section 2.3) and at the high local concentration of polymer in the particles some branching can be expected, even at low conversions. This causes problems in both obtaining a GPC trace, as branched polymer forms a gel fraction which may be retained on the GPC filters, and analysis of the GPC trace as the relationship between solvodynamic volume and molecular weight is affected by branching. If branching occurs it will be mainly to the seed polymer, thereby rendering subtraction (of the contribution to the GPC trace due to the seed) inaccurate. This can be minimised by collecting data at low conversion; however this results in a significant reduction in signal/noise (figure 5.10).

Unseeded emulsion polymerizations suffer from the poorly understood effects of the nucleation and retardation periods on the MWD. By the time the polymerization reaches a steady state, it is in the same unfortunate situation with regard to branching as for a seeded polymerization. The obvious area to explore next is heteroseeded emulsion polymerization with a seed that is not likely to participate in branching. However, as discussed in section 2.4.1.5 the pVAc macroradical will probably abstract backbone hydrogens from most, if not all, potential seed polymers.

The data presented below are for an unseeded emulsion polymerization at 62°C and a seeded emulsion polymerization at 40°C (figures 5.8 to 5.11).

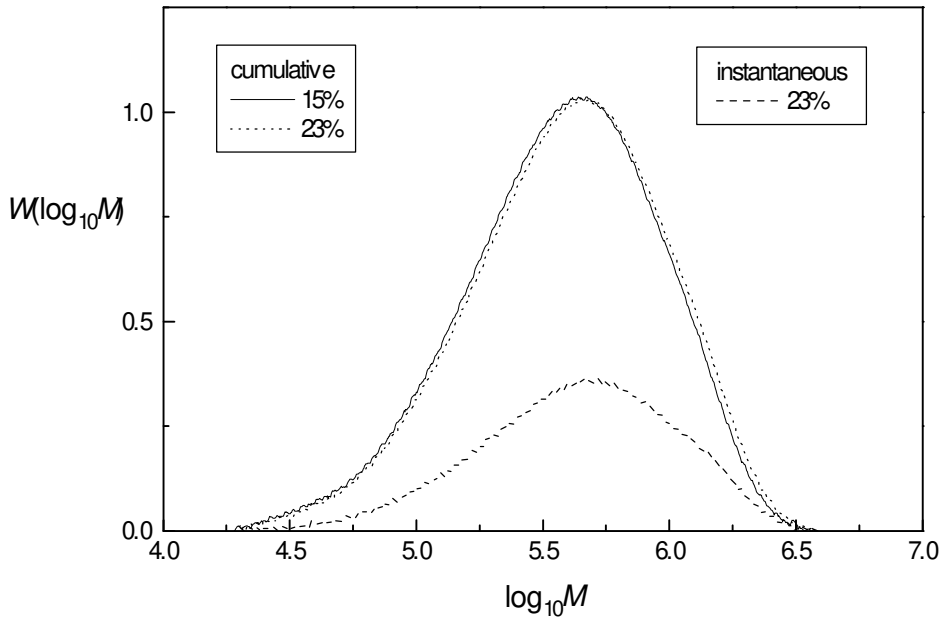

Figure 5.8: MWD for VAc emulsion polymerization, 62°C, 23% conversion, [persulfate] = 7.0×10^{-4} M.

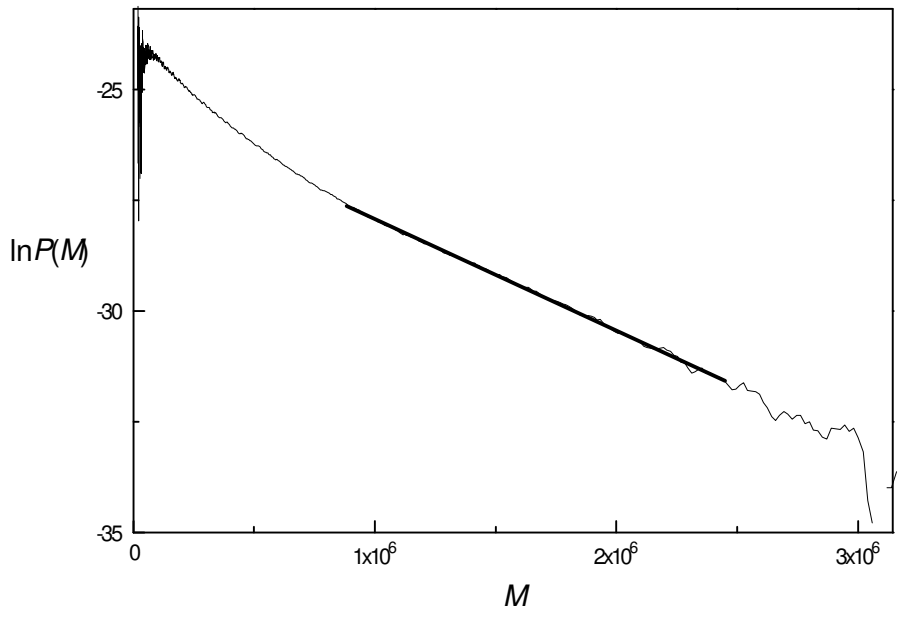

Figure 5.9: ln*P*(*M*) plot for VAc emulsion polymerization, 62°C, 23% conversion, [persulfate] = 7.0×10^{-4} M. The region of the plot used in equation 5.3 is shown in bold.

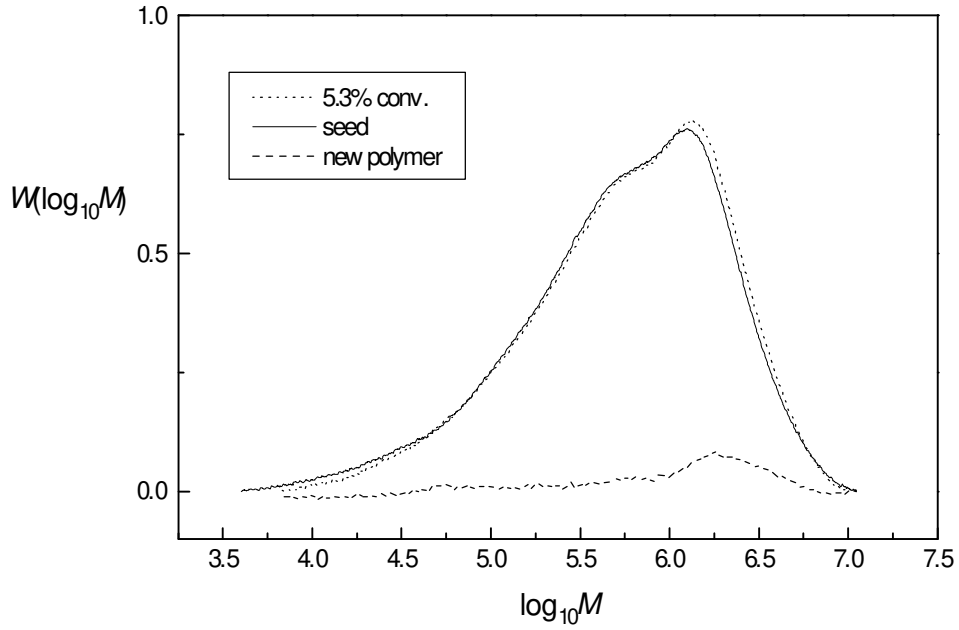

Figure 5.10: MWD for VAc emulsion polymerization, 40°C, 5.3% conversion, [persulfate] = 1.9×10^{-3} M.

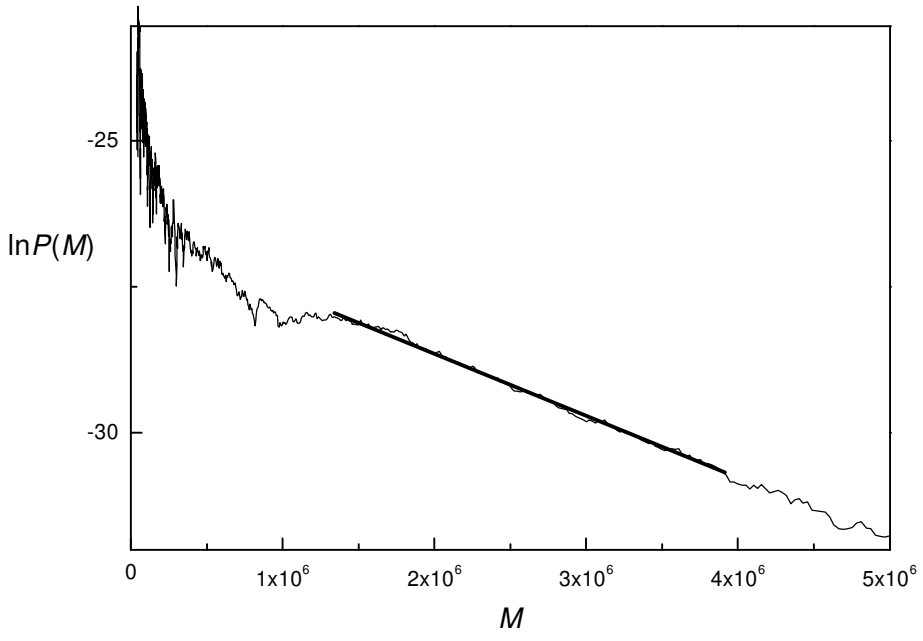

Figure 5.11: ln$P(M)$ plot for VAc emulsion polymerization, 40°C, 5.3% conversion, [persulfate] = 1.9×10^{-3} M. The region of the plot used in equation 5.3 is shown in bold.

From figure 5.9 it can be seen that the ln$P(M)$ distribution is linear from about 8×10^5 up to 3×10^6 daltons. It can be seen from figure 5.8 that this corresponds to most of the GPC trace to the high side of the peak molecular weight, as is generally desired for this type of analysis[116].

The low conversion sample in figure 5.10, demonstrates the signal/noise problem inherent in this experiment. However, the high molecular weight portion of the ln$P(M)$ distribution looks reasonable (figure 5.11) and k_{tr} determined from its slope is included in the final plot (figure 5.12) where it can be seen to be in general agreement with the rest of the data from this work and the literature.

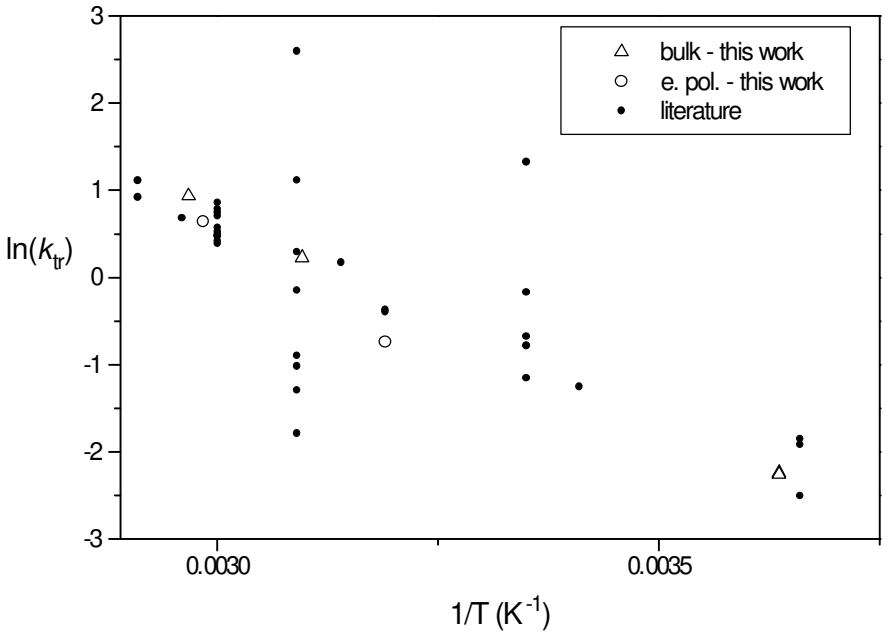

Figure 5.12: Arrhenius plot of transfer rate coefficients as determined for VAc bulk and emulsion polymerizations from this work, compared with literature data[54] reprocessed using Hutchinson's k_p[33].

The rate coefficient for transfer to monomer was found to obey the Arrhenius relation $\ln(k_{tr}$ /dm^3 mol^{-1} s^{-1}) = 14.7 - 38.8 kJ mol^{-1}/RT over the range 2° to 64°C. There was insufficient data to make any meaningful estimate of the errors.

5.4 Conclusions

There is little comparable data in the literature. Maeder and Gilbert's frequency factor for chain transfer in the BA system, ($2.9\pm0.9\times10^5$ M^{-1} s^{-1})[117] and Stickler and Meyerhoff's frequency factor for MMA (2.0×10^5 M^{-1} s^{-1})[108] are both about a factor of ten less than that measured for VAc in this work (2.4×10^6). This is not unreasonable, as the hydrogen abstraction sites (presumably the β and γ butyl carbons in BA and the methacrylic methyl carbon in MMA) are more hindered in the acrylates than in VAc. The activation energies for chain transfer in the homopolymerizations of BA and MMA are given as 32.6 and 46.1 kJ mol^{-1} respectively. The activation energy determined for VAc in this work, 38.8 kJ mol^{-1}, is in the middle of this range. Once again, this seems reasonable as the radicals formed by chain transfer to monomer in the BA system are secondary and therefore hydrogen abstraction occurs more readily than in VAc where a primary acetyl radical (possibly somewhat stabilised by conjugation with the carbonyl group) is formed. In the case of MMA both potential hydrogen donor groups are directly attached to electron withdrawing groups and therefore, the primary radicals so formed might be expected to form less readily than the acetyl radical in VAc.

Furthermore, while the reactivity ratios for BA and MMA with VAc (table 2.3) show that MMA monomer is more reactive than BA monomer, at least towards the pVAc macroradical, BA has a much higher k_p (table 2.1). This suggests that the pBA macroradical is extremely reactive. Combined with the ease of formation of the secondary radicals in BA, it is not surprising that the activation energy for transfer in the BA system is lower than that in the VAc system.

Finally, it has been shown by Ahmad et al.[119] that extensive chain branching occurs in the solution polymerization of BA. They have shown that chain transfer to polymer is primarily via abstraction of hydrogen from the tertiary backbone carbon and occurs to the extent of about 2.2 mole percent under conditions of relatively high initial monomer concentration (10%). This is greater than that reported for VAc (less than one mole percent)[64]. The comparison here is somewhat tenuous because of the different nature of the radicals formed in each case (tertiary for pBA versus primary for pVAc). However, the fact that the pBA macroradical succeeds in abstracting hydrogen from such a sterically hindered site to a greater extent than the pVAc macroradical does in the VAc system is further support for the notion that the pBA macroradical is extremely reactive in abstraction reactions and is consistent with the ordering of the activation energies reported above.

The main conclusion that may be drawn from the preliminary work described in this chapter is that the ln$P(M)$ method was found to be suitable for the determination of the rate coefficient for transfer to monomer in the bulk polymerization of VAc. However, care must be exercised in the choice of columns used in the GPC. It was found that mixed bed columns were necessary to achieve good separation of the MWD.

-oOo-

6 Conclusions and Recommendations

6.1 Conclusions

1. The kinetics of the emulsion polymerization of vinyl acetate have been the subject of many research efforts[8,9,68,97,102,106,114,120]. No satisfactory explanation of the behaviour of this system has been forthcoming. Particularly mystifying is the independence of the rate of polymerization from the monomer concentration in the latex particles.

   The difficulties with VAc appear to be related to the high chain transfer rate, uncertainty regarding the effect of polar solvents on k_p (particularly $k_{p,aq}^{i}$) and the relatively high water solubility of the monomer. The latter makes prediction of the behaviour of monomeric particle-phase radicals and aqueous-phase oligomeric radicals quite uncertain.

   The proposed "neat explanation" which this work set out to test, namely that if chain transfer to monomer was always followed by exit and subsequent radical loss (limit 1 or 2b) then R_p would be independent of C_p, was found not to be the case.

   With the benefit of hindsight, it can be seen that this was always going to be a difficult case to make. It required that reinitiation by $M_{tr}^{\bullet}$ be very slow in order that transfer to monomer should nearly always result in radical loss (i.e. $k_{p,M}^{1}$ must be small) and furthermore, that the induced decomposition of persulfate could provide the extra radicals required to reconcile the high radical-loss rate implied by the proposed mechanism, with the known k_p and measured R_p.

   Both of the above requirements were found not to be satisfied. Various arguments have been proposed over the years for a small $k_{p,M}^{1}$ and these have been discussed in section 2.3.1.7 where it was argued that most chain transfer to monomer is to the acetyl group and that $k_{p,M}^{1}$ is probably very large. Furthermore, it was shown in chapter 4, that the induced decomposition of persulfate does not produce more radicals than are produced by the normal thermal decomposition of persulfate. Hence, limits 1 and 2b are inconsistent with the measured rates of polymerization.

2. From the theoretical considerations discussed in chapter 2, it seems that VAc emulsion polymerizations are subject to zero-one-two kinetics and that the radical-loss mechanism is via long-long termination and/or transfer to monomer with

subsequent intra-particle short-long termination in particles which have two growing polymer chains. Modelling of this mechanism suggested an approximately 0.5 order dependence of R_p on C_p during interval III and as such goes half way to explaining the often reported zero-order dependence of R_p on C_p.

3. Two experimental artefacts were observed, of which researchers using γ relaxation techniques should be wary. The first was the "heat effect" described in chapter 3. It is easily detected but if ignored may play havoc with the interpretation of relaxation data. Testing for the "heat effect" is recommended as standard operating procedure, especially for those monomers with a high propagation rate coefficient or other characteristics that are likely to cause an exotherm. Secondly, the γ radiolysis relaxation method for determination of radical loss rates (as described in chapter 3) can not be applied to the emulsion polymerization of vinyl esters as the experiment is subject to another, as yet unidentified, experimental artefact.

4. In this work, it has been shown that the retardation period observed in the emulsion polymerization of VAc can be explained by the effect of traces of oxygen ($<10^{-6}$ M) on the entry efficiency of the initiator-derived aqueous-phase oligomeric radicals.

5. Acetaldehyde, was found to play a minor role in inhibition and retardation of VAc emulsion polymerizations. However, it is an effective chain transfer agent and may be responsible for a significant reduction in molecular weights.

6. It has also been shown that the mechanism for the induced decomposition of persulfate by VAc is chain transfer to initiator from aqueous-phase oligomeric radicals. A value has been determined for the rate coefficient for transfer to initiator, by fitting the data of Morris and Parts[14] to a model based on this mechanism.

7. Finally, Arrhenius parameters were determined for the rate coefficient for chain transfer. This section of the work is incomplete, for reasons detailed in chapter 5. However, as a preliminary indication it was found that the frequency factor was $10^{6.38}$ M^{-1} s^{-1} and the activation energy was 38.8 kJ mol^{-1}.

6.2 Recommendations

1. Construction of a γ facility that permitted rapid isolation of the experiment from the γ source, with better stirring and heat exchange may allow for more precise determination of radical loss rates.

2. Determination of the Arrhenius parameters for k_{tr} in a manner that satisfies the consistency checks described in chapter 5.

3. Photolysis relaxations of vinyl acetate and vinyl neo-decanoate emulsion polymerizations may not suffer from the possible γ-relaxation artefact found in this work. The inhomogeneity of radical production by photolysis of the turbid emulsions should not present insurmountable problems for photolysis relaxations.

4. Although a suitable mechanism has not been proven, the fundamental principle of termination being dependent on transfer is such an elegant solution to a perplexing problem that it warrants further investigation.

-oOo-

6.3 References

1) Klatte, F. U.S. patent 1084581 (1914).

2) Herrmann, W. O.; Haehnel, W. D.R. patent 450286 (1924).

3) Mark, H. F. *Encyclopedia of Polymer Science and Engineering*; John Wiley & Sons: New York, Vol. 17 (1989).

4) Gardon, J. L. *J. Polym. Sci., Part A-1*, **6**, 623 (1968).

5) Harkins, W. D. *J. Chem. Phys.*, **13**, 381 (1945).

6) Harkins, W. D. *J. Chem. Phys.*, **14**, 47 (1946).

7) Harkins, W. D. *J. Am. Chem. Soc.*, **69**, 1428 (1947).

8) Zollars, R. L. *Effects of Particle Number and Initiator Level on the Kinetics of Vinyl Acetate Emulsion Polymerizations*; in *Emulsion Polymerization of Vinyl Acetate*; El-Aasser, M. S. and Vanderhoff, J. W., Ed.; Applied Science Publishers Ltd.: London, (1981).

9) Litt, M.; Patsiga, R.; Stannett, V. *J. Polym. Sci., Part A-1*, **8**, 3607 (1970).

10) Trommsdorff, E.; Kohle, E.; Lagally, P. *Makromol. Chem.*, **1**, 169 (1948).

11) Norrish, R. G. W.; Smith, R. R. *Nature*, **150**, 336 (1942).

12) Ballard, M. J.; Napper, D. H.; Gilbert, R. G.; Sangster, D. F. *J. Polym. Sci. Polym. Chem. Edn.*, **24**, 1027 (1986).

13) Gilbert, R. G. *Emulsion Polymerization: A Mechanistic Approach*; 1st ed.; Academic: London, (1995).

14) Morris, C. E.; Parts, A. G. *Makromol. Chem.*, **119**, 212 (1968).

15) Henton, D. E.; Powell, C.; Reim, R. E. *J. Appl. Polym. Sci.*, **64**, 591 (1997).

16) Cutie, S. S.; Smith, P. B.; Henton, D. E.; Staples, T. L.; Powell, C. *J. Poly. Sci.: Part B*, **35**, 2029 (1997).

17) Sarkar, S.; Adhikari, M. S.; Benerjee, M.; Konar, R. S. *J. Appl. Polym. Sci.*, **39**, 1061 (1990).

18) Casey, B. S.; Morrison, B. R.; Gilbert, R. G. *Prog. Polym. Sci.*, **18**, 1041 (1993).

19) Sangster, D. F.; Davison, A. *J. Polym. Sci., Polym. Symp.*, **49**, 191 (1975).

20) Neta, P.; Huie, R. E.; Ross, A. *J. Phys. Chem. Ref. Data*, **17**, 1027 (1988).

21) Maxwell, I. A.; Morrison, B. R.; Napper, D. H.; Gilbert, R. G. *Macromolecules*, **24**, 1629 (1991).

22) Morrison, B. R.; Piton, M. C.; Winnik, M. A.; Gilbert, R. G.; Napper, D. H. *Macromolecules*, **26**, 4368 (1993).

23) Zammit, M. D.; Davis, T. P.; Willet, G. D. *J. Poly. Sci. A - Polym. Chem.*, **35**, 2311 (1997).

24) Lane, W. H. *Ind. Eng. Chem.*, **18**, 295 (1946).

25) Hutchinson, R. A.; Aronson, M. T.; Richards, J. R. *Macromolecules*, **26**, 6410 (1993).

26) Capek, I.; Barton, J.; Ordinova, E. *Chem. Zvesti*, **38**, 802 (1984).

27) Lyons, R. A.; Hutovic, J.; Piton, M. C.; Christie, D. I.; Clay, P. A.; Manders, B. G.; Kable, S. H.; Gilbert, R. G. *Macomolecules*, **29**, 1918 (1996).

28) Ballard, M. J.; Napper, D. H.; Gilbert, R. G. *J. Polym. Sci., Polym. Chem. Edn.*, **22**, 3225 (1984).

29) Halnan, L. F.; Napper, D. H.; Gilbert, R. G. *J. Chem. Soc. Faraday Trans. 1*, **80**, 2851 (1984).

30) Davis, T. P.; O'Driscoll, K. F.; Piton, M. C.; Winnik, M. A. *Macromolecules*, **23**, 2113 (1990).

31) Balic, R.; Gilbert, G.; Zammit, M. D.; Davis, T. P.; Miller, C. M. *Macromolecules*, **30**, 3775 (1997).

32) Hawkett, B. S. *BSc (Hons) thesis*; University of Sydney, Sydney (1974).

33) Hutchinson, R. A.; Paquet, D. A.; McMinn, J. H.; Beuermann, S.; Fuller, R. E.; Jackson, C. *DECHEMA Monographs*, **131**, 467 (1995).

34) Grant, R. D.; Rizzardo, E.; Solomon, D. H. *J. Chem. Soc., Perkin Trans.*, **2**, 379 (1988).

35) Poehlein, G. *Macromol. Symp.*, **92**, 179 (1995).

36) Heuts, J. P. A.; Radom, L.; Gilbert, R. G. *Macromolecules*, **28**, 8771 (1995).

37) Heuts, J. P. A. *PhD thesis*; University of Sydney, Sydney (1996).

38) O'Driscoll, K. F.; Mahabadi, H. K. *J. Polym. Sci., Polym. Chem. Edn.*, **14**, 869 (1976).

39) Yamada, B.; Kageoka, M.; Otsu, T. *Polym. Bull.*, **28**, 75 (1992).

40) Lorand, J. P. *Radical Reaction Rates in Solution*; in *Landoldt-Bornstein, New Series*; Fischer, H., Ed.; Springer-Verlag: Berlin, Vol. II,13a, (1984).

41) Moad, G.; Rizzardo, E.; Solomon, D. H.; Beckwith, A. L. J. *Polym. Bull.*, **29**, 647 (1992).

42) Krstina, J.; Moad, G.; Solomon, D. H. *Eur. Polym. J.*, **29**, 379 (1993).

43) Gridnev, A. A.; Ittel, S. D. *Macromolecules*, **29**, 5864 (1996).

44) Smoluchowski, M. *Z. Phys. Chem.*, **92**, 129 (1918).

45) Russell, G. T.; Gilbert, R. G.; Napper, D. H. *Macromolecules*, **25**, 2459 (1992).

46) Russell, G. T.; Gilbert, R. G.; Napper, D. H. *Macromolecules*, **26**, 3538 (1993).

47) Ballard, M. J.; Gilbert, R. G.; Napper, D. H.; Pomery, P. J.; O'Sullivan, P. W.; O'Donnell, J. H. *Macromolecules*, **19**, 1303 (1986).

48) Russell, G. T.; Napper, D. H.; Gilbert, R. G. *Macromolecules*, **21**, 2133 (1988).

49) Olaj, O. F.; Kauffmann, H. F.; Breitenbach, J. W. *Makromol. Chem.*, **177**, 3065 (1976).

50) Olaj, O. F.; Kauffmann, H. F.; Breitenbach, J. W. *Makromol. Chem.*, **178**, 2707 (1977).

51) Mayo, F. R. *J. Am. Chem. Soc.*, **90**, 1289 (1968).

52) Buchholz, K.; Kirchner, K. *Makro. Chem.*, **177**, 935 (1976).

53) Kauffmann, H. F.; Olaj, O. F.; Breitenbach, J. W. *Makro. Chem.*, **177**, 939 (1976).

54) Brandrup, A.; Immergut, E. H. *Polymer Handbook*; 3rd ed.; Wiley Interscience: New York (1989).

55) Terazima, M.; Okamoto, K.; Hityoa, N. *J. Chem. Phys.*, **102**, 2506 (1995).

56) Wu, J. Q.; Beranek, I.; Fischer, H. *Helvetica Chimica Acta*, **78**, 194 (1995).

57) Viswanadhan, V. N.; Mattice, W. L. *Makromol. Chem.*, **186**, 633 (1985).

58) Clarke, J. T.; Howard, R. O.; Stockmayer, W. H. *Makromol. Chem.*, **44**, 427 (1961).

59) Blackley, D. C. *Emulsion Polymerisation*; Applied Science: London, (1975).

60) Moad, G.; Solomon, D. H. *The Chemistry of Free Radical Polymerization*; 1st ed.; Elsevier Science Ltd.: Oxford, (1995).

61) Adelman, R. L.; Ferguson, R. C. *J. Polym. Sci., Polym. Chem. Ed.*, **13**, 891 (1975).

62) Flory, P. J.; Leutner, F. S. *J. Polym. Sci.*, **3**, 880 (1948).

63) Flory, P. J.; Leutner, F. S. *J. Polym. Sci.*, **5**, 267 (1950).

64) Britton, D.; Heatley, F.; Lovell, P. A. *Macromolecules*, **31**, 2828 (1998).

65) Mayo, F. R. *J. Amer. Chem. Soc.*, **65**, 2324 (1943).

66) McDowell, W. H.; Kenyon, W. O. *J. Am. Chem. Soc.*, **62**, 415 (1940).

67) Wheeler, O. L.; Ernst, S. L.; Crozier, R. N. *J. Polym. Sci.*, **8**, 409 (1952).

68) Challa, R. R.; Drew, J. H.; Stahel, E. P.; Stannett, V. *J. Appl. Polym. Sci.*, **31**, 27 (1986).

69) Bugada, D. C.; Rudin, A. *J. Appl. Poly. Sci.*, **30**, 4137 (1985).

70) Graessley, W. W.; Mittlehauser, H. M. *J. Polym. Sci., A2*, **5**, 431 (1967).

71) Graessley, W. W.; Hartung, R. D.; Uy, W. C. *J. Polym. Sci., A1*, **7**, 1919 (1969).

72) Nozakura, S. I.; Morishima, Y.; Murahashi, S. *J. Polym. Sci., A-1*, **10**, 2767 (1972).

73) Nozakura, S. I.; Morishima, Y.; Murahashi, S. *J. Polym. Sci., Part A-1*, **10**, 2781 (1972).

74) Nozakura, S. I.; Morishima, Y.; Murahashi, S. *J. Polym. Sci., Part A-1*, **10**, 2853 (1972).

75) Amiya, S.; Uetsuki, M. *Macromolecules*, **15**, 166 (1982).

76) Morishima, Y.; Nozakura, S. *J. Polym. Sci., Polym. Chem. Ed.*, **14**, 1277 (1976).

77) Melville, H. W.; Sewell, P. R. *Makromol. Chem.*, **32**, 139 (1959).

78) Wheeler, O. L.; Lavin, E.; Crozier, R. N. *J. Polym. Sci.*, **9**, 157 (1952).

79) Litt, M. H.; Chang, K. H. S. *The Reinvestigation of Vinyl Acetate Emulsion Polymerization (III) - Isotope Effect*; in *Emulsion Polymerization of Vinyl Acetate*; El-Aasser, M. S. and Vanderhoff, J. W., Ed.; Applied Science Publishers Ltd.: London, (1981).

80) Bartlett, P. D.; Tate, F. A. *J. Am. Chem. Soc.*, **75**, 91 (1953).

81) Starnes, W. H.; Chung, H.; Benedikt, G. M. *Polym. Preprints*, **34**, 604 (1993).

82) Fossey, J.; Lefort, D.; Sorba, J. *Free Radicals in Organic Chemistry*; John Wiley and Sons: Chichester, (1995).

83) Kotzeva, L. *J. Poly. Sci.: Part A: Poly. Chem.*, **27**, 1325 (1989).

84) Ruchardt, C. *Agnew. Chem., Int. Ed.*, **9**, 830 (1970).

85) Bueche, F. *Physical Properties of Polymers*; Interscience: New York, (1962).

86) Ferry, J. D. *Viscoelastic Properties of Polymers*; 2nd ed.; Wiley-Interscience: New York, (1980).

87) Scheren, P. A. G. M.; Russell, G. T.; Sangster, D. F.; Gilbert, R. G.; German, A. L. *Macromolecules*, **28**, 3637 (1995).

88) Griffiths, M. C.; Strauch, J.; Monteiro, M. J.; Gilbert, R. G. *Macromolecules*, **31**, 7835 (1998).

89) Smith, W. V.; Ewart, R. H. *J. Chem. Phys.*, **16**, 592 (1948).

90) Adams, M.; Napper, D. H.; Gilbert, R. G.; Sangster, D. F. *J. Chem. Soc. Faraday Trans. 1*, **82**, 1979 (1986).

91) O'Donnell, J. H.; Sangster, D. F. *Principles of Radiation Chemistry*; Edward Arnold: London, (1970).

92) Sunardi, F. *J. Appl. Polym. Sci.*, **24**, 1031 (1979).

93) Allen, P. E. M.; Burnett, G. M.; Downer, J. M.; Melville, H. W.; Molyneaux, P.; Urwin, J. R. *Nature*, **177**, 910 (1956).

94) Stannett, V. T.; Gervasi, J. A.; Kearney, J. J.; Araki, K. *J. Appl. Polym. Sci.*, **13**, 1175 (1969).

95) Buxton, G. V.; Greenstock, C. L.; Helman, W. P.; Ross, A. B. *J. Phys. Chem. Ref. Data*, **17**, 513 (1988).

96) Dunn, A. S.; Taylor, P. A. *Makromol. Chem.*, **83**, 207 (1965).

97) Chang, K. H. S.; Litt, M. H.; Nomura, M. *The Reinvestigation of Vinyl Acetate Emulsion Polymerization (I) - The Rate of Polymerization*; in *Emulsion Polymerization of Vinyl Acetate*; El-Aasser, M. S. and Vanderhoff, J. W., Ed.; Applied Science Publishers Ltd.: London, (1981).

98) Weiss, J. *Nucleonics*, **10**, 28 (1952).

99) Sack-Kouloumbris, R.; Meyerhoff, G. *Makromol. Chem.*, **190**, 1133 (1989).

100) Weast, C. R. *CRC Handbook of Chemistry and Physics*; 68 ed.; CRC Press Inc.: Boca Raton (1987).

101) Hidi, P., unpublished data.

102) Friis, N. *A Kinetic Study of the Emulsion Polymerization of Vinyl Acetate*, Danish Atomic Energy Commission, *RISO Report No. 282* (1973).

103) Dunn, A. S.; Chong, C. H. *Br. Polym. J.*, **2**, 49 (1970).

104) Patsiga, R. *thesis*; New York State University, Syracuse (1962).

105) Litt, M. H.; Chang, K. H. S. *The Reinvestigation of Vinyl Acetate Emulsion Polymerization (II) - The Induced Decomposition of Initiator*; in *Emulsion Polymerization of Vinyl Acetate*; El-Aasser, M. S. and Vanderhoff, J. W., Ed.; Applied Science Publishers Ltd.: London, (1981).

106) Stannett, V. T.; Challa, R. R.; Drew, J. H.; Stahel, E. P. *The Radiation Induced Emulsion Polymerization of Vinyl Acetate*; in *Emulsion Polymerization of Vinyl Acetate*; El-Aasser, M. A. and Vanderhoff, J. W., Ed.; Applied Science Publishers Ltd.: London, (1981).

107) Streitwieser, A.; Heathcock, C. H. *Introduction to Organic Chemistry*; 3rd ed.; Collier Macmillan Canada, Inc.: New York, (1985).

108) Stickler, M.; Meyerhoff, G. *Makromol. Chem.*, **179**, 2729 (1978).

109) Heuts, J. P. A.; Clay, P. A.; Christie, D. I.; Piton, M. C.; Hutovic, J.; Kable, S. H.; Gilbert, R. G. *Progress in Pacific Polymer Science; Proceedings*, **3**, 203 (1994).

110) Morrison, B. R.; Maxwell, I. A.; Gilbert, R. G.; Napper, D. H. *Testing nucleation models for emulsion polymerization systems*; in *ACS Symp. Series - Polymer Latexes - Preparation, Characterization and Applications*; Daniels, E. S., Sudol, E. D. and El-Aasser, M., Ed.; American Chemical Society: Washington D.C., Vol. 492, (1992).

111) Deady, M.; Mau, A. W. H.; Moad, G.; Spurling, T. H. *Makromol. Chem.*, **194**, 1691 (1993).

112) Sarkar, S.; Adhikari, M. S.; Benerjee, M.; Konar, R. S. *J. Appl. Polym. Sci.*, **35**, 1441 (1988).

113) Lloyd, D. G. *J. Appl. Polym. Sci.*, **1**, 70 (1959).

114) Chern, C. S.; Poehlein, G. W. *J. Appl. Polym. Sci.*, **33**, 2117 (1987).

115) Clay, P. A.; Gilbert, R. G. *Macromolecules*, **28**, 552 (1995).

116) Moad, G.; Moad, C. L. *Macromolecules*, **29**, 7726 (1996).

117) Maeder, S.; Gilbert, R. G. *Macromolecules*, **31**, 4410 (1998).

118) van Herk, A. M. *J. Chem. Ed.*, **72**, 138 (1995).

119) Ahmad, N. M.; Heatley, F.; Lovell, P. A. *Macromolecules*, **31**, 2822 (1998).

120) Kshirsagar, R. S.; Poehlin, G. W. *J. Appl. Polym. Sci.*, **54**, 909 (1994).

-oOo-